

Stiffener placement optimization for stressed skin topsides

by

B.E.J. Veltenaar

to obtain the degree of Master of Science
at the Delft University of Technology,
to be defended publicly on Wednesday August 31, 2022 at 02:00 PM.

Student number:	4559703	
Project duration:	Dec 1, 2021 – Aug 31, 2022	
Committee:	Ir. A. van der Stap	TU Delft, Chair
	Ir. A. Kaptijn	IV-Consult, Supervisor
	Dr. Ir. M. Veljkovic	TU Delft, Supervisor
	Ir. W. van den Bos	TU Delft, Examiner

An electronic version of this thesis is available at <http://repository.tudelft.nl/>

ABSTRACT

In this thesis, an automated buckling check method has been developed and validated for thin plated stiffened structures used in stressed skin topsides.

Thin plated stiffened structures are widely used in, for example, aircraft, bridges and ships. Recently, it has become competitive to use this type of construction to offshore topsides as well. Originally, topsides were built as a lattice structure, mainly for the oil and gas industry. Over the years, it was found that these lattice structures are sensitive to fluid and air leakage. Due to the later development of offshore wind farms with high voltage equipment, topsides were now also required as transformer houses for these farms. This necessitated topsides less sensitive to leakage, using a stressed skin structure.

Stiffened plated structures in compression are prone to fail by buckling. Therefore, each panel must be checked for every possible load case in the lifetime of the structure. There are three methods in which stiffened panels can be checked for buckling: full-scale experiments, FEA and by design code. Full-scale experiments are not cost-efficient because each topside is exposed to many different load conditions. Therefore, the only economically viable methods are FEA and design codes. Compared to non-linear plastic FEA, design codes are most economical and therefore the most cost-efficient choice for larger structures like topsides. However, the design code method yields more conservative results compared to non-linear plastic FEA.

Due to the use of many panels in a stressed skin topside, a demand has arisen for an automated application of the DNV-RP-C201 buckling standard for stiffened plated structures. This automated method opens up the possibility of stiffener placement optimization. This means that the stiffeners no longer need to be modelled in the design. In other words, during the design phase, non-stiffened panels can be modelled. At a later point in time, the optimization method can determine the number and type of stiffeners and stringers needed in the structure to ensure stability according to the DNV-RP-C201 design code.

Buckling analysis is dependent on a large set of variables and design considerations. The developed method sets clear boundaries for the applicability of the method and justifies the choices made.

Design codes have their limitation concerning assumptions which are not close to real conditions. Panels are subjected to uneven, distributed loads. Design codes provide rules for linear distributed loads over non-stiffened panels, but not for stiffened panels. For stiffened panels, because of the effective width method, an average stress distribution over a plate-stiffener is assumed. It was unclear whether large stress distributions over plate-stiffeners would cause a degrading effect on their ultimate resistance. Therefore, a validation study has been performed for uni-axially loaded stiffened panels. Non-linear plastic FEA has been used to determine the ultimate resistance.

From these “numerical experiments”, it can be concluded that the effective width method can be applied in most cases of stiffened panels. However, in the case of a plate slenderness between 3 and 4.28, large stress distributions can have a degrading effect on the ultimate resistance of the plate stiffener. Therefore, for plate of such slenderness, the maximum of a stress distribution should not exceed twice the minimum.

The stiffener optimization method developed in this thesis allows engineers to design stability-governed structures without modelling each individual stiffener. This enhances design flexibility and majorly simplifies the FE model. Later, the method can quickly generate a stiffener placement optimum, which would not be feasible by hand.

CONTENTS

List of Figures	iv
List of Tables	vi
Nomenclature	vii
1 Introduction	1
1.1 Research question	2
1.2 Outline of report	2
2 Background	3
2.1 Conventional topside versus stressed skin topside	3
2.2 Stressed skin topside design.	3
3 Load cases and failure mechanisms	6
3.1 Various Load cases; an overview	6
3.2 Structural members and their function in the structure; an overview	8
3.3 The dual structural function of plating creates complex stress developments	9
3.4 Failure criteria	10
3.5 Conclusion	11
4 Buckling	13
4.1 Column Buckling	13
4.2 Plate Buckling.	14
4.3 Post buckling reserve and effective width	16
4.4 Buckling of stiffened panels.	17
4.5 Cross-section classification	20
4.6 Bifurcation point, critical buckling strength.	21
4.7 Buckling check DNV-RP-C201.	22
4.8 Effect of lateral pressure.	24
4.9 Discontinuous or continuous stiffeners.	25
4.10 Ultimate resistance	26
5 Structural analysis	27
5.1 Global analysis	27
5.2 FEA	28
5.3 Ansys FEM software.	29
5.4 SDC-Verifier post-processing software	29
6 State of the art of a buckling analysis	30
6.1 Buckling analysis of ships versus topside	30
6.2 Buckling check methods	30
6.3 Automated buckling analysis software	31
6.4 Previously conducted research on buckling check automation	31
7 Problem statement	32
7.1 Simplification of the model	33
7.2 Effect of simplifications on FEA.	33
7.3 Linear elastic FEA	33
7.4 Design codes; how they deal with stress distributions.	35
7.5 Plate-stiffener.	37
7.6 Conclusion	37

8	Boundaries	38
8.1	Yielding; out of scope	38
8.2	Deformations; out of scope	38
8.3	Manual design stress selection	38
8.4	Continuous or discontinuous stiffeners and reduced buckling length.	40
8.5	Types of stiffeners	41
8.6	Stringer placement	41
8.7	Overlapping load cases	41
8.8	Conclusion	42
9	Optimization method	43
9.1	Simplifications	43
9.2	Inputs variables	46
9.3	Optimization criteria	46
9.4	Optimization method	46
9.5	Manual touch up	47
10	Future refinements	50
10.1	Automated design stress extraction	50
10.1.1	Normal stresses	50
10.2	Local buckling due to high stress distributions	51
11	Plate stiffener buckling due to distributed loads	52
11.1	General outline of experiment	52
11.2	Stress distributions	53
11.3	Experimental steps	54
11.4	Results of plate-stiffener experiment	56
11.5	Conclusion	60
12	Load redistribution in continuous plate structure	61
12.1	Result	61
12.2	conclusion	62
13	Validation and verification	64
13.1	Correct application of DNV-RP-C201	64
13.2	Validation of stress correction.	64
13.3	Validation of the developed model on a large set of panels	66
13.4	Full scale validation.	66
14	Conclusion	75
15	Recommendations and further research	76
	Bibliography	77
A	derivation of Euler Buckling criterion	79
B	Plate buckling	81
C	Effective widths for stress distributions	83
D	Load distribution plots	84
E	Stressed skin module	85
F	Contour plots full scale validation	86
G	Verification of design code application	91
H	Optimizer results	97
I	Code for second order plate-stiffener analysis	104

LIST OF FIGURES

1.1	Drawing of topside and jacket structure [23]	2
4.1	A "short" and "long" column [12]	13
4.15	Differential element of plate in cylindrical bending	22
7.1	Simple beam loaded in bending	32
7.2	Stressed skin platform	34
7.3	Contour plot of normal stress in z-direction (vertical) of stressed skin platform	34
7.4	Stress per node over selected panel	35
7.5	Nodal stresses Sz of close-up panel[5]	35
7.6	Plate stiffener with input variables[5]	35
7.7	Linearization of finite element stress results [10]	36
8.1	Longitudinal stresses in an unstiffened panel obtained by linear elastic FEA.	39
8.2	Width of plate stiffener in longitudinal stress results of stiffened panel.	40
9.1	Proposed design workflow of stability governed structures	43
9.2	Modelled stiffened panel with respect to structure. Boundaries denoted in red.	44
9.3	Schematic representation of modelled stiffened panel	44
9.4	Stiffener area divided by plate area	45
9.5	Flowchart of panel design method	48
9.6	Flowchart of panel design method	49
11.1	Schematic drawings of an effective width model (left) and a plate-stiffener (right)	52
11.2	Schematic drawing of two plate stiffeners inside a panel with a stress distribution	54
11.3	Normalized functions that the plate-stiffener will be subjected to	54
11.4	Plate-stiffener used in experiment	55
11.5	Plate-stiffener loaded into Ansys	55
11.6	Eigenvalue buckling result	56
11.7	Resistance to linear load distribution in average stress (left) and total force (right).	57
11.8	Peak stresses at positive edge for a linear distribution	57
11.9	Resistance to Sinusoidal load distribution in average stress (left) and total force (right).	58
11.10	Peak stresses in sinusoidal distribution	58
11.11	Resistance to Positive parabola load distribution in average stress (left) and total force (right).	58
11.12	Peak stresses in positive parabola load distribution	59
11.13	Resistance to negative parabola load distribution in average stress (left) and total force (right).	59
11.14	Peak stresses in positive parabola load distribution	59
12.1	Drawing of panel used in experiment	62
12.2	upright view of panel with stress distribution schematically drawn	63
12.3	Maximum resistance of panel for the middle plate-stiffener, the panel on average and by DNV	63
13.1	20MPa stiffener direction axial stress simulation with ANSYS. Stiffeners modeled	65
13.2	20MPa stiffener direction axial stress simulation with ANSYS. Stiffeners not modeled	65
13.3	Wall on which the developed method is applied	66
13.4	four-panel geometry used in validation	67
13.5	Boundary conditions applied to the validation geometry	68
13.6	Line pressures applied to the geometry	69
13.7	Validation geometry with proposed stiffeners	71
13.8	First buckling mode of panels	72

13.9 Total deformation due to load case 1	73
13.10 Total deformation due to load case 2	73
13.11 Total deformation due to load case 3	74
A.1 Pin ended beam [12]	79
A.2 Graph of buckling load solutions [12]	80
E.1 HV equipment module	85
E1 Contour plot of normal stress in longitudinal direction	86
E2 Contour plot of normal stress in transverse direction	87
E3 Contour plot shear stress	87
E4 Contour plot of normal stress in longitudinal direction	88
E5 Contour plot of normal stress in transverse direction	88
E6 Contour plot shear stress	89
E7 Contour plot of normal stress in longitudinal direction	89
E8 Contour plot of normal stress in transverse direction	90
E9 Contour plot shear stress	90

LIST OF TABLES

4.1 Ultimate limit state Cross-section classification [18]	21
9.1 Input parameters model	46
11.1 Plate-stiffener geometry used in experiment	55
12.1 Panel geometry used in experiment	62
13.1 Verification plates	64
13.2 Simulation data	65
13.3 Geometry of panel and stiffeners	68
13.4 Boundary conditions	68
13.5 Line pressures per load case	69
13.6 Stiffener placement results load case 1	70
13.7 Stiffener placement results load case 2	70
13.8 Stiffener placement results load case 3	70
13.9 Maximum number of stiffeners out of every load case	71

NOMENCLATURE

Symbols

b	Plate width	[m]
b_{eff}	Effective plate width	[m]
C_{xs}	Reduction factor due to stress in x-direction	[-]
C_{ys}	Reduction factor due to stress in y-direction	[-]
E	Young's modulus	[Pa]
f_k	Equivalent buckling strength	[N]
f_T	Torsional buckling strength	[N]
f_y	Characteristic yield strength	[Pa]
I_e	Effective moment of inertia	[Kg m ²]
k	Buckling factor	[-]
k_{sp}	Reduction factor for plate buckling due to lateral pressure	[-]
l_k	Reduced buckling length	[m]
L	Length	[m]
M	Moment	[N/m]
M_{yyy}	Resistance parameters for interaction formulas	[N/m]
N_{xxx}	Resistance parameters for interaction formulas	[N]
p_f	Lateral pressure giving yield in outer-fibre of a continuous stiffener using elastic section	[Pa]
p_{sd}	Design lateral pressure	[Pa]
P	Load	[N]
σ	Design stress	[Pa]
s	Plate-stiffener width	[m]
s_e	Effective plate-stiffener width	[m]
S	Section modulus	[m ³]
t	Plate thickness	[m]
t_w	Minimal throat thickness of weld	[mm]
t_0	Web thickness of stiffener	[mm]
W_{es}	Section modulus	[m ³]
z_t	Distance	[m ³]

Greek symbols

γ_M	Material factor	[-]
λ_T	Reduced torsional slenderness	[-]
λ	Plate slenderness	[-]
λ_p	Plate slenderness	[-]
μ	Coefficient, geometric parameter	[-]
ν	Poisson ratio	[-]
ρ	Reduction factor	[-]
σ_{yw}	Yield strength of weld material	[Pa]
σ_y	Yield stress	[Pa]
σ_{cr}	critical yield stress	[Pa]
$\sigma_{x,Sd}$	Lateral design stress in longitudinal direction	[Pa]
$\sigma_{x,Rd}$	Lateral resistance stress in longitudinal direction	[Pa]
$\sigma_{y,Sd}$	Lateral design stress in transverse direction	[Pa]
$\sigma_{y,Rd}$	Lateral resistance stress in transverse direction	[Pa]

τ_{Sd}	Design shear stress	[Pa]
τ_{Rd}	Design resistance shear stress	[Pa]
ψ	Factors	[-]

Abbreviations

DNV	Det Norske Veritas
FEA	Finite Element Analysis
FE	Finite Element
HVDC	High Voltage Direct Current
HV	High Voltage
HTV	Heavy Transport Vessel
SLS	Serviceability Limit State
ULS	Ultimate Limit State

1

INTRODUCTION

Topsides are widely used in offshore engineering. Their primary function is to support equipment for hydrocarbon extraction or as transformer housing near an offshore wind turbine facility. [Figure 1.1](#) shows a drawing of a topside with a jacket structure to support it on the sea floor.

Traditionally, a topside is designed as a lattice structure, which is later closed with non-structural, architectural walls. Due to deformation in the lattice structure, and insufficient clearance at the supports of these non-structural walls, they are unintentionally provided with a load. Over time, this construction has proven to be sensitive to leakage of air and fluids. For adequate performance of HVDC equipment, humidity is crucial and moist or insufficient cooling could damage the equipment. Therefore, a new concept was developed where the entire topside is constructed out of reinforced steel panels. This new topside design is called a 'stressed skin' design and is already widely used in the aeroplane and shipping industry. In a stressed skin offshore topside, the walls have a structural function opposite to the traditional platforms where the walls do not have a structural function.

A topside is subjected to various load cases related to environmental loads during operation and loads during transportation and installation. The stresses that the structural members endure during these load cases can be predicted by linear elastic FEA. These results are used as an input to check whether the structural members will fail.

Topsides are checked for fatigue, buckling, yielding and deformations. This thesis will focus on the stability related limit state of a stressed skin topside. Fatigue, due to cyclic loading of the structure, is therefore out of scope. Because of the slender nature of stressed skin topsides, the sudden loss of stability (buckling) is considered the most governing failure mechanism.

In the industry, buckling checks are performed with widely accepted design codes such as 'Eurocode 3 - Design of steel structures - part 1-5', 'DNV-RP-C201 - recommended practice: Buckling strength of plated structures' and 'ABS - Buckling and ultimate strength assessment for offshore structures'. These design codes provide rules and manufacturing limits to which stiffened thin plated structures can be checked for buckling.

This approach to a buckling check requires an engineer to model each stiffener and plate throughout the structure, and later check it for buckling with one of the earlier mentioned buckling codes. For reasons described in [chapter 7](#) it is not necessary to model each individual structural element in order to determine whether buckling occurs. Not doing so saves labour and cost, simplifies the FEA model and improves flexibility during the design process.

This thesis examines to what extent buckling analyses by linear elastic FEA in combination with design codes can be automated and optimized. The focus lies on a particular structure, that of a stressed skin offshore topside, but it can be assumed that other stability governed thin walled structures could be checked for buckling in the same way with minor adjustments.

1.1. RESEARCH QUESTION

The aim of this research can be described in the following research question: "How to develop a method with which stiffener placement in stability governed thin walled structures can be automated and optimized for cost of execution."

In order to answer this question, all relevant literature will be presented and a method for stiffener placement optimization will be developed and validated.

1.2. OUTLINE OF REPORT

chapter 2 will state the background of the research and its relevance. chapter 3 will explain the load cases to which the topside is subjected and explains the function of the structural elements in the structure. chapter 4, chapter 5 and chapter 6 will state all the relevant literature on: buckling, structural analysis, previously performed research and automated buckling analysis methods. chapter 7 will state the problem to be solved in this research, whereas chapter 9 proposes a solution through an analysis method. chapter 11, chapter 12 and chapter 13 validates for the proposed method through experiments. chapter 14 summarizes and concludes this research project.

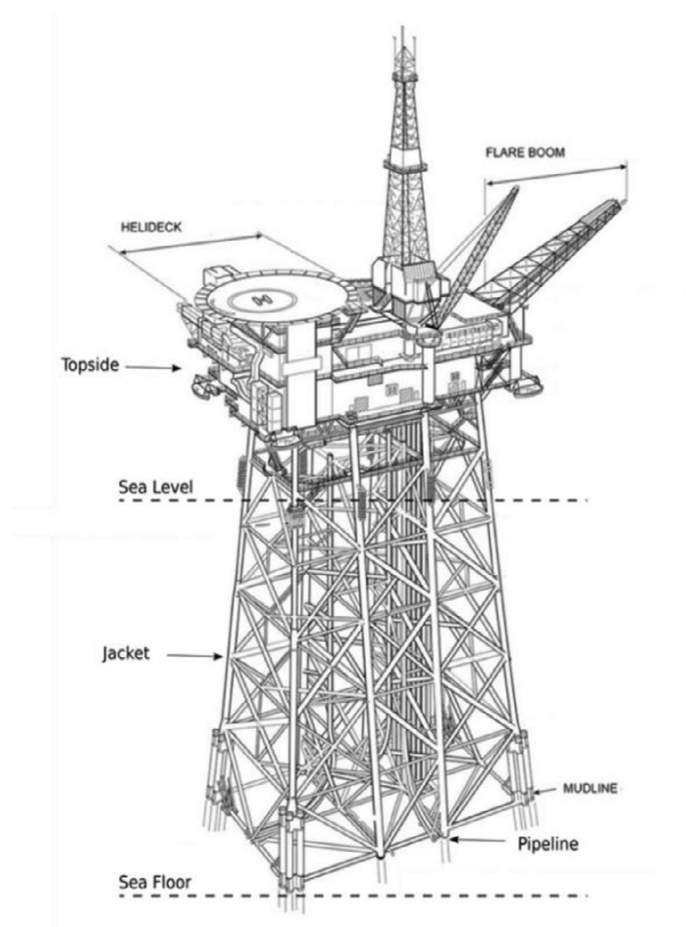


Figure 1.1: Drawing of topside and jacket structure [23]

2

BACKGROUND

This chapter provides the relevant background for the research at hand. Differences between stressed skin- and lattice structure-topsides, their architecture and the structural elements of a topside are discussed.

2.1. CONVENTIONAL TOPSIDE VERSUS STRESSED SKIN TOPSIDE

Offshore exploitation of hydrocarbons dates back until 1947 and is still common practice. The earlier topsides were built as lattice structures, i.e. triangles of steel, as no other feasible constructions existed. Back then, computing power was limited; stress calculations were done by hand. As computers and finite element software developed over time, this task was taken over by computers. Nevertheless, lattice structures stayed the industry standard as there was no incentive to change.

In conventional offshore topsides, the lattice structure was (partially) closed with non-structural, architectural walls. These walls were not included in the structural analysis of the lattice structure, but unintentionally still got a load-bearing function because of the way the walls were attached to the lattice structure. Since these walls were not designed to bear loads, they caused water- and air leakages over time.

A relatively new purpose of topsides is the housing of transformers and other high voltage electrical equipment near offshore wind turbine facilities. This created the need for a more reliable water and airtight construction because high voltage equipment requires a dry, appropriately cooled and ventilated closed facility.

These additional requirements lead to the development of an entire topside out of reinforced steel panels. This new way of topside design is called a 'Stressed skin' topside. In a stressed skin offshore topside the walls now do have a structural function and are therefore also incorporated in the structural analysis. In this type of topside, steel panels are reinforced by stiffeners and no longer fail because their load-bearing effects are now included in the structural analysis.

2.2. STRESSED SKIN TOPSIDE DESIGN

The main objective of this thesis is to find the optimal architectural configuration of structural members in a stressed skin topside with regard to cost and weight, taking into account (practical) boundaries. To understand the load distribution throughout a topside, the architecture and structural parts of the topside will be reviewed, using a more or less standard topside design.

ARCHITECTURE OF A STRESSED SKIN TOPSIDE

The broad outlines of the design are drawn by the project architect of the platform. This outline is based on the equipment required for the platform, the weight of this equipment, the size and number of personnel quarters, and the required air supply of rooms. The design of a stressed skin offshore topside can vary widely between sites because of different requirements. Although the geometry is different, the structural integrity is achieved in the same way, by choosing sufficient beam geometries, beam spacing and plate thicknesses.

In general, the topside can be seen as a large beam with the decks as flanges and the transverse walls as webs. This results in a preliminary structural function of the skin because it serves as the second flange of an H-beam. Each deck (horizontal dividers) and structural wall (vertical dividers) has its own function. Decks support the equipment and are constructed out of girders, stiffeners and stringers. The load that is supported by the decks is transferred to the bottom by the walls, which are supported by columns, stringers and stiffeners. Each structural member has its unique structural function, as addressed in [section 3.2](#). The topside will be supported on a discrete set of points provided by the jacket on which it stands. In order to support these loads, the topsides are often equipped with a double bottom, which works as a beam to transfer the load to the jacket.

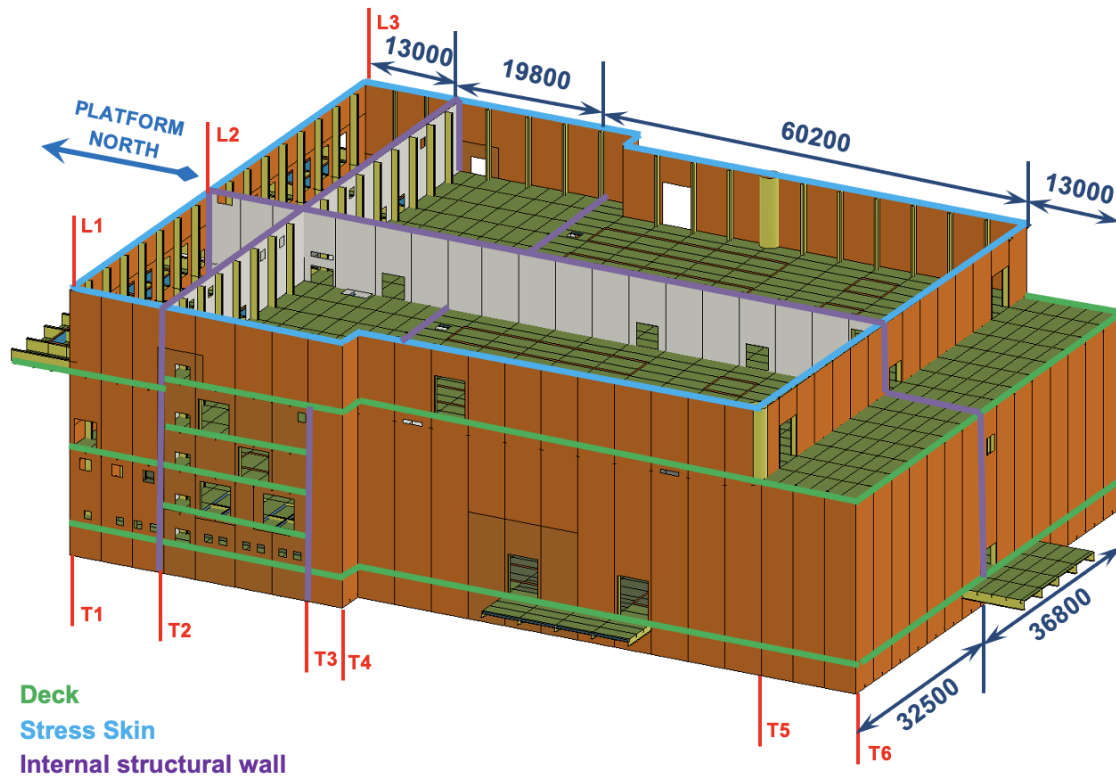


Figure 2.1: Section of a typical stressed skin offshore topside

Figure 2.1 illustrates the inside of a typical stressed skin topside. The green lines denote the decks, the purple lines the internal structural walls and the blue lines the stressed skin. The walls and decks of the platform are constructed out of steel plated material and is referred to as the skin of the platform. To provide the plate material with sufficient structural integrity, beams with varying stiffness and functions are applied. These beams will be referred to as girders, columns, stringers and stiffeners. [section 3.2](#) will further clarify their function.

STRUCTURAL BEAMS

The structure is composed of beams and steel plates. Not all beams are of the same geometry and therefore differ in stiffness. Naturally, the largest beams in the decks have the highest stiffness. These so-called girders are positioned in the direction of the shortest span, in order to minimize deflection and stress. The girders are supported by columns at both the inside and outside walls. The girders and columns are welded T-sections that, in combination with the skin, form an H-beam. The spacing of the girders and columns is based on the various openings that are required for access and material handling purposes in both walls and floors. To avoid interrupted girders and columns, the spacing of the girders and columns has to be larger than the largest opening in the wall or deck.

In order to prevent the skin/deck from buckling and to allow for limited local loads, plate stiffeners are required. The plate stiffeners are oriented in the same direction as the girder/columns and deliver an additional effective area to the skin/deck plates when acting as second flanges to the girders/columns. Spacing of the stiffeners depends on the plate thickness and local stress.

To reduce the buckling length of the stiffeners, stringers are introduced. Stringers are placed perpendicular to the girders/columns and stiffeners, transferring the out-of-plane load created by the stiffener. In addition, the stringers redistribute local loads over multiple girders/columns.

STRUCTURAL PLATING

The plating applied between beams in the structural walls and decks have two functions. The first function is to ensure the shape of the platform by accommodating shear forces. Lateral forces on the structure will mainly be counteracted by the wall of the structure in which the lateral force acts. The second function is to act as the second flange of the columns, girders, stringers and stiffeners. The slenderness of the structure, dependent on the thickness and width of the plates, determine the effective width of the plate as flange of the supporting beams. Because the topside is a thin-walled structure, the skin between columns, girders, stringers and stiffeners will generally not be fully effective.

3

LOAD CASES AND FAILURE MECHANISMS

A structural analysis of the design is performed to ensure stability during its lifetime. The structure is therefore checked for the following failure criteria as defined by its ultimate limit state (ULS): Yielding, buckling and reaction forces on its support. An additional serviceability limit state (SLS) is introduced due to deformations in the decks.

3.1. VARIOUS LOAD CASES; AN OVERVIEW

During the lifetime of the topside, it will be exposed to various load cases. These load cases can be distinguished into the following groups: in place, transport on HTV, transport on barge, float over, crane lift and a catamaran lift. Each topside has its own installation requirements, so not all installation methods will be considered for each topside. Each load case will be discussed briefly below.

In place

The in place load case represents the loads acting on the structure while it is in service. Loads acting on the structure originate from the environment (wind), cranes, helicopter and gravity.

Load-out and Load-in

Prior to transportation, the topside is loaded onto some kind of vessel or support structure. During this process, accelerations and gravity induce loads on the structure. The process is shown by figure 3.1.

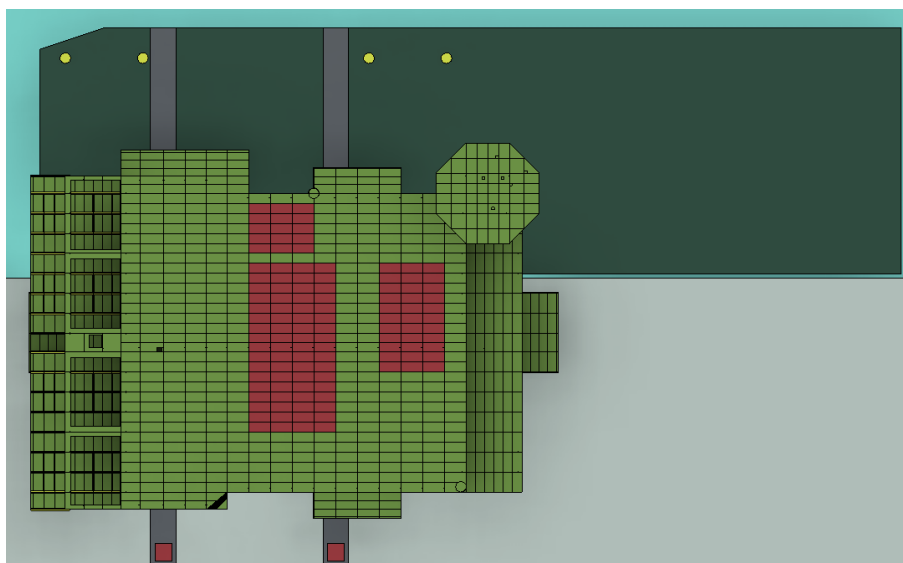


Figure 3.1: Load out on barge

Transport on Heavy Transport Vessel

Generally, due to lower wages, topsides are manufactured outside Europe and often transported to their final destination on a Heavy Transport Vessel (HTV). It is assumed that during transport all High Voltage equipment is installed, and that the topside is supported by the jacket leg stubs. During this phase, loads on the structure originate from hogging and sagging, accelerations and gravity. Hogging and sagging is a phenomenon that occurs when a beam or in this case ship is dynamically loaded. Loads will act on the structure because of deformations in the HTV.

Transport on barge

During a barge transport, the topside is supported in the same way as during the Heavy Transport Vessel transport. In this load case, hogging and sagging will not be considered as this transportation method will only be used during the installation phase and therefore in calm weather conditions with little dynamic loading on the barge. Acceleration and gravity should still be considered.

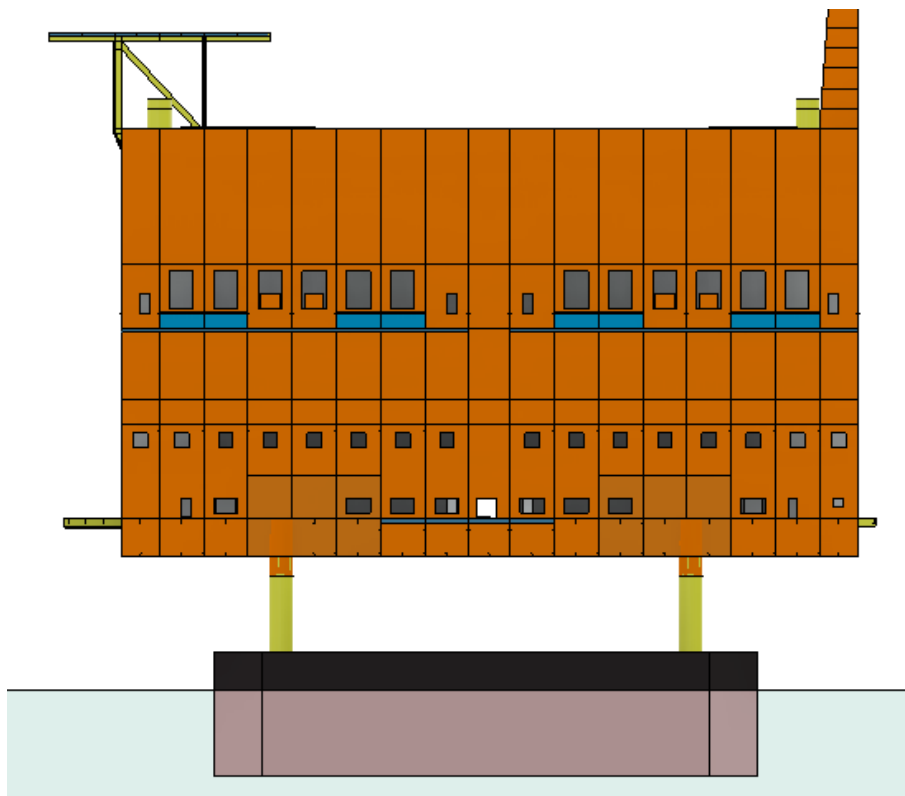


Figure 3.2: Topside on barge

Float over

During a float over, the topside will be positioned on a semisubmersible vessel, floated over the jacket and then lowered by sinking the semisubmersible. This load case involves gravity and accelerations.

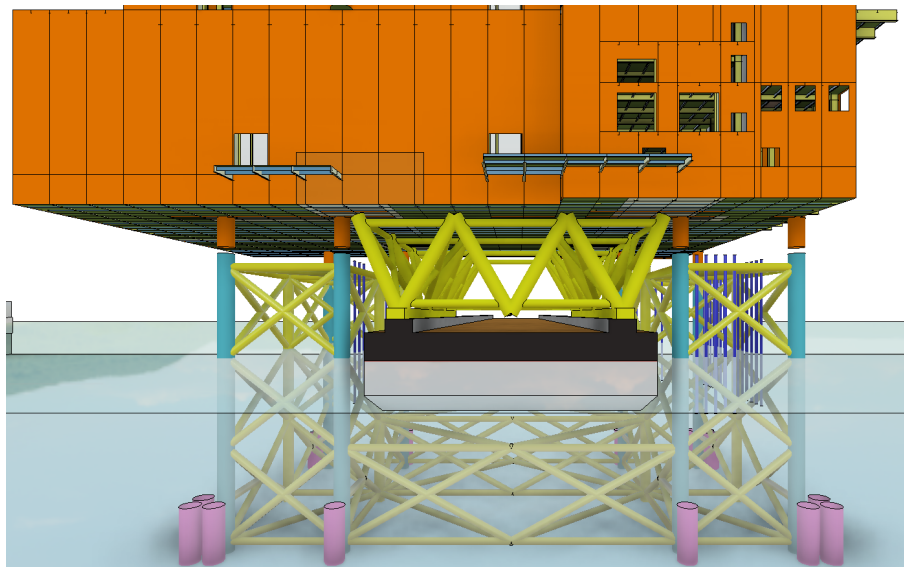


Figure 3.3: Float over

Catamaran lift

The catamaran lift is known from the Pioneering Spirit. During this installation practice, the topside is first loaded onto a barge, then transported to the catamaran, which then lifts it from the barge and places it onto the jacket. The load out on a barge and the catamaran lift are illustrated by Figure 3.1 and Figure 3.4 respectively.

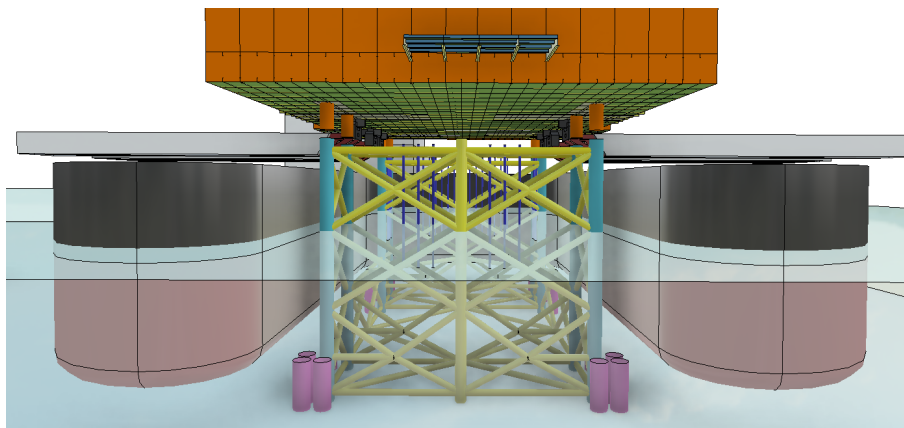


Figure 3.4: Catamaran lift with pioneering spirit

Conclusion

Each load case results in a different set of stresses developing throughout the structural members of the topside. To understand how stresses develop in the structural members of the topside, each member will be discussed briefly.

3.2. STRUCTURAL MEMBERS AND THEIR FUNCTION IN THE STRUCTURE; AN OVERVIEW

Structural members have the function of transferring loads through the structure, these loads cause stresses in the structural members. Structural members vary in geometry and therefore in their capacity to transfer loads and to bear stresses. In order to ensure the stability of the structure, the general function of each structural element should be known. Each structural member and its function will be briefly explained below.

Columns

Columns are the largest beams in vertical direction in the structure. Their main function is to transfer vertical loads in the platform to the bottom of the structure and eventually to the jacket. The main loads on columns are therefore compressive forces and moments along its length, applied by the girders.

Girders

The girder's geometry is in the same order of magnitude as the columns and are being used in horizontal direction underneath the decks. The weight of the equipment on the decks causes a bending load on the girders. The girders are supported by the columns.

Stringers

Second in magnitude in the structure are stringers, used to reduce the buckling length of the stiffeners applied to the plating. This results in a perpendicular load with respect to the attached plating on the girder. Another function of a stringer is the reduction of plate width in case of transverse stresses.

Stiffeners

Stiffeners are the smallest beams in the structure. To avoid local buckling of the plates between the columns/girders, stiffeners are applied to the plating. The main function of a stiffener is to prevent buckling due to loads in the direction of the stiffener. In addition, a stiffener helps to transfer out-of-plane loads to supporting beams. It should be noted though that this is not the main function of a stiffener. Therefore, high out-of-plane loads should be placed on larger beams like columns and girders.

Plating

The plating used in walls and decks have a dual structural function. Firstly, they act as the second flange of the columns, girders, stringers and stiffeners. Because the topside is a thin-walled structure, the skin between columns, girders, stringers and stiffeners will generally not be fully effective.

Secondly, they ensure the shape of the platform by accommodating shear forces. Lateral forces on the structure will mainly be counteracted by the wall of the structure in which the lateral force acts.

Plating also has a non-structural function; as room dividers to ensure the structure is water and airtight.

Panel

In this thesis, a distinction is made between a panel and a plate. When referring to a plate, this refers to the plating bounded by stiffeners and stringers. A panel is the plating between columns and stringers, on which stiffeners are applied.

3.3. THE DUAL STRUCTURAL FUNCTION OF PLATING CREATES COMPLEX STRESS DEVELOPMENTS

The dual function of plating results in a complex stress development throughout the structure. This is caused by two general mechanisms that contribute to stress development. Firstly, moments create axial loads in a structure and are accommodated by the plates, acting as flanges of the beams. This creates an internal compressive force on the plates. Secondly, shear forces are induced in the entire plating to ensure the initial shape of the structure.

The sheer number of structural members and their dual function makes it impossible to solve for stress development throughout the structure by hand calculations. This necessitates the use of linear elastic FEA. Finite element analysis generates all local stresses throughout the beams and plating. Once these stresses are known, it is then possible to check all members against various limitation criteria. Further information on finite element analysis can be found in [section 5.2](#)

3.4. FAILURE CRITERIA

The various loads as described in [section 3.1](#) generate stress developments in the topside. A variety of mechanisms can lead to failure of the structure. Failure of the structure can be subdivided into Ultimate Limit State (ULS) failure and Serviceability Limit State failure (SLS). The Ultimate Limit State of this structure is determined by yielding or loss in stability, in the Serviceability Limit State the operation can not proceed due to large deformations.

YIELD CHECK

The structure is checked for yielding as this causes permanent deformations. The yield stress of plates up to $t = 40\text{mm}$ is 345MPa . With the material safety factor provided by DNV of $\gamma_m = 1.15$ this results in a design resistance of 300MPa . Linear elastic FEA analysis will provide local peak stresses in areas with profound geometrical changes. Such stresses are allowed to exceed the yield stress, provided the adjacent structural parts have sufficient capacity for redistribution of the stresses (DNVGL-OS-C101 [6] chapter 2 section 4; 1.4.2).

It should be noticed that the structure is relatively thin walled and therefore buckling is the governing failure mode. This results in a relative low utilization of the yield check.

BEAM BUCKLING

Girders and columns are welded T-sections that form an H-section together with the skin/deck plate. In an FEA model, the girders and columns are modelled as shell elements and are verified against the design resistance. In the preliminary design phase it is made sure that girders and columns are of at least category 3 so that they can be loaded up until its yield strength without buckling, more on that can be found in [section 4.5](#).

PLATE BUCKLING

Loads encountered by the topside cause the plating to be subjected to normal stresses in axial and transverse direction and shear stresses. Because of these loads, the plating can buckle elastically and therefore lose stability. Checking stiffened plates for buckling is the main objective of this research.

DEFORMATIONS

The supports of the equipment that is being placed in the topside can be subjected to limited deformations. For HV equipment, the supports are allowed to maximally deform at a ratio of 1:500 and decks without HV equipment can deform 1:300.

In case these limits are reached, additional stiffening must be applied to the decks. The stiffness of the deck is highly dependent on the number of beams, beam geometry and plate thickness that is being used. It is relatively easy to check for deformations during the preliminary design phase, therefore, this requirement is being checked and fulfilled prior to the buckling check.

FATIGUE

Fatigue is the weakening and ultimately failure of the structure because of cyclic loading. This failure mechanism is out of the scope of this research and should be addressed separately.

WELDING

Residual stresses and distortions near the weld bed originate from localized heating by the welding process and subsequent rapid cooling. High residual stresses near a weld bed can lead to brittle fractures, fatigue, or stress corrosion cracking [25]. Due to the residual stresses, the buckling strength of the baseplate may be reduced. Residual welding stresses occur as compressive and tensile stresses in the structure, the course of the stress distribution is smooth but can be idealized as shown in [Figure 3.5](#). Welding residual stresses are an integral part of design codes and should not be accounted for separately. Only during non-linear plastic FEA analysis, welding residual stress will be accounted for through the application of additional initial deformations to the structure as prescribed by Eurocode 3 [8].

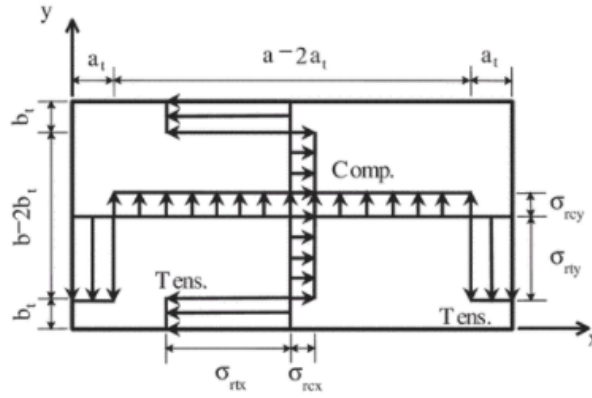


Figure 3.5: Idealized distribution of the welding residual stresses in a plate [11]

WELD SIZE

The strength of a weld is dependent on its throat thickness and effective length. The throat thickness is determined as the height of the largest triangle in the fillet weld, schematically denoted as 'a' in figure 3.6.

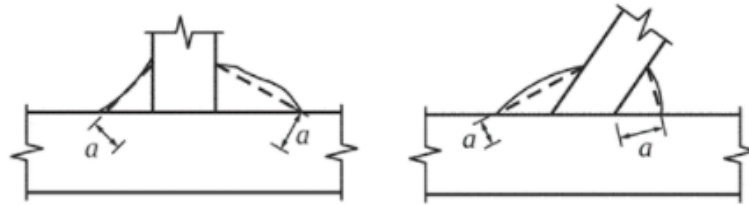


Figure 3.6: Throat thickness of fillet weld [28]

Eurocode 3 [8] describes 2 ways of calculating the strength of welds; the directional method and the full strength method. The directional method is more refined and could therefore yield the minimal weld volume.

In literature, throat thicknesses are usually referred to as integers in millimetre with an 'a' in front of it. A 6-millimete throat thickness fillet weld would be referred to as 'a6'. The size of a fillet weld determines to a large extent the weld volume and therefore the labour involved in realizing a connection. Though 3 mm welds are technically still possible, throat thickness of a weld connection generally exceeds 4 mm because of efficiency considerations[16].

The minimal throat thickness of double continuous fillet welds is given by Equation 3.1 and 3.2 [6].

$$t_w = 0,43 f_r t_0 \text{ (mm), minimum 3 mm} \tag{3.1}$$

$$f_r = \left(\frac{f_y}{\sigma_{fw}} \right)^{0,75} \text{ minimum 0.75} \tag{3.2}$$

CORROSION

As the structure operates in harsh environments, corrosion could lead to potentially unsafe situations. The structural reliability is for the structural elements reduced by loss of section thickness and for the overall structure by loss of integrity through pitting corrosion [17]. The effect of corrosion can be minimized by applying protective measures such as coatings and galvanization. Corrosion becomes particularly critical in situations where these protections become ineffective. For the design of a topside, it is assumed that the entire topside is sufficiently protected against corrosion.

3.5. CONCLUSION

During the lifetime of a topside, it is exposed to different load cases. During transport these are caused by accelerations, weight, hogging and sagging. Once in place, the topside is exposed to the environment, heli-

copters and cranes. To ensure the shape and structural integrity of the topside during transport and during its lifetime, beams and plates are used.

These members are designed in such a way that the ULS and SLS are not met during the lifetime of the topside. These limits can be met by various failure mechanisms such as corrosion, fatigue, deformations, buckling and yielding. For this research, it is assumed that fatigue and corrosion have been accounted for in previous design steps and are out of scope.

A yield check is performed to ensure no plastic deformation is present. However, it is expected that the final utilization of the yield check will be relatively low because buckling is governing in thin walled structures. Deformation limits should be checked as well, however, this is expected to be a limited problem and therefore, like the yield check, will be performed prior to the buckling analysis and are out of scope of this research.

In most areas, buckling is expected to be the governing failure mode for this structure.

4

BUCKLING

In engineering, structures are designed for various limit states such as ULS, SLS, and ALS. Analysis methods have been developed to determine under what circumstances these limits are reached. One of the phenomena that cause these limit states to be reached is buckling. It refers to the sudden loss in stability due to a compressive force. Because it can result in the loss of almost all structural capacity, it can lead to overall failure of a structure.

During the lifetime of a structure, it is subjected to all sorts of loads that lead to stresses in the structure, these stresses are subdivided into in-plane stresses and shear stresses. A buckling limit is defined as a limit of a combination of these stresses, at which the buckling phenomena will occur. All load cases must not exceed the buckling limit to ensure structural integrity.

4.1. COLUMN BUCKLING

Compressive loads are being carried by compressive members, the most widely used is a column. A column is characterized by its straight vertical shape and greater length relative to the cross-section dimensions. Columns can be subdivided into long and short columns, as shown in Figure 4.1. A short column under an incremental axial load will shorten and finally collapse by fracture or a large deformation. A long column under similar loading will develop the same shortening, but will eventually develop a deformation normal to that of the loading axis. This phenomenon is referred to as buckling. Figure 4.1 shows the buckled shape of a long column.

The buckling resistance of a column is largely dependent on the bending stiffness and the length of the beam. Buckling is therefore of the biggest concern in 'slender' structures; long beams with small bending stiffness. Because of the high yield strength of structural steel, steel beams tend to be slender and buckling is therefore of particular interest when using these compressive members.

The buckling stress of a uniform, pin-ended strut can

be found by the classical Euler analysis, of which the derivation can be found in Appendix A.

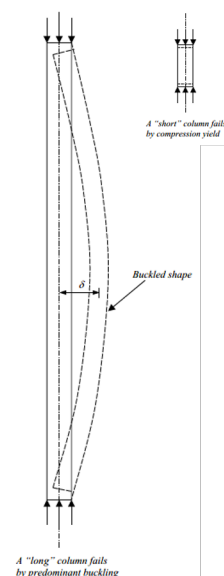


Figure 4.1: A "short" and "long" column [12]

4.2. PLATE BUCKLING

In [section 4.1](#) a column is defined as a straight vertical structural member with a length substantially larger than its cross-sectional dimension. Plates are characterized by their significant width in comparison to their length, and are therefore modelled as two-dimensional plane members.

Just as columns, plates tend to buckle out-of-plane when subjected to compressive loads in the axial direction. The buckling shape depends on loading conditions, geometry and support conditions. However, because of the slender nature of plates, they stay stable even after buckling has occurred. This phenomenon is referred to as the 'post buckling reserve' and can be used in the engineer's advantage, when applied correctly.

The critical plate buckling stress was first derived by G.H. Bryan in 1891 and is stated in [Equation 4.1](#). The constant k is dependent on the width to length ratio of the plate and can be derived analytically or be read from [Figure 4.2](#). With ' a ' the length of the plate in the direction of the stress and ' b ' the perpendicular in plane width.

As σ increases towards the critical buckling stress, just as a column, the plate tends to deform out of plane. The width of the plate gives resistance to this deformation, as tensile stresses are formed in transverse direction. If only one half-wave would form in the plate, the curvature in longitudinal direction would be less than the curvature in transverse direction, this would cause a higher resistance than a tendency to buckle. For this reason, a plate tends to buckling in squares as shown in [Figure 4.3](#) and k converges to a value of 4 for simply supported plates with $a/b > 1$. The full derivation of [Equation 4.1](#) can be found in [Appendix B](#). Other edge boundary conditions, such as clamped or free, yield different values for k varying from 0.5 to 7, which can be found in [Figure B.2](#). It should be noticed that the edge boundary conditions are therefore of great influence to the ultimate resistance of a plate.

$$\sigma_{cr} = k \frac{\pi^2 D}{b^2 t} = k \frac{\pi^2 E}{12(1 - \nu^2)} \left(\frac{t}{b} \right)^2 \quad (4.1)$$

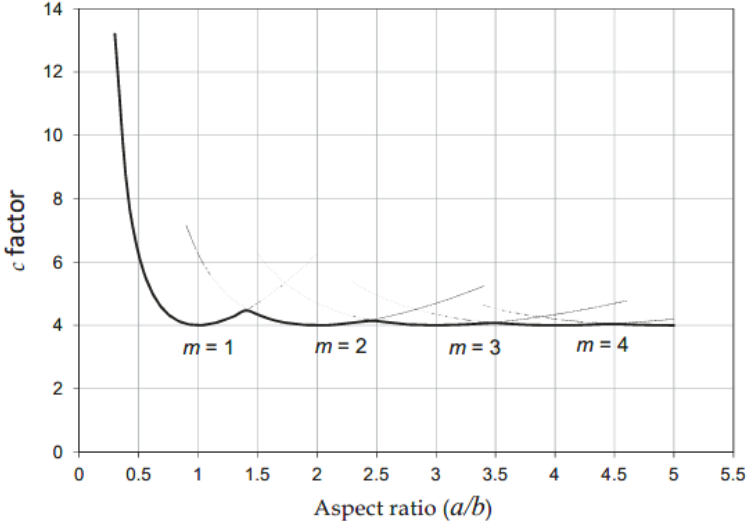


Figure 4.2: Buckling coefficient versus plate aspect ratio [2]

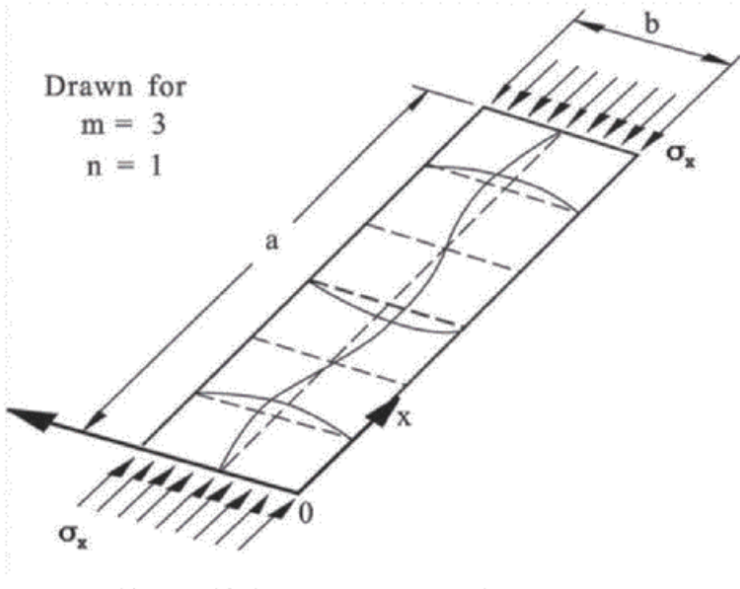


Figure 4.3: Buckled shape of a long plate [11]

4.3. POST BUCKLING RESERVE AND EFFECTIVE WIDTH

Just as columns, plates have a critical buckling strength that differs from its ultimate resistance. The difference originates from geometric imperfections, structural imperfections (due to welding or rolling) and the fact that steel is elastic to a limited extent.

Plates do not always plastically deform when they buckle, allowing them to be loaded beyond the critical buckling stress as long as this causes solely elastic deformation. This is illustrated in Figure 4.4; strip 'C-D' redistributes stress from the middle of the plate to the edges. Because of the boundary conditions imposed at the edges, these can be loaded until the yield strength. Not taking the post buckling reserve into account would result in a very conservative design. For that reason, buckling design codes make use of the effective width method. Figure 4.5 illustrates the stress distribution over the plate: prior to the critical buckling stress, in the post buckling reserve and at its ultimate strength. $\sigma_{x,y}$ varies from the yield strength at the edges to the critical buckling strength in the middle at its ultimate stress. The effective width is a representation of the ultimate strength of a plate with respect to this yield strength and can be found with Equation 4.2.

$$b_{\text{eff}} = \rho \cdot b \leq b \tag{4.2}$$

With ρ the reduction factor due to plate buckling as a function of the plate slenderness factor λ_p and $\psi = \sigma_2/\sigma_1$. A table for effective width calculations of unstiffened plates, in case of linear stress distributions, can be found in Appendix C. The effective width is calculated identically by the Eurocode 3 [9] and DNV [6] by use of Winter's correction factor.

$$\rho = \frac{b_{\text{eff}}}{b} = \frac{1}{\lambda} \left(1 - \frac{0,22}{\lambda} \right) = \frac{\bar{\lambda}_p - 0,055(3 + \psi)}{\bar{\lambda}_p^2} \leq 1 \tag{4.3}$$

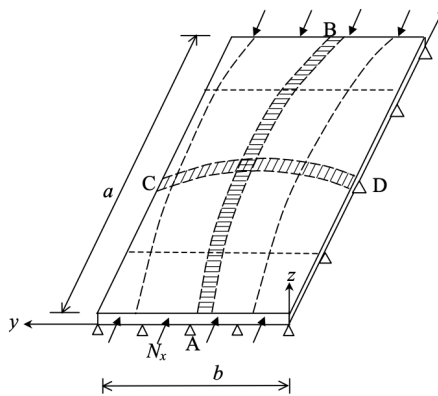


Figure 4.4: Plate buckling under Uni-axial Compression [13]

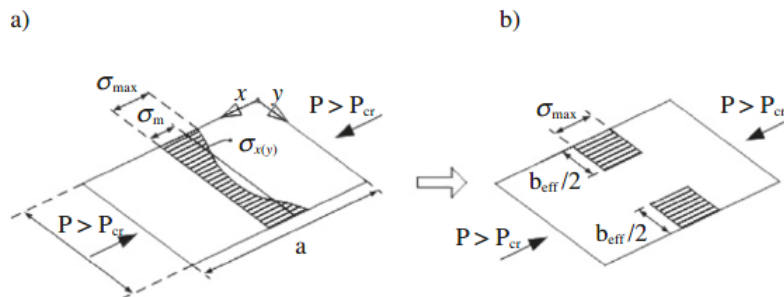


Figure 4.5: Stress distribution: a) at post-buckling state and b) according to effective width [?]

4.4. BUCKLING OF STIFFENED PANELS

A stiffened panel is usually referred to as a steel plate that is reinforced and therefore stabilized by stiffeners and stringers. It is extensively used in structures that require a high strength to weight ratio; offshore-structures, aeroplanes, ships, lock gates and box girder bridges. Due to flexure of the structure, the stiffened panels are subjected to longitudinal and transverse compressive loads as well as shear stresses, with or without lateral pressure. The slender character of the stiffened panels make them prone to instability failure. A stiffened panel is an assembly of plates and support members, the interaction of those structural elements is therefore of great importance to the ultimate strength of the panel. A stiffened panel in tension is fairly easy to evaluate, as it will fail by gross yielding of the material. The ultimate strength of a panel in compression, however, can be caused by buckling or plastic deformation. The following six collapse patterns of panels have been identified by Paik [21]:

- Overall collapse of plating and stiffeners as a unit
 - Mode I-1: Mode I for uniaxially stiffened panels
 - Mode I-2: Mode I for cross-stiffened panels (grillages)
- Mode II: Plate collapse without distinct failure of stiffener
- Mode III: Beam-column collapse
- Mode IV: Collapse by local web buckling of stiffener
- Mode V: Collapse by lateral-torsional buckling of stiffener
- Mode VI: Gross yielding

MODE I

Mode 1 is the failure mode of a panel with relatively weak stiffeners. In this scenario, the stiffeners and plate buckle as one unit, as shown in Figure 4.6. A slight distinction is being made between mode 1-1 and mode 1-2 as the latter represents the buckling of an orthotropic plate (Figure 4.7) in contrast to mode 1-1. The buckling behaviour of a Mode 1 is initially elastic and can sustain further loading after initial buckling has occurred in the elastic regime. Ultimate strength is reached by large yielding inside the panel or along the edges. An initial imperfection in the orthotropic plate is considered, but the welding-induced residual stress are ignored because tensile and compressive residual stresses will effectively cancel each other in a plate with multiple small stiffeners.

In this case, the stiffeners have a limited effect on the overall strength of the panel. This mode is therefore checked by DNV-RP-C201 in section 6 'buckling of unstiffened plates'.

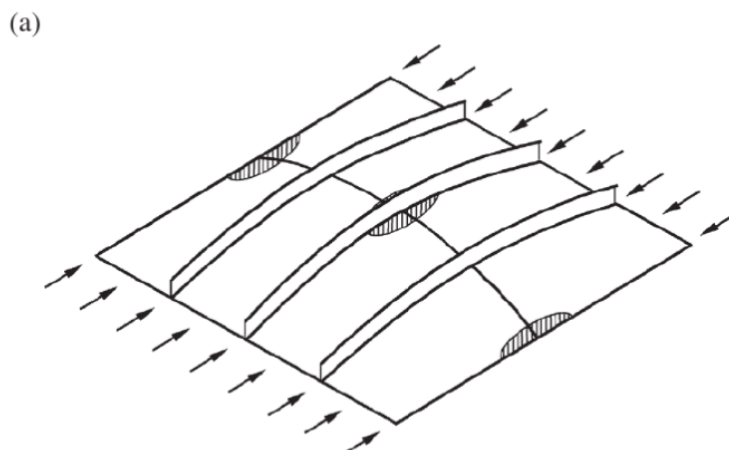


Figure 4.6: Buckling mode 1-1 [21]

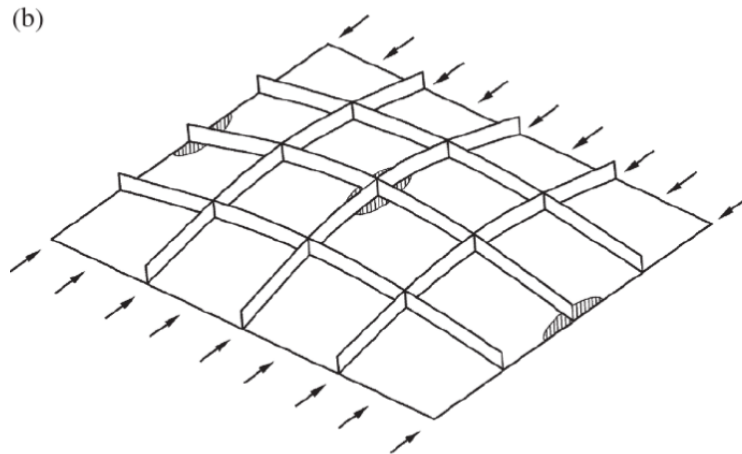


Figure 4.7: Buckling mode 1-2 [21]

MODE 2

Mode 2 failure is characterized by yielding at the plate stiffener intersection at the edges. This mode is especially interesting in case of biaxial loading of the panel. This mode assumes that, at ultimate strength, the stiffeners do not fail. It occurs in panels with relatively strong stiffeners compared to the plating.

DNV-RP-C201 checks for this failure mode in section 7.4, 'Resistance of plate between stiffeners'. Since the stiffeners do not fail, this failure mode is not dependent on the stress in longitudinal direction. Stress in transverse direction and shear stress are governing here. The resistance to this failure mode does increase with the amount of stiffeners (decrease in stiffener distance) but does not depend on stiffener dimensions.

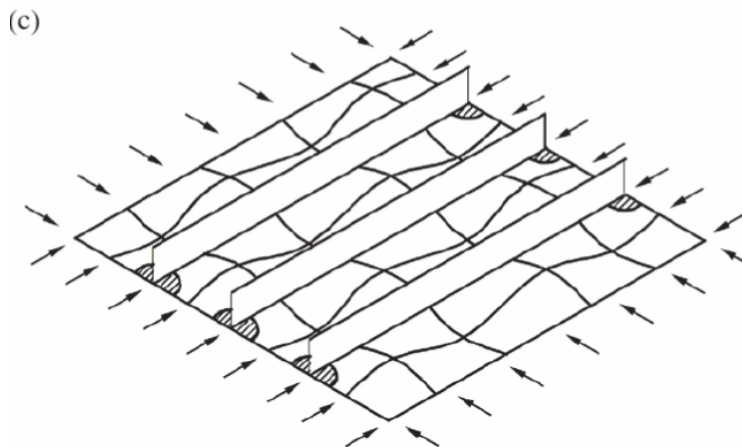


Figure 4.8: Buckling mode 2 [21]

MODE 3

When the plating is relatively weak, the slenderness is high and therefore the strength of the panel is mainly dependent on the stiffeners. This is the case in failure modes 3,4 and 5, for this reason the stiffened panel is represented as a plate-stiffener combination shown in Figure 4.9.

Mode three occurs at intermediate stiffener strength with respect to the plate. In this case, the plating is fully effective and fails as a beam-column by yielding of the extreme outer fibre.

DNV-RP-C201 checks for this failure mode in section 7.5, 'Characteristic buckling strength of stiffeners'.

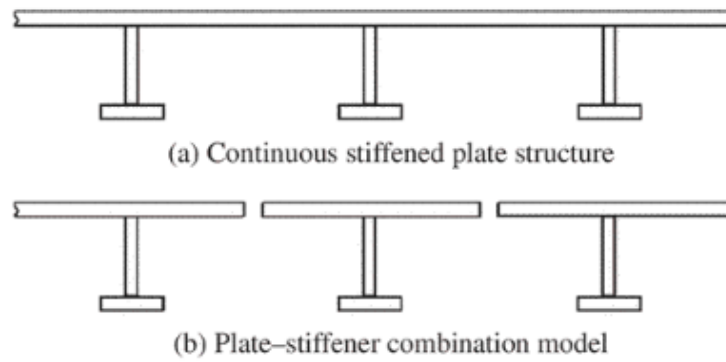


Figure 4.9: Plate stiffener combination model representing the entire stiffened panel [21]

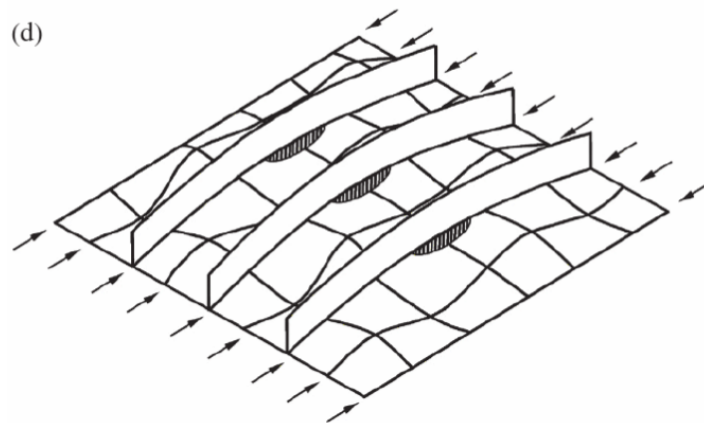


Figure 4.10: Buckling mode 3 [21]

MODE 4

In case of failure mode 4, displayed in Figure 4.11, the web of the stiffener is relatively high compared to its thickness and local buckling can occur. This can be overcome by choosing sufficient stiffener dimensions as described in section 4.5.

DNV-RP-C201 checks for this failure mode in section 9 'Local buckling of stiffeners, girders and brackets'.

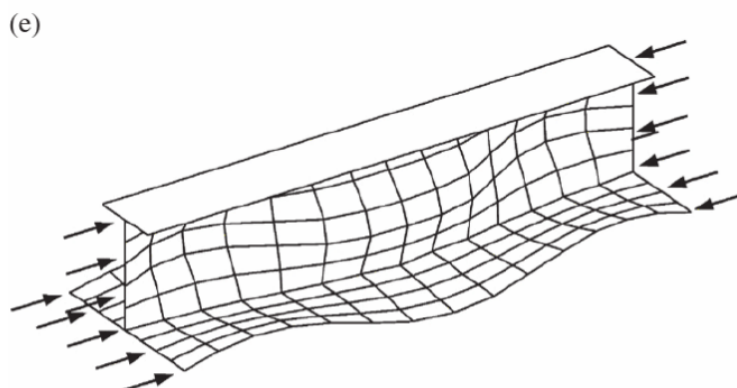


Figure 4.11: Buckling mode 4 [21]

MODE 5

Failure mode 5 is illustrated in Figure 4.12 and occurs when the most highly stressed stiffener in the panel collapses by flexural-torsional buckling or tripping. This is caused by insufficient torsional resistance of the stiffener and can be overcome by increasing the flange thickness.

This failure mode is checked by the DNV-RP-C201 code in section 7.5.2, 'Torsional buckling of stiffeners'. In practice, this type of buckling can be relatively easily prevented by installing tripping brackets.

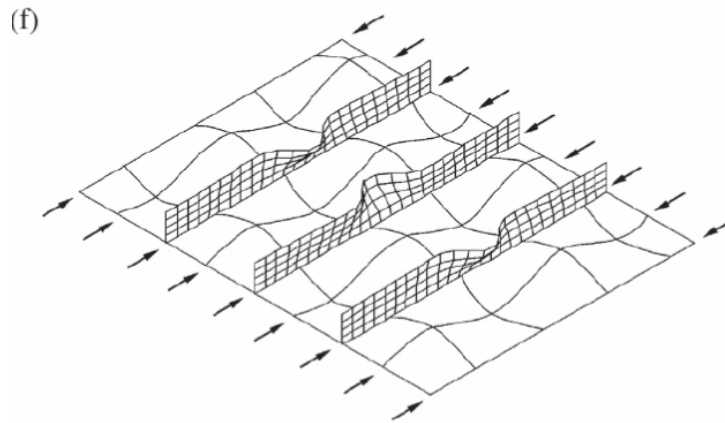


Figure 4.12: Buckling mode 5 [21]

MODE 6

Failure mode 6 is due to gross yielding by tensile stresses, and therefore out of scope when studying buckling.

4.5. CROSS-SECTION CLASSIFICATION

Sections used in steel structures can be classified as closed and open sections. Closed sections are defined as box sections whereas H-sections, channel-sections and angle sections are classified as open. Sections can be seen as an assembly of thin-walled sheets. As discussed earlier in section 4.2 the buckling limit of plates depends on the edge boundary conditions and plate slenderness ratio. Figure 4.13 displays local buckling in an H-section with a wave pattern in the flange, whereas the closed rectangular section develops a wave pattern in the flanges and webs.

The shape of a member is therefore of large influence on the local buckling limit. E.g. an H-section has a free end in its flange whereas the web is fully enclosed by simply supported edges. Figure B.2 shows that the free flange end causes a buckling factor 8 times smaller than the simply supported web.

The shape and slenderness of a section is therefore of great influence when considering local buckling. Local buckling restricts a section to be loaded to its yield strength. Eurocode clause 5.5.2 [9] therefore defines cross-section classes to find its ultimate resistance. The definitions of these simplified models are listed in Table 4.1.

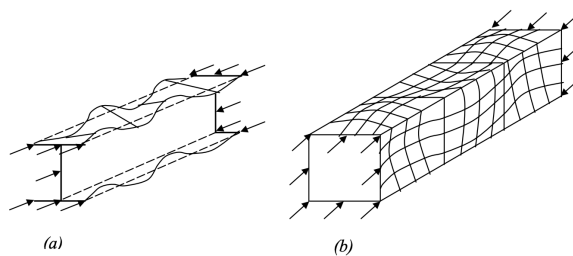


Figure 4.13: Local buckling of compression members [14]

Table 4.1: Ultimate limit state Cross-section classification [18]

Cross-section class	General analysis method	Calculation of Member Cross-section Resistance
1	Plastic	Plastic
2	Elastic	Plastic
3	Elastic	Elastic
4	Elastic	Elastic Plate Buckling

According to clause 5.5.2 the classes can be defined as follows[9]:

- Class 1 cross-sections are those which can form a plastic hinge with the rotation capacity required from plastic analysis without reduction of the resistance
- Class 2 cross-sections are those which can develop their plastic resistance moment, but have limited rotation capacity because of local buckling
- Class 3 cross-sections are those in which the stress in the extreme compression fibre of the steel member, assuming an elastic distribution of stresses, can reach the yield strength. However, local buckling is liable to prevent development of the plastic resistance moment
- Class 4 cross-sections are those in which local buckling will occur before the attainment of yield stress in one or more parts of the cross-section

Figure 4.14 gives an overview of the cross-section behaviours with M_{el} and M_{pl} ; the elastic and plastic limits of the members respectively. Hot rolled sections usually have enough wall thickness to avoid local buckling prior to yielding and are classified as 1,2 or 3 Cross-sections. Class 4 sections are usually fabricated (welded) sections like plate girders. It should be kept in mind that these compression members can be restricted to reach their full elastic resistance when in class 4.

Compression members used to stiffen plated structures are preferred in class 3 as they can be fully utilized to their elastic limit. Higher classes are undesirable because a plastic capacity is not to any use of the structure. A distinction is made between the compression members to form the stiffened panel and the assembly itself. The compression members should be chosen to be class 3, however, the assembly with the plate as second flange is generally a class 4 beam due to the slender nature of the design.

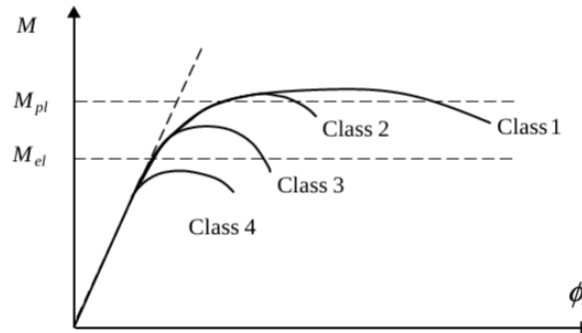


Figure 4.14: Cross-section behaviour in bending [7]

4.6. BIFURCATION POINT, CRITICAL BUCKLING STRENGTH

To evaluate the critical buckling strength of a stiffened plated structure, the buckling strength of a basic element must be determined. A basic plate in such a structure is surrounded by support members (stringers or stiffeners) which imply a rotational restraint at the plate edges of neither zero nor infinite. For the sake of simplicity, the conservative assumption is made that the plates are simply supported and are therefore not rotationally restrained at the edges.

Basic plate elements will be subjected to in-plane and out-of-plane loads. In-plane loads contain longitudinal and transverse axial compression/tension, edge shear and longitudinal and transverse in-plane bending.

Out-of-plane loads come from lateral pressure on the plates induced by environmental or local loads. It should be noted that buckling is a phenomenon that occurs due to compression; buckling will therefore not occur due to axial tension and out-of-plane loads alone.

The approach of determining the resistance of a stiffened panel can be categorized into two consecutive steps. The first step is to determine the characteristic buckling limit by searching for the bifurcation point, i.e. the stress at which the plate buckles because the flat form of the plates becomes unstable. The second step is to investigate the post-buckling strength behaviour by solving the equilibrium and compatibility equation. The equation that describes plate behaviour under a lateral load was first derived by Timoshenko [27]. The derivation as presented here is adopted from his work. The theory is applicable under the following conditions:

1. Plane cross-sections remain plane
2. The deflections of the plate are small ($w_{max} < t$)
3. The maximum stress nowhere exceeds the plate yield stress (i.e. the material remains elastic)

When considering a differential element of a bent cylindrical plate as shown in Figure 4.15, the curvature of the plate be described as $-d^2w/dx^2$, where w is the deflection of the plate in Z-direction. The unit elongation of a fibre at distance z from the middle surface is then $-zd^2w/dx^2$. Hooke's law describes the unit elongations in terms of normal stresses σ_x and σ_y .

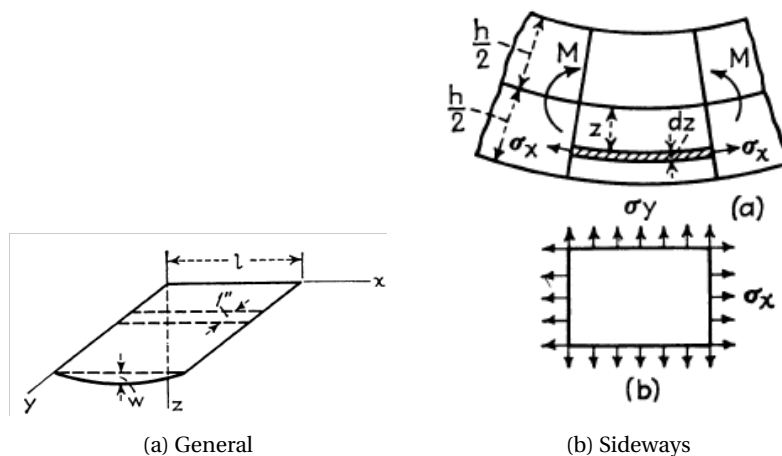


Figure 4.15: Differential element of plate in cylindrical bending

4.7. BUCKLING CHECK DNV-RP-C201

The optimization method presented in this thesis is based upon the general design considerations provided by DNV in DNV-RP-C201 [5]. These general design considerations are hereinafter referred to as the 'DNV design code'. This code provides a recommended practice for stiffened and unstiffened panels, but does not cover the failure modes of gross yielding of the plate due to a lateral load and buckling of very slender plates due to high span to thickness ratios. These failure mechanisms are covered in DNV-OS-C101.

All checks and important steps will be briefly mentioned here. A detailed description can be found in DNV-RP-C201 [5].

PLATE BETWEEN STIFFENERS

In case of a stiffened panel, the plate between the stiffeners is one of the first checks to be performed. Since the load in axial direction is mainly carried by the stiffener and its effective plating, the plate in between the stiffeners does not need to be checked separately. However, in cases with substantial σ_{ySD} , the plate between the stiffeners should be checked in transverse direction by clause 7.4 which is defined by the following equations.

$$\tau_{Sd} \leq \tau_{Rd} = \frac{f_y}{\sqrt{3} \cdot \gamma_M} \quad (4.4)$$

$$\sigma_{y,Sd} \leq k_{sp} \cdot \sigma_{y,Rd} \quad (4.5)$$

$$k_{sp} = \sqrt{1.0 - 3 \cdot \left(\frac{\tau_{Sd}}{f_y} \right)^2} \quad (4.6)$$

EFFECTIVE PLATE WIDTH

The effect width of a continuous stiffener subjected to a longitudinal, transverse and shear force is calculated as follows:

$$\frac{S_e}{s} = C_{xs} C_{ys} \quad (4.7)$$

$$C_{xs} = \frac{\bar{\lambda}_p^{-0.22}}{\bar{\lambda}_p^2}, \quad \text{if } \bar{\lambda}_p > 0.673$$

$$= 1.0, \quad \text{if } \bar{\lambda}_p \leq 0.673 \quad (4.8)$$

$$\bar{\lambda}_p = 0.525 \frac{s}{t} \sqrt{\frac{f_y}{E}} \quad (4.9)$$

$$C_{ys} = \sqrt{1 - \left(\frac{\sigma_{y,Sd}}{\sigma_{y,R}} \right)^2 + c_i \left(\frac{\sigma_{x,Sd} \cdot \sigma_{y,Sd}}{C_{xs} \cdot f_y \cdot \sigma_{y,R}} \right)} \quad (4.10)$$

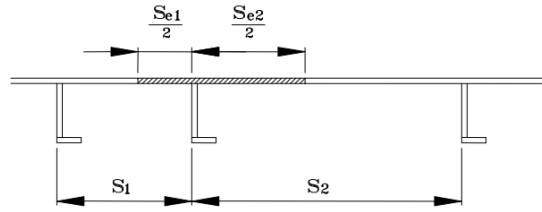


Figure 4.16: Effective width for varying stiffener distance [5]

$$c_i = 1 - \frac{s}{120 \cdot t} \quad \text{for } \frac{s}{t} \leq 120$$

$$c_i = 0 \quad \text{for } \frac{s}{t} > 120 \quad (4.11)$$

CHARACTERISTIC BUCKLING STRENGTH OF STIFFENERS

The characteristic buckling strength of stiffeners with its effective plating is calculated by the following equations:

$$\frac{f_k}{f_r} = 1 \quad \text{when } \bar{\lambda} \leq 0.2 \quad (4.12)$$

$$\frac{f_k}{f_r} = \frac{1 + \mu + \bar{\lambda}^2 - \sqrt{(1 + \mu + \bar{\lambda}^2)^2 - 4\bar{\lambda}^2}}{2\bar{\lambda}^2} \quad (4.13)$$

TORSIONAL BUCKLING OF STIFFENERS

Torsional buckling of stiffeners with its effective plating is calculated by the following equations:

$$\frac{f_T}{f_y} = 1.0 \quad \text{when } \bar{\lambda} \leq 0.2 \quad (4.14)$$

$$\frac{f_T}{f_y} = \frac{1 + \mu + \bar{\lambda}_T^2 - \sqrt{(1 + \mu + \bar{\lambda}_T^2)^2 - 4\bar{\lambda}_T^2}}{2\bar{\lambda}_T^2} \quad (4.15)$$

However, torsional buckling can be easily overcome by the placement of brackets. In case torsional buckling of stiffeners is governing, brackets should be considered.

INTERACTION FORMULAS

Because of loads induced by wind, the topside will endure (limited) lateral pressure on the plates. This results in an interaction effect between axial compression and lateral pressure. Therefore, the following interaction formulas for axial compression and lateral pressure at the plate side must be fulfilled:

$$\frac{N_{Sd}}{N_{ks,Rd}} + \frac{M_{1,Sd} - N_{Sd} \cdot z^*}{M_{s1,Rd} \left(1 - \frac{N_{Sd}}{N_E}\right)} + u \leq 1 \quad (4.16)$$

$$\frac{N_{Sd}}{N_{kp,Rd}} - 2 \cdot \frac{N_{Sd}}{N_{Rd}} + \frac{M_{1,Sd} - N_{Sd} \cdot z^*}{M_{p,Rd} \left(1 - \frac{N_{Sd}}{N_E}\right)} + u \leq 1 \quad (4.17)$$

$$\frac{N_{Sd}}{N_{ks,Rd}} - 2 \cdot \frac{N_{Sd}}{N_{Rd}} + \frac{M_{2,Sd} + N_{Sd} \cdot z^*}{M_{st,Rd} \left(1 - \frac{N_{Sd}}{N_E}\right)} + u \leq 1 \quad (4.18)$$

$$\frac{N_{Sd}}{N_{kp,Rd}} + \frac{M_{2,Sd} + N_{Sd} \cdot z^*}{M_{p,Rd} \left(1 - \frac{N_{Sd}}{N_E}\right)} + u \leq 1 \quad (4.19)$$

In case of sniped stiffener conditions, the interaction formulas are reduced to:

$$\frac{N_{Sd}}{N_{ks,Rd}} - 2 \cdot \frac{N_{Sd}}{N_{Rd}} + \frac{\left|\frac{q_{Sd} l^2}{8}\right| + N_{Sd} \cdot z^*}{M_{st,Rd} \left(1 - \frac{N_{Sd}}{N_E}\right)} + u \leq 1 \quad (4.20)$$

$$\frac{N_{Sd}}{N_{kp,Rd}} + \frac{\left|\frac{q_{Sd} l^2}{8}\right| + N_{Sd} \cdot z^*}{M_{p,Rd} \left(1 - \frac{N_{Sd}}{N_E}\right)} + u \leq 1 \quad (4.21)$$

4.8. EFFECT OF LATERAL PRESSURE

Lateral pressures in stiffened plated structures can arise from cargo, wind and water pressure. [Figure 4.17](#) shows the buckling pattern of plates with and without lateral pressure. In case of no lateral pressure (situation a) there is no restriction to the full development of the buckling shape. Therefore, no rotational constraints are present at the boundary of the plates.

The remaining situations shown in [Figure 4.17](#) endure a lateral pressure on the plates. This lateral pressure results in a bending moment in the edges and eventually a rotational constraint at the edges. This rotational constraint increases buckling factor, k as can be seen from [Figure B.2](#). Therefore, lateral pressure usually increases the buckling strength of plated structures. DNV-RP-C201 accounts for this phenomenon with a reduced buckling length presented by [Equation 4.22](#), [Equation 4.23](#) and [Equation 4.24](#)

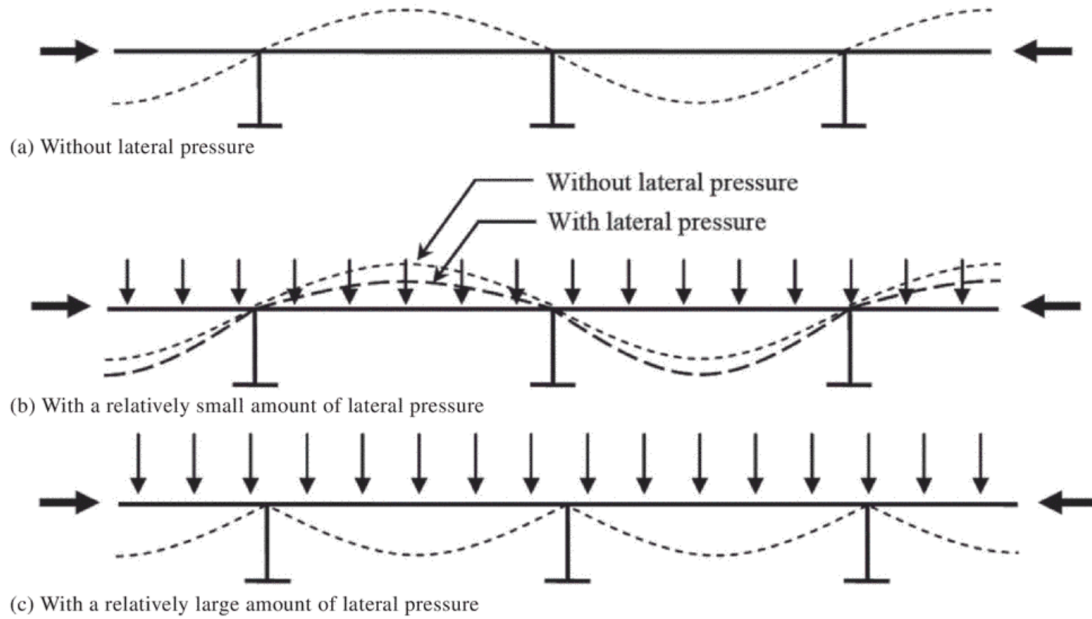


Figure 4.17: Schematic of the axial compressive buckling pattern of a plate with and without lateral pressure [11].

$$l_k = l \left(1 - 0.5 \left| \frac{p_{sd}}{p_f} \right| \right) \quad (4.22)$$

$$p_f = \frac{12 W f_y}{l^2 \cdot s \gamma_M} \quad (4.23)$$

$$W_{es} = \frac{I_e}{z_t} \quad (4.24)$$

4.9. DISCONTINUOUS OR CONTINUOUS STIFFENERS

Stiffeners can be added continuous or discontinuous, as shown in Figure 4.18. In case of continuous stiffening, the webs and flanges of the stiffeners are welded to the transverse beams and therefore to the opposing panels stiffeners.

When continuous stiffeners are chosen, bending moments are able to transmit from panel to panel, which can result in a reduced buckling length as described in section 4.8, whenever sufficient lateral pressure is present. The downside is that the flanges and webs of the stiffeners must be welded to the transverse stiffener, which results in significant additional welding costs. To benefit of a reduced buckling length, the stiffener pattern must also be mirrored with respect to the adjacent panel. After all, the transverse stiffening is not torsionally stiff.

In case of small lateral pressures, long panels and nonsymmetric stiffener patterns. Continuous stiffening will not add a significant benefit, in that case, discontinuous stiffeners are the most economic option.

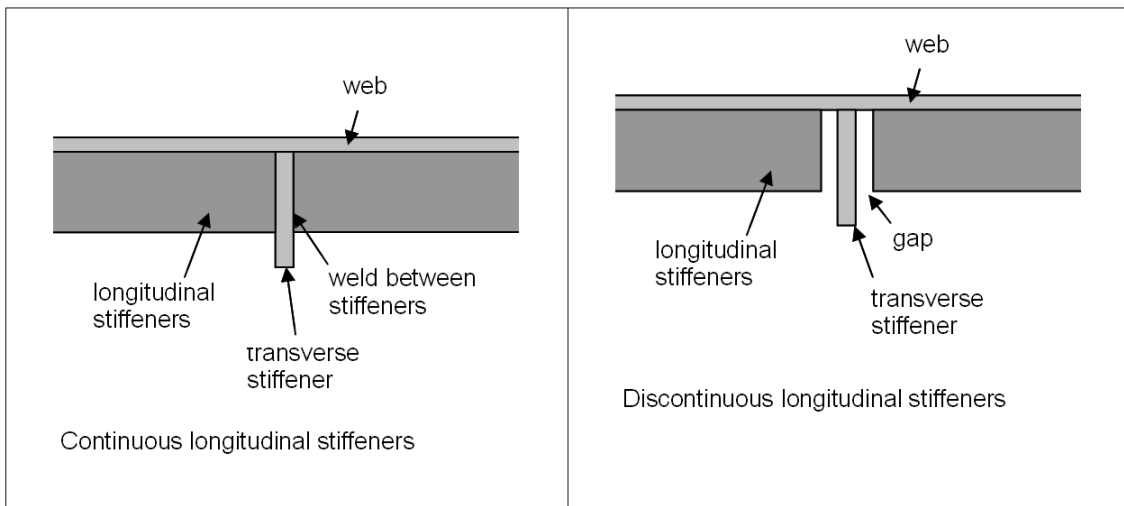


Figure 4.18: Schematic drawing of sniped and continuous stiffeners [24].

4.10. ULTIMATE RESISTANCE

Calculating the bifurcation point and solving for the compatibility equation is not a straight forward procedure. A simulation can be performed by non-linear plastic FEA, but is computationally very expensive. More on this can be found in [section 5.2](#). For this reason, design codes have been developed over the years. Eurocode 3, DNV and ABS are the most widely recognized codes. The codes provide guidelines for a safe design of stiffened plated structures at a much lower computational cost. In order to apply these codes to a stiffened plate, the stiffener location, steel type, beam geometry and stresses it is subjected to must be known.

Topsides are geometrically fairly large and complex structures that are even further complexified by introducing columns, girders, stringers and stiffeners. In order to simplify the geometry during the design phase, there is a cost incentive against modelling the stiffeners and stringers as this saves labour. An additional incentive against modelling is that it allows for an automated approach that opens up the possibility of fast iteration and therefore optimization of the structural member configuration. How this can be accomplished will be elaborated in [chapter 9](#).

5

STRUCTURAL ANALYSIS

Limit states are defined by load cases because they trigger a failure mechanism. In order to identify what failure mechanisms might impose a limit state, the stresses throughout the structure must be determined. This chapter provides an overview of the relevant literature regarding a structural analysis, in order to identify these stresses.

5.1. GLOBAL ANALYSIS

Stresses that develop in individual structural members should be checked against failure criteria. For this purpose, the internal (member) forces and moments should be derived from a global analysis. This analysis can be performed in four different ways [19]:

- linear elastic - initial geometry and fully linear material behaviour
- non-linear elastic - deformed geometry and fully linear material behaviour
- linear plastic - initial geometry and non-linear behaviour
- non-linear plastic - deformed geometry and non-linear material behaviour

The chosen calculation should accurately reflect the structural behaviour of the structure for the load case under consideration. For these load cases, there are two limit states of interest. The serviceability limit state due to deformations in the deck and the ultimate limit state that arises from global buckling of one or more structural members.

The choice between a linear or non-linear structural analysis should be based on the flexibility of the structure. In case of large deformations, ignoring second order effects can cause an unsafe approach, as the internal forces and moments are being underestimated. For stressed skin topsides, deformations will be small. Therefore, an elastic global analysis method is sufficient.

The choice between fully linear or non-linear material behaviour should be based on the relevance of non-linear material behaviour. A thin walled plated structure will initially buckle in an elastic manner, at a lower stress than the yield stress because the plating is not fully effective. Even if the plating would be fully effective, then the developed stresses should be always lower than the yield stress, as plastic deformation is defined as a limit state. Therefore, linear material behaviour should be assumed.

Many finite element analysis software packages are currently on the market, which mainly differ in user-friendliness and performance. For the global analysis of this structure, Ansys is chosen as the designated FEA tool as it is widely recognized in the offshore industry.

5.2. FEA

Finite Element Analysis (FEA) is widely used in the industry of structural mechanics, fluid flow, electromagnetic potential, mass transport and heat transfer. FEA is a numerical method that solves sets of algebraic equations for steady state problems and ordinary differential equations for transient problems. In the method, a larger model is subdivided into smaller parts, which are called finite elements. The size and shape of these elements is referred to as the mesh.

For steady state problems, a large set of linear algebraic equations is constructed and solved with numerical linear algebra methods. This linear mathematical approach is generally considered as a simple method and is computationally inexpensive. Transient problems are generally more difficult and lead to a set of ordinary differential equations which are solved by numerical integration techniques, this is referred to as non-linear FEA.

The transient failure modes of buckling and yielding could be checked for by non-linear FEA, but this would lead to unreasonable long computation times. For this reason, design codes have been developed to check for buckling, which only require stresses as inputs. Stresses alone can be obtained by elastic linear FEA. It is therefore only necessary to conduct a linear static FEA for a stressed skin offshore topside when using design codes as a buckling check method.

LINEAR ELASTIC FINITE ELEMENT ANALYSIS

In this section, a compact description of a linear elastic finite element analysis is provided. It is derived from the more detailed explanations by Hughes [26] and Okereke [20].

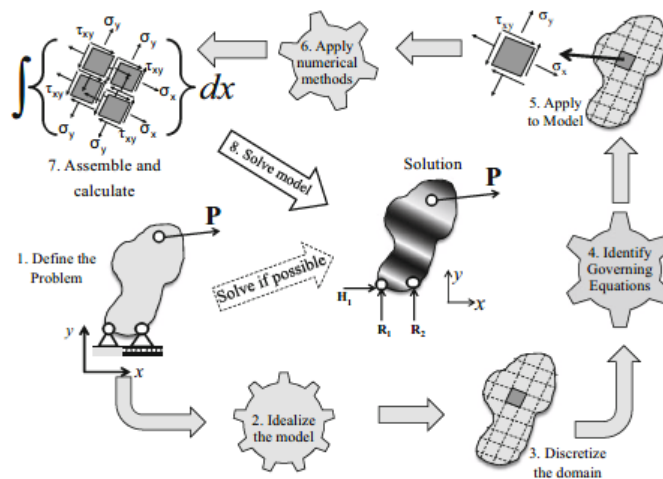


Figure 5.1: A schematic representation of the key processes that comprise the finite element method [20]

As can be seen in Figure 5.1 a finite element process consists of three steps in order to solve the problem.

1. Idealization of the defined problem by describing the system into smaller solvable parts (finite elements).
2. Identifying the governing equations.
3. Apply a numerical method to solve for these equations.

The result of the numerical model applied is dependent on the shape and size of the finite elements, also known as the mesh. FEA is an idealization of a physical model into a mathematical model. The FEA solves the mathematical model. After solving the model the accuracy is evaluated and if needed the model is refined and recalculated.

There are two ways of evaluating the mathematical model [3]:

1. Effectiveness of the model

The most effective mathematical model for the analysis yields the required response with sufficient accuracy and at the lowest computational cost.

2. Reliability of a mathematical model

The chosen mathematical model is reliable if the required response is known to be predicted within a selected level of accuracy.

For this reason, it is important to estimate the required accuracy that is needed for the problem.

5.3. ANSYS FEM SOFTWARE

Because of the many computational steps involved in solving a finite element model, it is crucial to set up the model as efficiently as possible. Applying the correct mathematical model can drastically reduce the number of computational steps. FEA is a field of engineering in itself. The chosen FEA software for this project is Ansys, Ansys is widely recognized in the (offshore) industry. The software helps the relatively inexperienced user to build an efficient FEA model and provides the user with an easy to use graphical interphase to define geometry, loads and boundary conditions. The Ansys solver is based upon APDL and its exact function is out of the scope of this research.

5.4. SDC-VERIFIER POST-PROCESSING SOFTWARE

SDC-Verifier is post-processing software for Ansys and Femap. It allows the user to efficiently check structures to different standards and load cases and automatically generates a report. The power of the tool lies in the automated recognition of joints, beams, welds and plates. The latter is of interest for this research. In order to automate a buckling check, the stresses and geometries of each panel should be extracted from the linear elastic FEA solution. This is a very time-consuming process and not feasible by hand. Therefore, SDC-Verifier is being used to automate this process. Although it is a very useful tool, it comes with a compromise. SDC-Verifier can only return the average, maximum or minimum stress over a panel and does not allow the user to request the stress development over a recognized panel. SDC-Verifier has indicated their desire to add this functionality to the software, so refinement can be realized.

For each horizontal or vertical wall, the software will return a text file with the geometry, location and stresses acting on every the panel. This can be used as an input for a buckling check. An example of such a result is presented in [Appendix H](#).

6

STATE OF THE ART OF A BUCKLING ANALYSIS

Structural instability due to compressive loads is caused by buckling. As mentioned in [section 3.5](#), buckling is the governing design criteria in case of stressed skin offshore topsides. This chapter provides an overview of all relevant literature concerning a buckling analysis.

6.1. BUCKLING ANALYSIS OF SHIPS VERSUS TOPSIDE

In comparison to ships and lock gates, which are often stiffened plated structures, the lateral pressure on the plates of a topside is relatively low. This is because wind-induced pressure is many times lower than the water pressure experienced by ships or lock gates.

As stated in [section 4.8](#), the buckling strength of plates under high lateral pressure is often larger because of the reduced buckling length. In case of ships and lock gates, due to the high out-of-plane pressure, the governing failure mechanism is yielding due to the bending of the stiffener. In these cases, the buckling check is a rather procedural check as buckling rarely causes problems. In case of topsides, buckling is the governing failure mechanism however, and is therefore normative during the design phase.

6.2. BUCKLING CHECK METHODS

There are three options in order to check for buckling: firstly the non-linear FEA, secondly the analytical approach by searching for a bifurcation point ('eigenvalue analysis') of the panel in combination with virtual work and thirdly by using design codes. The non-linear plastic FEA is computationally expensive and not feasible for large structures. The analytical approach has as pro that the buckling phenomenon can be proven mathematically, but the drawback is that it yields complex differential equations that must be solved numerically. On top of that, imperfections and welding residual stresses must be accounted for separately.

The design codes are therefore the most straight forward approach and are widely used in the industry. The benefit of using these codes is that they are relatively easy to implement, set manufacturing boundaries and incorporate welding residual stresses and imperfections. The only drawback is that it makes use of (semi-)empirical values that are not always (mathematically) justified.

In the industry, three design codes are most common for performing buckling checks on stiffened plated structures:

1. Eurocode 3 - Design of steel structures - Part 1-5: Plated structural elements [9]
2. DNV-RP-C201 - recommended practice: Buckling strength of plated structures [5]
3. ABS - Buckling and ultimate strength assessment for offshore structures [1]

Buckling checks will be determined through one of the here mentioned design code methods, as this is the simplest approach and often required by the industry. It's the actual standard approach as to date. In this research, DNV-RP-C201 has been chosen as this design code is used in IV-consults workflow.

6.3. AUTOMATED BUCKLING ANALYSIS SOFTWARE

The most common way of performing a buckling analysis is to model each beam and plate element in the structure, perform a linear static FEA and check every plate and beam segment for buckling by design code. FEMDS, Dlubal and SDC-Verifier are software packages currently on the market that allow users to perform an automated buckling check. These software packages work as add-ons on FEA software. They can reduce engineering time drastically by quickly performing a buckling check. However, a drawback is that the location and geometry of each individual compression member must be determined and fed into the software. This is straight forward as long as buckling is a non-governing failure mechanism, but causes major engineering limitations when it is. More on this can be found in [chapter 7](#).

6.4. PREVIOUSLY CONDUCTED RESEARCH ON BUCKLING CHECK AUTOMATION

O. Hillers first performed research on the automation of buckling analysis in 2011 [10]. In this thesis, a post-processing tool has been developed that is able to perform buckling checks on unstiffened plates based on FEA results in the form of text files.

The major challenge Hillers research faced was the automated recognition of plates and stiffeners, especially with complex geometries. At the time his research was performed, SDC-Verifier did have a buckling check feature, but the plates needed to be manually selected by the user. The developed recognition tool as developed by Hillers was therefore a welcome and novel addition to an automated buckling check, but was not able to identify panels in large, complex structures. Currently, SDC-Verifier features a superior automated tool that automatically identifies panels and can handle large, complex geometries.

7

PROBLEM STATEMENT

In comparison to other stiffened plated structures like ships and sluice gates, the lateral pressure on the plates of a topside are relatively low due to the lack of water pressure.

For ships and sluice gates, strength used to be the governing failure mechanism. In structures designed to withstand those pressures, buckling is not a major problem. A buckling check is performed, but will only rarely fail. In case of stressed skin topsides, buckling is the governing failure mechanism and is therefore normative during the design phase. This creates an optimization challenge because a buckling check only yields a boolean; the structure either buckles or not.

This can be further illustrated with a simple strength calculation, where yielding at the outer fibre of the beam is set as the ultimate strength.

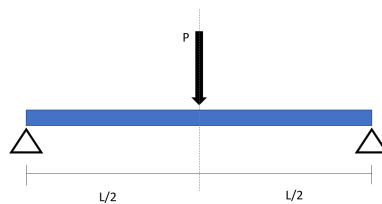


Figure 7.1: Simple beam loaded in bending

When considering [Figure 7.1](#) the maximal moment in the beam is found underneath the force and is equal to $M = \frac{PL}{4}$. Yielding of the outer fibre of a beam occurs when $M = M_y$ with $M_y = S \cdot \sigma_y$. It can be concluded that the yield moment is only dependent on the section modulus (S) and material yield strength.

A buckling check is dependent on many more variables and only returns a pass or a fail. Efficient design of a structure, with buckling as the governing failure mechanism, must therefore be done by (intelligent) trial and error. Currently, an engineer must make an initial guess for a stringer and stiffener configuration that he/she thinks to be sufficient to later verify it according to a design code. In case the check fails, the process must be iterated until sufficient resistance of the configuration is realized. Due to the large amount of variables, e.g. stiffener geometry, stiffener spacing, stringer geometry, stringer spacing, plate thickness and stresses, the optimization process generally requires many iteration steps, each step coming with a considerable calculation effort. Because of the large number of panels assembled in a topside and the geometrical complexity, this optimization process has its economical boundaries. At some point, further optimization costs more than the economical aggregate of benefits to be found.

Once automated, the economical boundaries of the optimization process are greatly reduced, as the costs of additional iteration steps are relatively low.

The aim of this research is to develop an automated method that can efficiently determine the optimal stiffener and stringer configuration. An optimum is defined as the point where the cost of execution is lowest.

In order to use this method, it is not necessary to model stiffeners and stringers in a linear elastic FEA model, which majorly simplifies the design process. Although the method is designed for stressed skin topsides, with limited adjustments it should be applicable to all stability governed, thin walled structures.

7.1. SIMPLIFICATION OF THE MODEL

A simplification in the model is realized by reducing the amount of compression members being modelled.

To justify simplifications, certain assumptions are made:

1. Stringers and stiffeners are of an order of magnitude smaller than columns and girders. For this reason, stringers and stiffeners are less stiff than columns and girders and will absorb a small amount of out-of-plane loads. This means that the loads perpendicular to the deck (due to the weight of the equipment) will be absorbed in bending by the girders. Local peaks are avoided by placing the equipment on girders.
2. The second assumption is that all shear forces will be absorbed by the plating in the structural walls and decks. Although four beams in a square ('Vierendeel truss') can absorb some lateral forces in bending, this is a relatively weak mechanism [22]. When a plate is applied to the Vierendeel truss, it is assumed that all forces will be absorbed in shear by the plating in line with the applied load. Not in bending and therefore does not load any compression member in bending, including stringers and stiffeners.

Because of these two assumptions, stringers and stiffeners are not loaded in bending and can therefore be left out of the global analysis.

7.2. EFFECT OF SIMPLIFICATIONS ON FEA

A linear elastic FEA yields stresses throughout the structure. The software calculates the deformation due to the applied forces of each individual element, but does not account for the effect that deflections have on the adjacent members. Because plasticity is defined as a limit state of the structure, it should be checked that the stresses in the members do not exceed the yield strength (yield check).

Because stringers and stiffeners are not loaded in bending, it is redundant to check them for strength, which presents an opportunity. This opens the possibility of segregating the analysis. Stress developments can be determined by a simplified model without stiffeners and stringers. This drastically simplifies the model.

With these results, buckling checks can be performed according to a design code. In this research, DNV-RP-C201 has been chosen as this is a desire of IV-Consult. The method should propose a favourable configuration of stringers and stiffeners.

An additional benefit of this approach is that it saves labour by not having to draw the stiffeners and stringers, and it enhances the flexibility during the design process.

7.3. LINEAR ELASTIC FEA

In this section, a portion of a linear elastic FEA analysis is presented and discussed. [Figure 7.2](#) shows the outer wall of the topside that will be discussed. Stiffeners and stringers are **not** modelled in this platform. The analysis starts by defining the geometry, applying boundary conditions and defining loads. The linear elastic FEA analysis will simulate stress developments throughout the model. Depending on the desired solution, contour plots with stress developments can be constructed, such as shown in [Figure 7.3](#). The figure shows a contour plot of normal stresses in Z-direction of the outer longitudinal wall of the platform shown in [Figure 7.2](#).

It is clearly visible from the contour plot that the panels are not uniformly loaded and that stress gradients throughout the outer wall of the platform exist. Near the supports of the platform, high stress peaks can be found. The unsymmetrical stress pattern is explained by the high shear stress in the plates, reducing the normal stress over their length. As a result, there are also stress distributions within individual panels (indicated by black lines). Figure 7.4 shows a close-up of the panel shaded in black indicated by Figure 7.3.

As input for the optimization method, a design stress must be determined. Due to the much stiffer compression members surrounding the panel, the largest stresses can be found at the edges of the panel. Therefore, the stress distributions found in the top and bottom of the panel, shown in Figure 7.5 are extracted from the linear elastic FEA solution. The design stress of the panel is obtained by superimposing both results and extracting the maximum for each node.

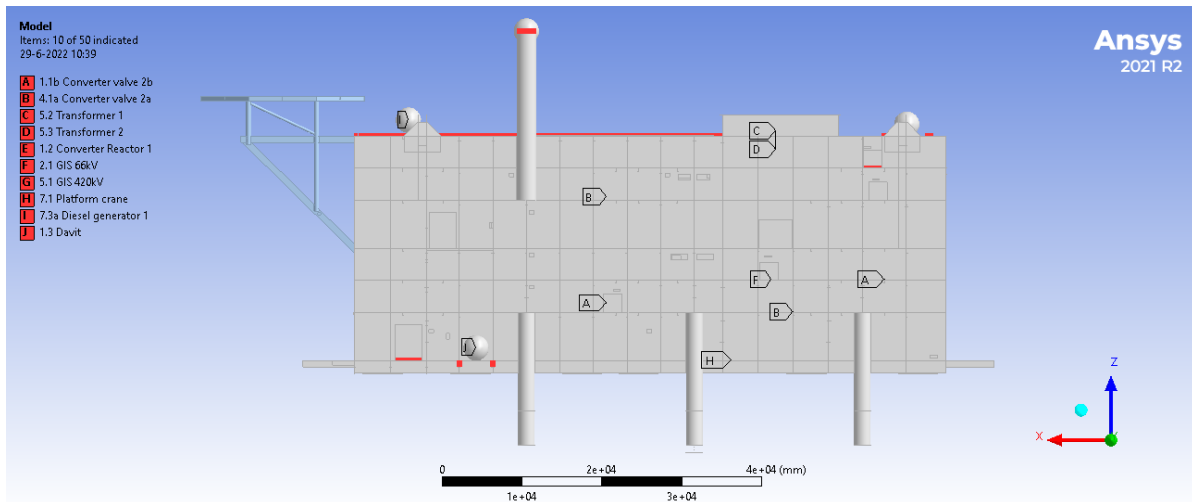


Figure 7.2: Stressed skin platform

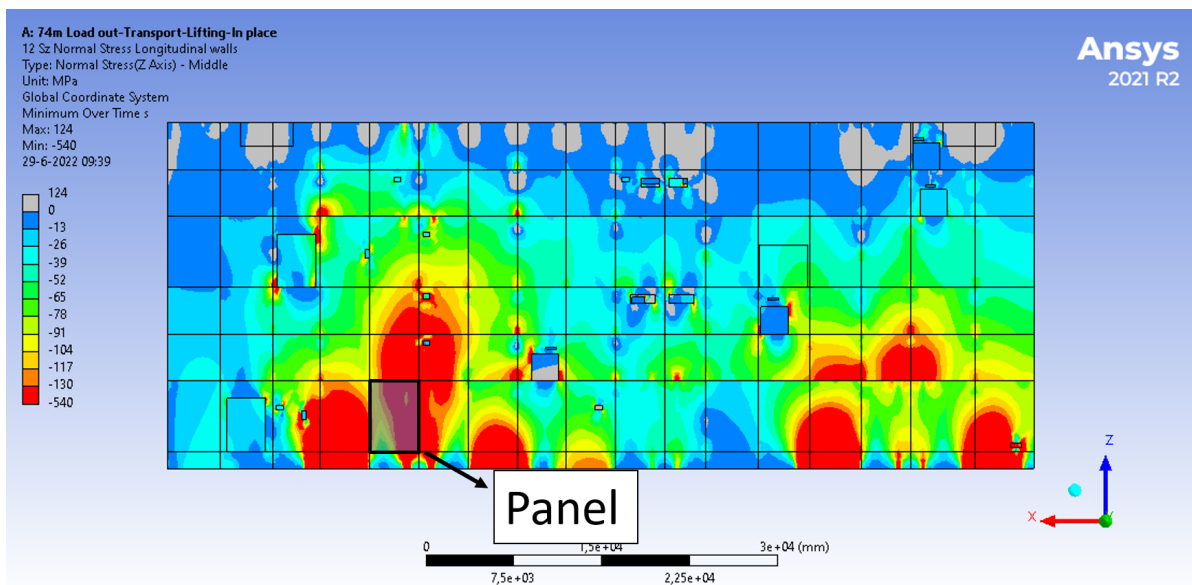


Figure 7.3: Contour plot of normal stress in z-direction (vertical) of stressed skin platform

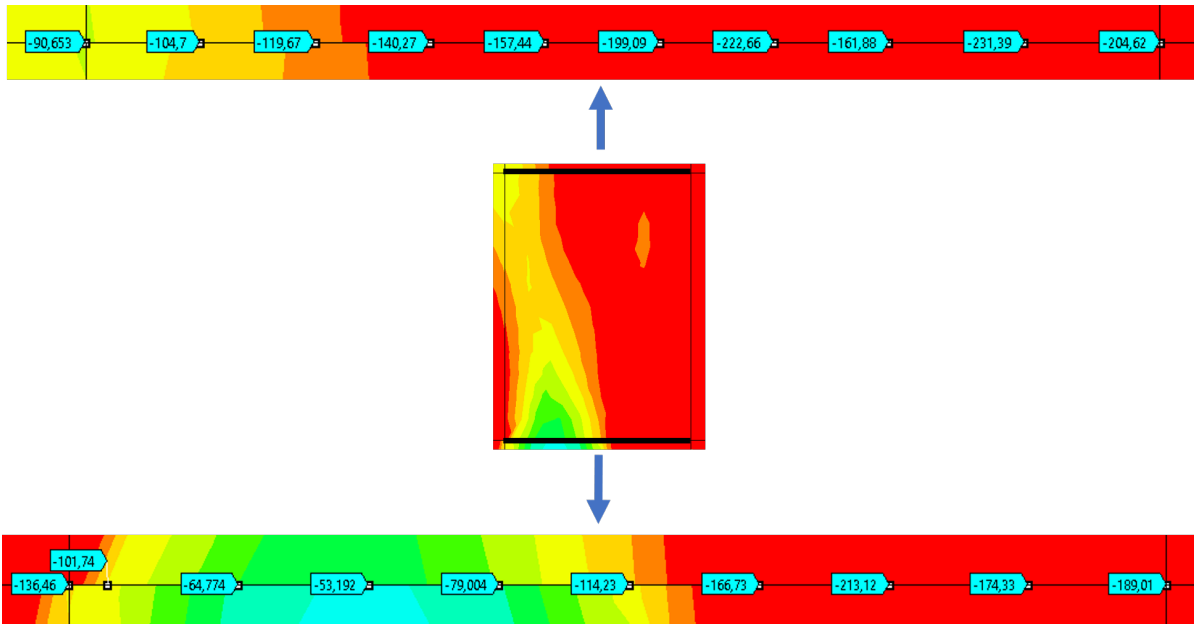


Figure 7.4: Stress per node over selected panel

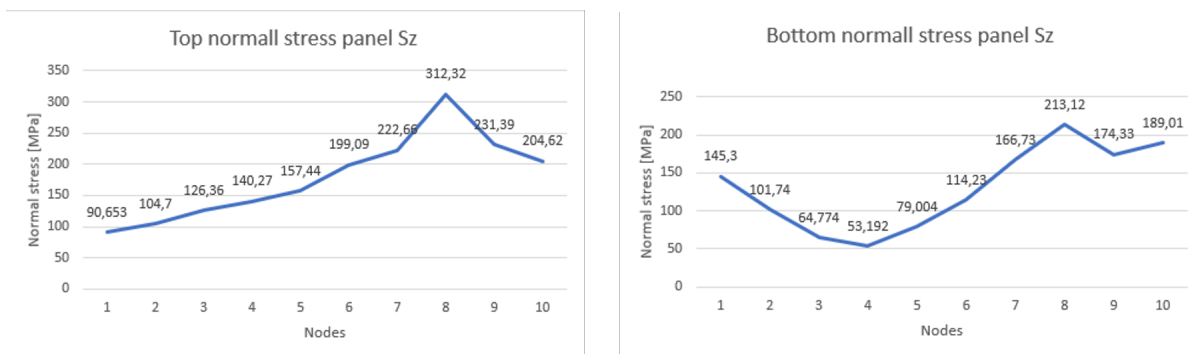


Figure 7.5: Nodal stresses Sz of close-up panel[5]

7.4. DESIGN CODES; HOW THEY DEAL WITH STRESS DISTRIBUTIONS

Stressed skin topsides can be considered slender structures with a slenderness above 1.282, which means that the plating is not fully effective. In case of a high slenderness, the panel's strength is mainly dependent on the strength of the stiffener, with the plate acting as second flange. This was earlier described in section 4.4 and, for this reason, the panel can be represented as a set of plate-stiffeners as shown in Figure 4.9.

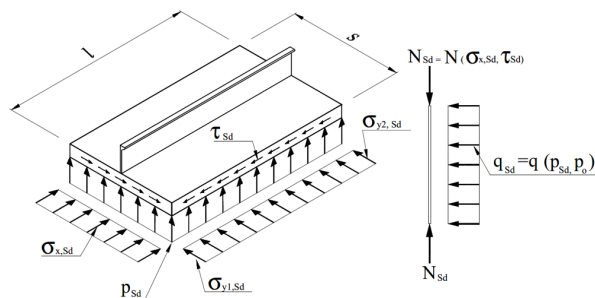


Figure 7.6: Plate stiffener with input variables[5]

A limitation of best practices such as the DNV-RP-C201 is that they only provide guidelines for linear stress distributions over plates. In reality, stress developments are non-linear and non-symmetrical, as shown in section 7.3.

Hillers [10] has identified this problem and proposed linearization and overestimation as a solution. Figure 7.7 shows a schematic panel with FEA results represented as gray circles, for each node. The yellow line represents the linearization of these results, and the blue line represents the linearization shifted to its maximum to ensure the result is conservative. Hiller's approach was constructed for unstiffened plates and was assumed to be conservative. This approach is applicable to unstiffened panels, or to transverse stresses in stiffened panels, because longitudinal reinforcement does not contribute to transverse loadings. Therefore, Hiller's approach is most suitable for obtaining the transverse normal stress.

Figure 7.6 shows a plate-stiffener with the input variables provided by DNV. In transverse direction, $\sigma_{y1,sd}$ and $\sigma_{y2,sd}$ refer to the maximum and minimum of the linear stress distribution in transverse direction. In longitudinal direction, the stresses are averaged over the width ('s') of the plate-stiffener. With this stress average and the width of the plate-stiffener, a resultant force in the longitudinal direction is constructed. The stiffener, with the effective width of the plate acting as a second flange, is then checked for buckling. More on the effective width method can be found in section 4.3.

Extracting a design shear stress is tricky in the case of stress distributions. The design code does not give guidelines for this scenario. In the event of panels subjected to large shear stress deviations caution is needed. Choosing the maximum found along a panel would lead to a very conservative design. Whenever an average is chosen, it is unsure whether this is sufficient. Those cases should therefore be evaluated by a professional, and a conservative design should be implemented. Fortunately, these circumstances are not very common and are typical of panels that are heavily loaded and therefore require extra attention anyway.

A linear elastic FEA results can result in nonlinear and unsymmetrical stress distributions over the panels. For an accurate application of the code, a way must be found to translate these stress distributions into input variables which can be applied to the code. In transverse direction, perpendicular to the direction in which the stiffeners will be applied, the approach by Hillers is most suitable. In longitudinal direction, due to the effective width method, the stresses should be averaged over the width of each plate stiffener. Shear forces should be averaged over the panel whenever a semi uniform stress pattern is present. Whenever a stress distribution is present, a conservative value should be selected manually. The amount of conservatism that should be chosen is debatable and should be decided by an engineer. Usually, panels subject to load distributions in shear are heavily loaded and should in general be handled with extra care.

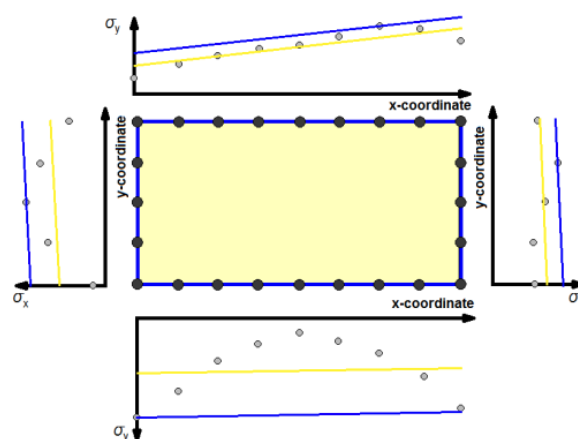


Figure 7.7: Linearization of finite element stress results [10]

7.5. PLATE-STIFFENER

Due to the slender nature of the structure, the panel's strength is mainly dependent on the strength of the stiffener with the plate acting as second flange. This was earlier described in [section 4.4](#) and, for this reason, the panel can be represented as a set of plate-stiffeners as shown in [Figure 4.9](#).

Some panels throughout the platform encounter large stress distributions, as shown in [section 7.3](#). In case of large stress distributions, the plate-stiffener model, will lead to load differences per stiffener within one panel. In theory, when the plating is not fully effective, the panel could be reinforced with gradually changing stiffener types depending on the load condition. This could lead to material savings compared to a homogeneous stiffener profile where the most heavily loaded stiffener is normative for the entire panel.

However, this would drastically complexify the construction of such large structures. The increased complexity of the construction makes such reinforcement uneconomical. For this reason, the plate-stiffener encountering the largest stress average, and therefore load, is governing.

SDC-Verifier, gives the user the option to extract minimum, average and maximum stresses over a panel. Selecting the average stress over a panel, and no data on the distribution of this average is dangerous because individual plate-stiffeners could be designed insufficiently strong. Selecting a maximum however leads to an undesirable conservative result, as stresses near boundary conditions may rise locally. Such a local peak is not representative for the entire panel. This issue is further addressed in [section 8.3](#).

7.6. CONCLUSION

Determining adequate stiffening for each individual panel in a stresses skin topside is a tedious and therefore costly process due to the large number of variables involved in a buckling check by design codes. In order to determine an optimal stiffener configuration for each panel, an automated approach is desired.

Because stiffeners and stringers are subjected to small out-of-plane loads, they can be left out of the global analysis, which leads to a major simplification of the linear elastic FEA of a structure. A linear elastic FEA results in stress distributions over panels, of which the largest stresses are found at the edges of a panel. In order to find the most critical stresses, results at both edges are superimposed and the maximum per node is extracted. These stress distributions should then be translated into input variables applicable to a design code. In perpendicular direction of the applied stiffening this is done by linearization of the results and shifting the function to the maximum found in the distribution as described by Hillers [10]. In the direction of the stiffeners, the stresses are averaged over the width of a plate-stiffener due to the effective width method.

8

BOUNDARIES

The stability of a stressed skin topside depends on a large range of variables. To achieve an automated methodology, boundaries are set, each of these will be discussed and justified.

8.1. YIELDING; OUT OF SCOPE

Yielding is a limiting criterion of the structure, but is out of scope of this research. The yielding criteria will be met throughout the structure prior to the buckling checks by applying sufficient steel plating thickness so that the yield strength of the material is not met during the initial linear elastic FEA. The final utilization of the yield limit will probably be low because buckling is the governing failure mechanism. In the majority of cases, the yield limit determines the plate thickness throughout the structure.

It can be debated whether this is an optimal choice. After all, the panel thickness is chosen conservatively in this way because the stress in the panels will later be reduced by adding additional steel in the form of stiffeners. Preventing the occurrence of buckling is more efficient by adding stiffeners than increasing the slab thickness. Therefore, there is a chance that a better optimum exists when the yield strength is not decisive for the slab thickness.

However, a boundary is drawn here for practical reasons. The linear elastic FEA results are strongly dependent on the chosen plate thickness. These results will be used as a starting point for the buckling analysis, which also strongly depends on the plate thickness. Finding an optimum would therefore mean that the linear elastic FEA analysis would have to be integrated in the optimization loop, with all its challenges.

An additional argument is found in common fabrication sizes. For large structures, common sizes are used. Sheet thicknesses are available in two millimetre increments and otherwise have to be specially manufactured. Obviously, reducing the plate thickness by two millimetres after finding a stiffener optimum will lead to instability.

8.2. DEFORMATIONS; OUT OF SCOPE

Deformation criteria are met prior to the buckling analysis. Additional stiffening in the panels has limited impact on the deformations within the structure because local high loads are placed on girders, columns or stringers. Meeting the deformation limits prior to the buckling analysis and adding stiffeners afterwards is a conservative choice, as the added steel will make the structure stiffer.

8.3. MANUAL DESIGN STRESS SELECTION

For normal stresses in the direction of the stiffener, DNV-RP-C201 allows the user to average the stress over a plate-stiffener. However, the post-processing software SDC-verifier does not allow the user to extract a stress distribution over a panel, only the minimum, maximum and average.

A conservative solution would be to choose the maximum stress over a panel. The disadvantage of this is that imposed boundary conditions such as supports, can cause local high peak stresses within a panel. In [Figure 8.1](#) such a peak can be found in the upper right panel. Designing the panel for this peak stress would lead to a far too conservative design.

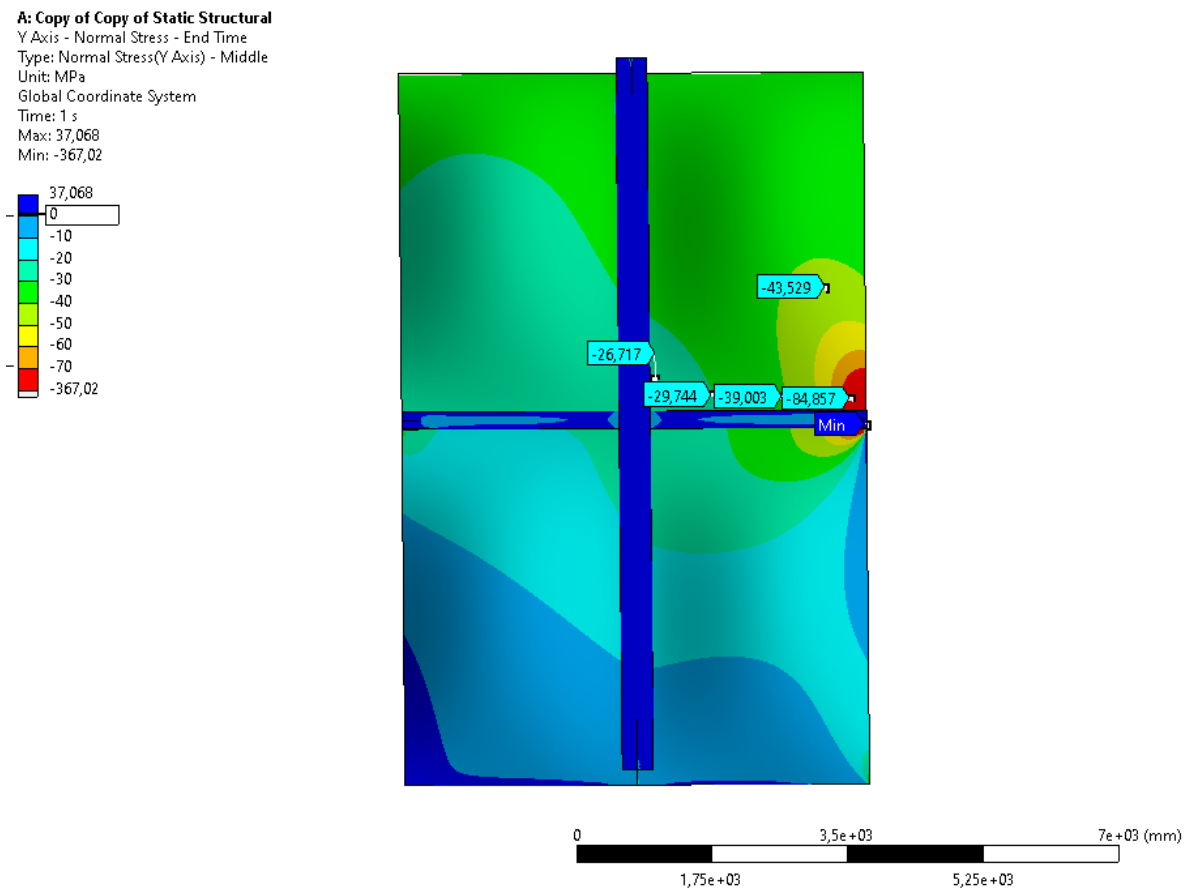


Figure 8.1: Longitudinal stresses in an unstiffened panel obtained by linear elastic FEA.

In case of a uniform stress pattern with a local peak, the average stress over the panel should be taken. Considering average stress only, not looking at the stress peak, is justified because the width of a plate stiffener does not incorporate the far right strip of the panel, as shown in [Figure 8.2](#). This far right strip, where the peak is located, acts as the second flange of the surrounding column. Because this column is far stiffer than the panel or stiffeners, elastic buckling or limited yielding in this flange is not considered a problem.

However, as described by [section 7.3](#), some panels are subjected to large stress distributions. This generally occurs near boundary conditions like supports, where the stresses are the highest. Because of these boundary conditions, it is also likely that the earlier described local peaks are present. Simply extracting the maximum stress over the panel edge is therefore not feasible.

Unfortunately, no automated solution is available to filter out local high peaks and extracting the maximum stress over a panel edge. Therefore, a reasonable maximum stress found at the edges of these panels should be manually extracted from the linear elastic FEA solution.

The consequence of this approach is that each plate-stiffener within a panel will be designed to this manually determined reasonable maximum stress. It could be debated whether this is an optimal solution, as the majority of plate-stiffeners are loaded less severely. However, optimizing a panel with varying stiffener sizes within a panel would be far too complicated to fabricate and is therefore undesirable.

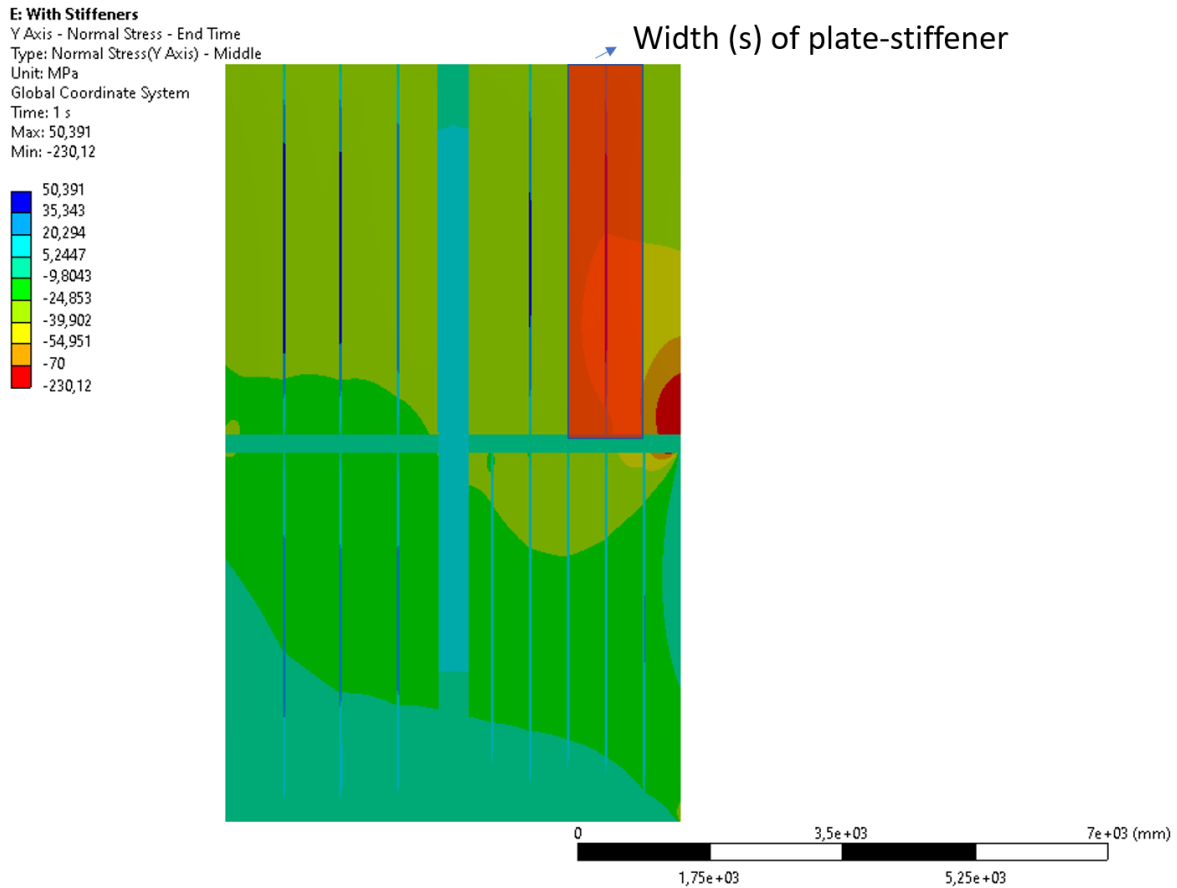


Figure 8.2: Width of plate stiffener in longitudinal stress results of stiffened panel.

Shear stresses can be averaged over a panel whenever they are subjected to a somewhat uniform stress distribution. In case of large shear stress distributions, a conservative value should be manually extracted as described in [section 7.4](#).

[section 7.4](#) describes how normal stresses in the direction of the stiffener can be averaged over a plate-stiffeners width. This means that the selection of a reasonable maximum is a conservative approach but the alternative of extracting the entire stress distribution manually is not feasible.

Panels which need manual selection of the design stress are often heavily loaded and therefore, in most cases, need extensive stiffening. Defining the maximum stress as design stress in the event of extensively stiffened panels yields a marginally conservative solution, as the width of these plate-stiffeners over which the stresses may be averaged, is limited.

8.4. CONTINUOUS OR DISCONTINUOUS STIFFENERS AND REDUCED BUCKLING LENGTH

As explained in [section 4.8](#), a lateral pressure on panels causes a beneficial effect with respect to the buckling strength of the panel due to a reduced buckling length. However, lateral pressures imposed by wind do generally not exceed 0.0021 MPa and are therefore considered relatively small. For this reason, the reduced buckling length effect due to lateral pressure is limited. This effect is even further reduced by the large length of the panels. Although the lateral pressure on the panels is small, it cannot be neglected.

The great advantage of continuous stiffeners over discontinuous stiffeners is the possibility of making use of the reduced buckling length effect applies to continuous stiffeners only, reason why this type of stiffener is

preferred over discontinuous stiffeners. When the reduced buckling length effect is limited, the added value of continuous stiffeners is also reduced. The big advantage of not using continuous stiffeners is that the webs and flanges do not have to be welded to the transverse reinforcement. This welding is a time-consuming process that has to be done manually.

Stressed skin topsides endure large stress deviations from panel to panel throughout the structure. In order to reduce the overall weight and welding cost of the structure, the minimal amount of stiffeners is found by the optimization method. However, this leads to an inhomogeneous solution with a different number and type of stiffeners from panel to panel. Therefore, continuous stiffener conditions according to DNV-RP-C201 can not be assumed. Although the stiffener web and flange connection to transverse reinforcement impose some torsional stiffness, it is not possible to determine to what extent. This is another motivation for choosing discontinuous stiffeners because nonsymmetrical stiffener configurations for continuous stiffeners are not covered by any design code.

For the case study of stressed skin offshore topside with limited lateral pressure, discontinuous stiffeners will be chosen.

8.5. TYPES OF STIFFENERS

The chosen types of stiffeners are of great influence on the result of the optimization. After determining the minimum amount of stiffeners needed in a panel, the algorithm lowers the cross-sectional area of the stiffener in order to maximize the utility ratio of the plate-stiffeners. It is for the engineer to decide what stiffeners may be used by the method. Larger stiffeners may lead to less welding length, but will lead to a heavier structure. The engineer should therefore make a consideration based on the welding costs at the production location and installation method that might come with a weight limit. Steel cost are of influence, but are considered less important than welding length (section 9.3).

The more stiffener types are included in the method, the more accurately the utility ratio limit can be reached. A higher utilization of the utility ratio means more efficient use of the applied steel and therefore a material and weight saving. A weight limit of the structure could be a motivation to include a large set of stiffener types. However, this comes at the cost of complexity during the construction of the structure. It is up to the engineers to decide how many stiffener types they want to incorporate in the analysis.

8.6. STRINGER PLACEMENT

Adding a stringer to a panel has two effects; it carries transverse stresses and it halves the length of a panel. Halving a panel's length decreases the buckling length of the stiffeners, which improves the buckling strength. Determining the option with the smallest weld length is therefore not straightforward. In some cases, with substantial transverse stresses, it is more economical in terms of weld length to apply a stringer to the panel because this reduces the number of stiffeners needed. A simplification is therefore introduced here: the application of a stringer requires an additional operation in which a transverse beam is welded to a panel. It is assumed that this extra operation requires more labour than adding extra longitudinal stiffeners on a panel. The reason for this is that longitudinal stiffeners have to be installed anyway, and the installation of additional stiffeners in the same operation does not outweigh the additional work required for the installation of a transverse beam. A panel will therefore only be fitted with a stringer when the maximum amount of stiffeners set for a panel does not yield sufficient buckling resistance.

8.7. OVERLAPPING LOAD CASES

The topsides endure various load cases during their lifetime. Every load case leads to a different stress pattern throughout the topside. For this result, the optimization algorithm will generate a stiffener pattern for each panel. Because all load cases must fulfil the buckling requirement, the most governing configuration is chosen from all the load cases. This is possible because the developed methodology considers no interaction effect between the panels.

To do so, every configuration is indexed based on two categories: number of stiffeners and stiffener cross-sectional area. To extract the most governing stiffener configuration, first the number of stiffeners is com-

pared between all load cases. The load cases with the largest number of stiffeners are filtered. In case multiple load cases yield the same number of stiffeners, the load case with stiffeners that have the largest cross-sectional area will be selected as the final configuration.

Because the most critical panel is chosen from all load cases, this leads to a conservative design.

8.8. CONCLUSION

In order to achieve an automated stiffener placement methodology, boundaries to the method have been set, including their justification. Yielding and deformations limits are met prior to stiffener placement analysis and are out of scope of the developed method.

Panels are either subjected to a homogeneous or a distributed stress pattern. Due to local high loads near panel boundaries, a representative maximum stress can not be automatically extracted with SDC-verifier. Therefore, for panels subjected to a homogeneous stress pattern the average stress can be extracted, while for panels with a distributed stress pattern the maximum stress must be manually extracted from the linear elastic FEA solution.

Due to small lateral pressures endured by the panels, discontinuous stiffeners are the most economical option. The number and type of stiffeners used in the methodology will be decided by the engineer. Including many stiffener cross-sections lead to a lighter structure due to higher utility ration, but this comes at the cost of a more complex structure.

Stringers shall only be placed when the ascribed maximum number of stiffeners provides insufficient buckling resistance. A final stiffener configuration is realized by overlapping results of every load case and selecting the most governing configuration.

9

OPTIMIZATION METHOD

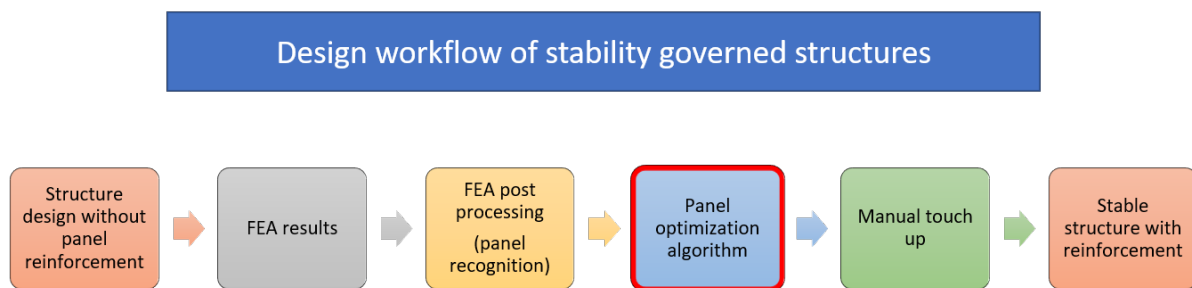


Figure 9.1: Proposed design workflow of stability governed structures

The stability analysis of a large structure is divided in several stages, as shown in [Figure 9.1](#). Linear elastic FEA, FEA post-processing, panel optimization and manual touch up of design. The use of linear elastic FEA and the FEA post-processing tool has been justified in [section 5.2](#) and [section 5.4](#) respectively.

The further focus of this research lies in the development and validation of an efficient and accurate method for determining optimal stiffener configurations for each panel throughout the structure. The method is developed for stressed skin topsides, but would be applicable to all stability governed structures with little adjustments.

A stiffened panel is referred to as a steel plate, bounded by stiffer members (columns, girders or perpendicular panels) that is reinforced by stringers and stiffeners. [Figure 9.2](#) pictures the modelled stiffened panel and its boundaries.

9.1. SIMPLIFICATIONS

The stiffened panel denoted in [Figure 9.2](#) can be schematically presented as show in [Figure 9.3](#). Based on the literature study conducted in , [chapter 5](#) and [chapter 6](#), and the research boundaries set in [chapter 8](#), some assumptions can be made in order to simplify the problem. All simplifications will be stated and later briefly discussed and justified:

1. Panel stresses are known
2. Stiffeners and stringers are left out of the FEA
3. Stability is governing
4. A design code is the preferred buckling analysis method

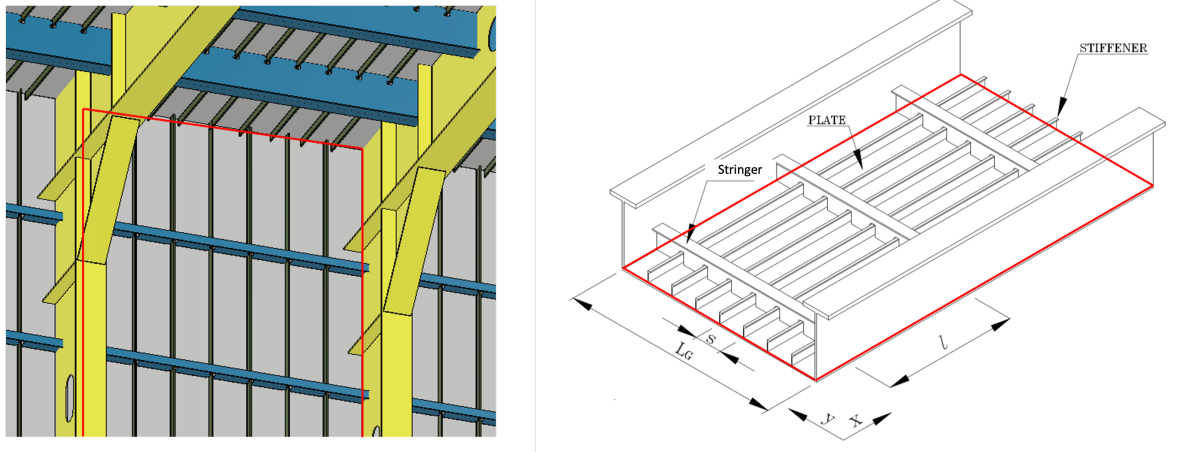


Figure 9.2: Modelled stiffened panel with respect to structure. Boundaries denoted in red.

5. Stringers, columns and girders are welded T-sections, stiffeners are bulb- or L-steels

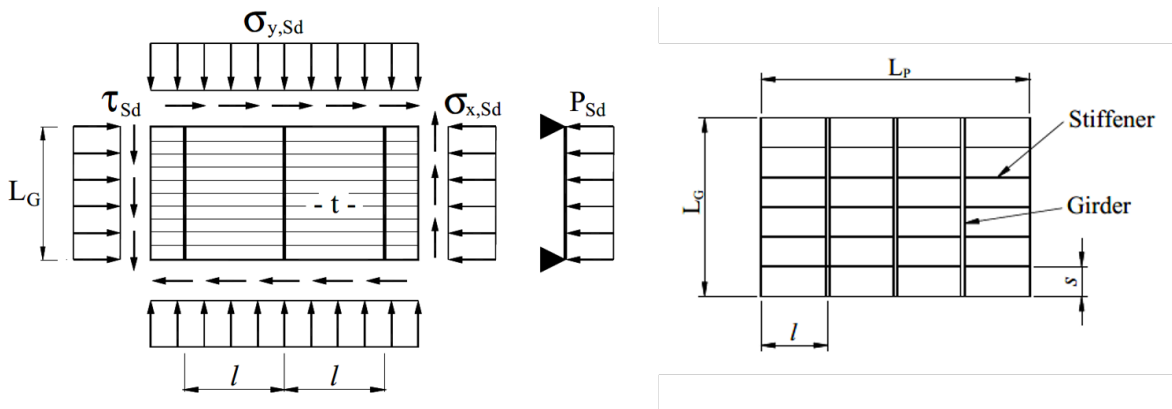


Figure 9.3: Schematic representation of modelled stiffened panel

1) PANEL STRESSES ARE KNOWN

As discussed in section 3.1, load cases are determined by the equipment location, architecture, size, transportation method and environmental conditions. Each load case causes different stress patterns throughout the topside. Linear elastic FEA is a well-developed field of engineering to determine component stresses with reliable results (section 5.2). The plate thickness, column- and girder- size is of influence on the stress developments throughout the structure and must be set prior to the linear elastic FEA analysis.

In order to obtain longitudinal-, transverse- and shear stresses over each individual panel, the FEA post-processing software of SDC-Verifier is used. Currently, it is not yet possible to retrieve stress distributions across the edges of a panel from the software, although this feature is expected in the future, The currently available software allows for the extraction of minima, average or maxima only.

As mentioned in section 8.3, near boundary conditions imposed on a structure, stresses in a panel can locally reach high values. Therefore, for panels subjected to uniform load distributions, the average stress over a panel is set as design stress. In case of stress distributions, the reasonable maximum over a panel should be manually extracted from the linear elastic FEA solution.

Once SDC-Verifier or different software allows to retrieve stress distributions at the edges of a panel, a method of refinement has been developed, which is covered in section chapter 10.

2) STIFFENERS AND STRINGERS CAN BE LEFT OUT OF THE FEA MODEL

In [section 7.1](#) it was discussed that stiffeners and stringers can be left out of the global analysis of the structure. Leaving the stiffeners and stringers out of the FEA model will have limited influence on the shear- and axial-stress results in the transverse direction of the stiffener. Stresses in the direction of the stiffener will yield higher results because the cross-sectional area of the stiffener is not present in the model.

Not including the area of the stiffeners in the linear elastic FEA will lead to a stress overestimation in the direction of the stiffeners. After all, the force is distributed over a smaller surface area. [Figure 9.4](#) shows the portion of stiffener area with respect to the plate area for a number of different HP200x10 stiffeners and plate thicknesses. This graph illustrates how in some cases the stiffener surface area is not negligible, and can lead to a considerable overestimation of the stresses in a panel. For this reason, the stresses found by the finite element method are corrected for the stiffener surface area in the direction of the stiffeners. The relationship between pressure and surface area is linear, and the stress is therefore easily corrected proportionally to the plate and stiffener surface area. Validation according to a linear elastic FEA can be found in [section 13.2](#).

$$\sigma_{Stiffeners} = \sigma_{withoutStiffeners} \frac{A_{plate}}{A_{plate} + A_{stiffeners}} \quad (9.1)$$

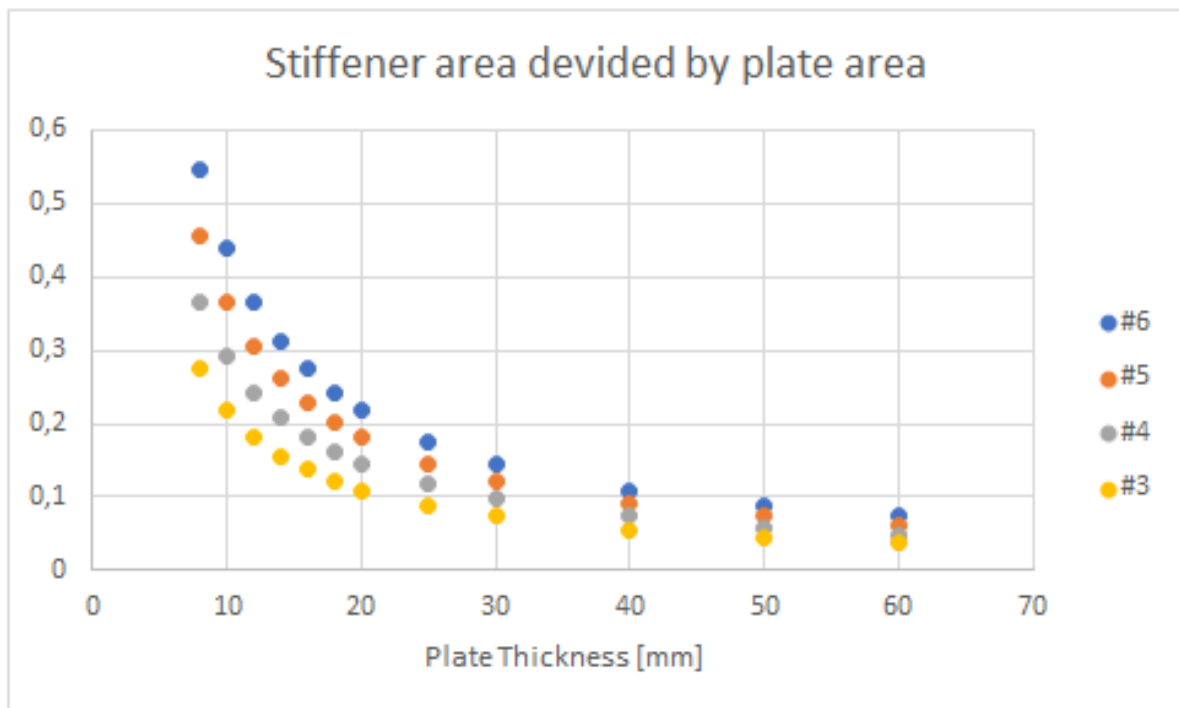


Figure 9.4: Stiffener area divided by plate area

3) STABILITY IS GOVERNING

Local loads induced by equipment on the decks will be placed on the girders so that the stiffeners and stringers will not endure large lateral loads. The panels in the walls are subjected to wind induced lateral loads, but these are assumed to be small (<0.0021MPa). Therefore, stiffeners and stringers will not fail by strength. All other structural members in structure are checked for yielding prior to the buckling analysis. Therefore, stability is considered the governing failure mechanism.

4) DESIGN CODES ARE MOST SUITED FOR BUCKLING ANALYSIS

As discussed in [section 6.2](#), design codes set accurate buckling limits that are widely recognized throughout the industry. They are best suited for buckling analyses as they are the most straight forward approach, computationally inexpensive and account for fabrication imperfections and residual welding stresses. In this research, DNV-RP-C201 is being used as this code is used within IV-Consults workflow.

5) STRINGERS, COLUMNS AND GIRDERS ARE WELDED T-SECTIONS, STIFFENERS ARE BULB- OR L-BEAMS.

Stringers, columns and girders are larger cross-sections that can not be rolled and are therefore welded T shapes. These beams form into an H-beam with the plating acting as a second flange.

Bulb steels or L-beams are the second least expensive stiffener type available. Flat strips are the least expensive type, but have limited torsional stiffness. Therefore, bulb steels or L-beams are chosen to ensure some torsional stiffness at the expense of the limited extra cost. As discussed in [section 4.5](#) all sections should be of at least category three to be able to fully utilize their elastic limit.

9.2. INPUTS VARIABLES

In order to perform a buckling analysis by a design code, all parameters presented in [Table 9.1](#) are needed, as well as the stiffener and girder location. As has been described in [section 6.3](#), when all these parameters are known, various software packages such as SDC Verifier, Dlubal and FEMDS are available to perform an automated buckling check.

However, [chapter 7](#) described that it is desirable to develop a method where optimal stiffener and stringer locations can be determined. Benefits of not modelling stringers and stiffeners is that it simplifies FEA models, saves dedicated drawing labour, increases flexibility of the design and allows for execution cost optimization. Whenever different stiffener cross-sections want to be considered, a set of stiffener types should be provided.

Table 9.1: Input parameters model

Panel	Loading	Material properties	Set of stiffeners and stringers
Length	Max longitudinal stress	Young's modulus	Flange width
Width	Min longitudinal stress	Poisson's ratio	Flange thickness
Thickness	Max transverse stress	Yield stress	Web height
Edge boundary conditions	Min transverse stress		Web thickness
	Shear stress		
	Lateral pressure		

9.3. OPTIMIZATION CRITERIA

Optimization is a relative term and depends on the context. In the case of stressed skin topsides, an optimal construction is found when the cost of execution is minimal. Cost of execution depends mainly on weight and the weld volume needed for construction.

[Equation 3.1](#) shows that the minimal throat thickness of a weld is dependent on the material yield strength and the thickness of the web. Although a throat thickness of 3 millimetres is possible in theory, these require additional care. Therefore, the more practical minimum of 4 millimetres is set. Up to a web thickness of 10 millimetres, this results in the minimum throat thickness of 4 millimetres. The largest stiffener in this case study has a web thickness of 10 millimetres, which makes the weld volume only dependent on weld length. Therefore, an optimum is found based on weld length.

In the Netherlands, labour accounts for approximately 90% of the total welding cost [16]. Welding costs vary greatly from country to country, as labour costs vary. Welding volume is proportional to cost; the user can therefore apply their own cost figure per unit volume.

9.4. OPTIMIZATION METHOD

A method has been developed to efficiently find a stiffener optimum, of which the hierarchy is visually presented in [Figure 9.6](#). The method uses the various checks performed in the DNV-RP-C201 code. For every load case the structure is subjected to, the method will provide a stiffener configuration. Later, the results of every load case will be overlapped and the most critical panel configuration of every load case will be selected, as was described in [section 8.7](#). The method has been automated by the programming language Python.

The method starts by retrieving a panel's geometry, axial-, transverse- and shear-stresses. subsequent to that the following checks are performed:

1. The plating between the stiffeners is checked for buckling due to shear- and transverse-stresses. If no stiffeners are present the plating is also checked for axial stresses during the first iteration
2. The resistance of the panel to shear is checked
3. The buckling strength of the stiffener is checked
4. The torsional buckling strength of the stiffener is checked
5. The interaction resistance of the stiffeners is checked

Whenever a check fails, an additional stiffener will be added and the analysis will be rerun until all checks have been passed or until the maximum number of stiffeners, as defined by the user, has been reached.

When the maximum amount of stiffeners, as defined by the user, does not yield a sufficient utility ratio for all checks, a stringer is applied in the middle of the panel and the check is rerun with half the length of the panel.

Whenever all checks yield a sufficient utility ratio, the number of stiffeners and stiffener type is logged as a feasible solution. Subsequently, the panel check is rerun with a smaller stiffener cross-section until a check fails.

Although all solutions with sufficient utility ratios are logged, the one with the smallest stiffener cross-sectional area is selected as the optimal solution with minimal steel volume and weld length.

Figure 9.6 represents a flow chart of the algorithm. Feedback loops in the algorithm prevent unnecessary calculations. For each load case of a panel it returns at set of possible stiffener configurations. The optimal configuration is met by minimizing the cost of execution and therefore weld length (see section 9.3).

9.5. MANUAL TOUCH UP

The panel optimization method can yield two types of results. The first is a list of panel ID's with its optimal stiffener and stringer configuration. The second is a list of panel ID's with all stiffener checks passed. Due to load differences from panel to panel, optimizing for each individual panel leads to an inhomogeneous result. This could result in a complex and therefore costly topside to manufacture. An engineer might want a more conservative result in order to favour a homogeneous design.

The optimization method results in the form of a text file, which is hard and therefore time-consuming for human interpretation. An application to manually adjust the generated results is therefore proposed and a mock-up is presented in Figure 9.5. It should be noted that only a few stiffener results are drawn into the mock-up for explanatory purposes. A real life result would show stiffener suggestions for almost all panels.

The application follows the following steps:

1. List of panels and stresses from SDC-Verifier are loaded
2. The panel optimization algorithm is run
3. The results of the panel optimization algorithm are loaded
4. The application reads the location and geometry of the panels and draws a scaled representation of the wall (Figure 9.5 leftside)
5. The optimal stiffener and stringer configurations are drawn into the panels with dashed lines and colours that denote the stiffener type
6. the user can click on a panel to review all other possible configurations according to the design code
7. The user can either confirm the suggested configuration or adjust it to improve homogeneity along the wall. Whenever confirmed, the lines turn solid

- When the configuration is as desired, it can be downloaded as a text file with a corresponding image of the wall

Development of this interpretation tool is out of scope of this research, as it adds no academic value. However, when homogenization of the results are desired, this method significantly speeds up the process.

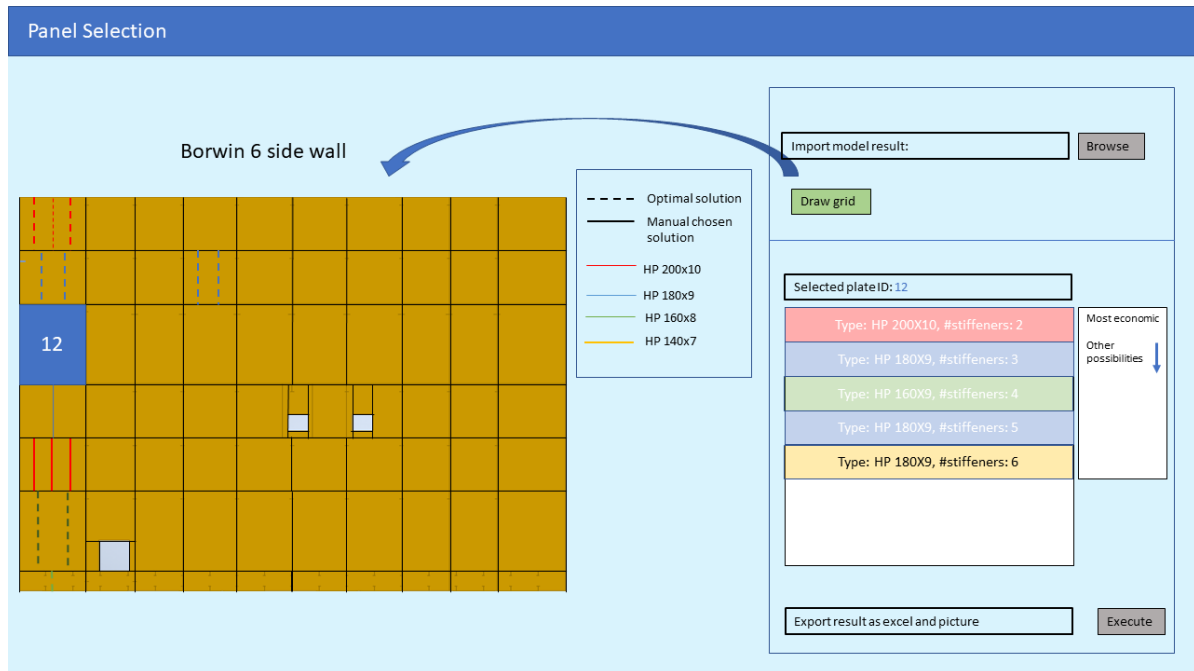


Figure 9.5: Flowchart of panel design method

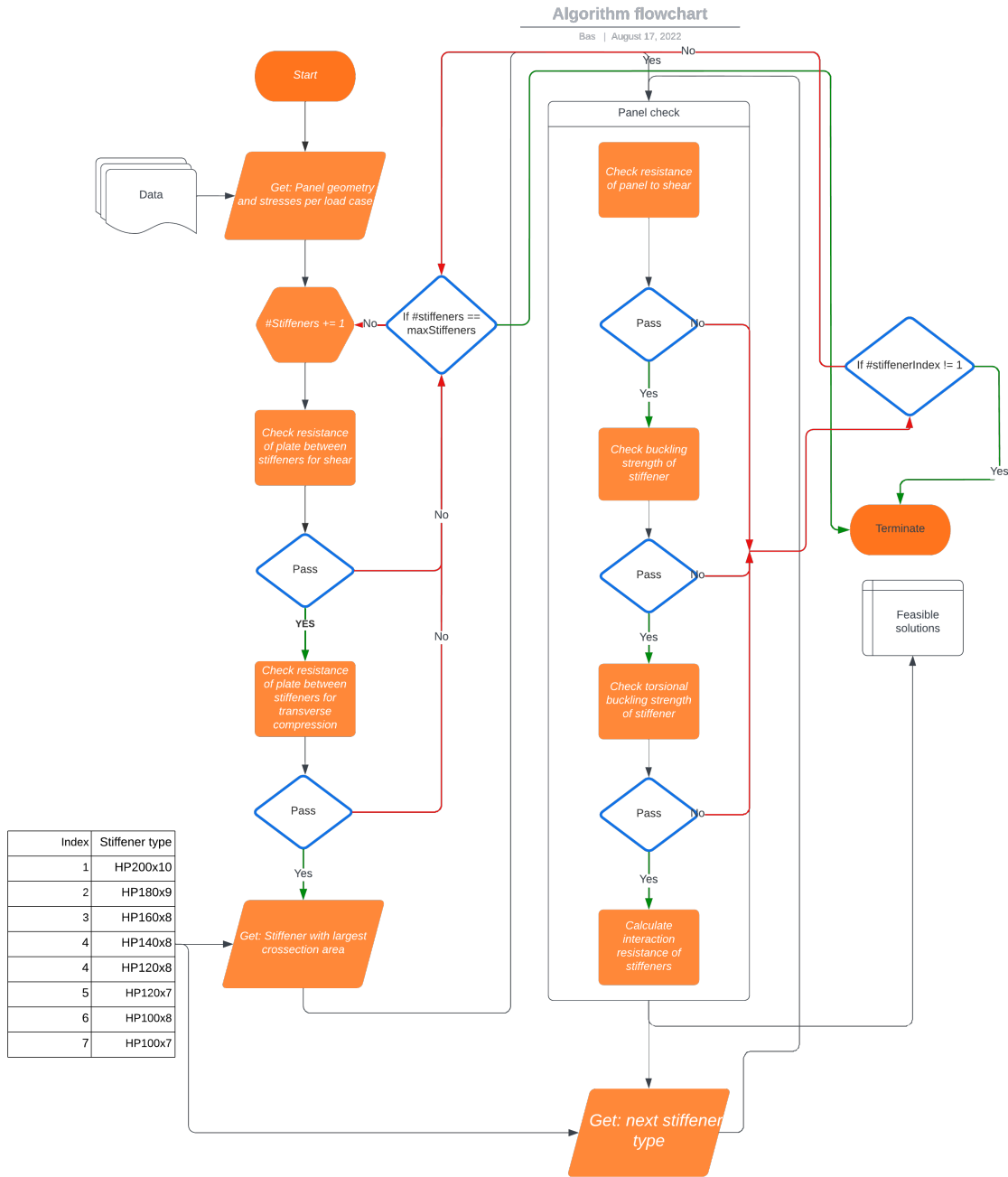


Figure 9.6: Flowchart of panel design method

10

FUTURE REFINEMENTS

In case of stress distributions, automated stress recognition for each panel does not yield a correct design stress as mentioned in [section 8.3](#). Manual evaluation of linear elastic FEA results is still necessary, causing a high workload and increasing the chances of human error.

SDC-Verifier has mentioned the desire to add a new feature; the functionality of extracting stress distributions over a panel. In this case, a refinement is possible. With the stress distributions over the panel edges known, automated selection of the desired node stresses yield automated and specific results which can be used as input for the developed method.

In this chapter, an additional method will be described that allows the stiffener optimization method to be fully automated.

10.1. AUTOMATED DESIGN STRESS EXTRACTION

To describe the proposed method, it is now assumed that the software automatically extracts stresses from the finite element model at any node within a panel. This includes stresses at the edges. For uniformly loaded panels, this method is not necessary but also has no downside. With regard to the analysis of an entire topside, it does have the advantage that no distinction needs to be made between uniform and distributed stress distributions across panels. The automated design stress extraction will be stated for longitudinal-, transverse- and shear stresses.

10.1.1. NORMAL STRESSES

Normal stresses are largest at the boundaries of a panel. Out of conservatism, the stresses at the edges of the panel are therefore extracted as illustrated in [Figure 7.4](#), in longitudinal direction. The same process for transverse normal stresses is applicable.

LONGITUDINAL NORMAL STRESSES

[Figure 11.2](#) shows a schematic of two stress distributions over two plate-stiffeners. It can be seen from the figure that the plate-stiffeners encounter a load distribution over their widths. In the direction of the stiffeners, the stresses may be averaged over their widths according to DNV-RP-C201. Whenever this stress distribution is known, an average stress can be constructed for every plate-stiffener and the largest average is chosen as design stress. When implemented in the optimization method, this results in the reevaluation of the design stress whenever the number of stiffeners in the analysis is changed. When automated, this is a fairly simple adjustment. This refinement improves the reasonable maximum selection as described in [section 8.3](#), because it yields a better representation of reality, leading to a less conservative result.

TRANSVERSE STRESSES

In case the stress distribution over the edge of a panel in the perpendicular direction of the stiffeners is known, the shifted linearization method by Hillers [10], discussed in [section 7.4](#), can be applied. This leads to a less

conservative result with respect to selecting a reasonable maximum out of the stress distribution, as described in [section 8.3](#)

SHEAR STRESSES

Shear forces are chosen to be averaged over the entire panel, because choosing a maximum over the panel yields far too conservative results. In cases of high shear stress distributions throughout a panel this could lead to a not conservative result. Therefore, panels with high shear stress distributions can not be checked automatically. They should be carefully checked by a professional and conservatively engineered.

10.2. LOCAL BUCKLING DUE TO HIGH STRESS DISTRIBUTIONS

The effective width method suggests that the average stress over a plate-stiffener may be taken. However, it is unclear whether there is a limit to the slenderness of a plate at which extensive local buckling due to a high stress distribution causes a degrading effect on the strength of the plate-stiffener.

Whenever the refinement method is adopted in the optimization method, less conservatively chosen design stresses will be used. Therefore, it is crucial to know whether the high stress distributions will cause a degrading effect. This is investigated on the basis of non-linear plastic FEA experiments in [chapter 11](#).

11

PLATE STIFFENER BUCKLING DUE TO DISTRIBUTED LOADS

chapter 7 identifies that some stiffened panels are loaded by stress distributions. For unstiffened plates, DNV-RP-C201 provides rules for applying linear stress distributions. section 7.5 states an approach by Hillers [10] to simplify non-symmetrical and non-linear distributions to that of a linear distribution that can be used in best practices.

Due to the application of the effective width method, a stiffened panel can be simplified to that of a plate-stiffener, schematically drawn in Figure 11.1 b. In case of a distributed load over a plate-stiffener, in longitudinal direction, the effective width method allows the average stress across the plate-stiffener to be used for evaluation. In extreme cases however, this could lead to peak stresses over the plate stiffener much higher than the average buckling stress limit. For very slender plates, it is expected that a peak load could lead to local buckling of the plate between the stiffeners which has a degrading effect on the plate-stiffeners strength. It is unclear whether the described failure mechanism applies to the researched structure.

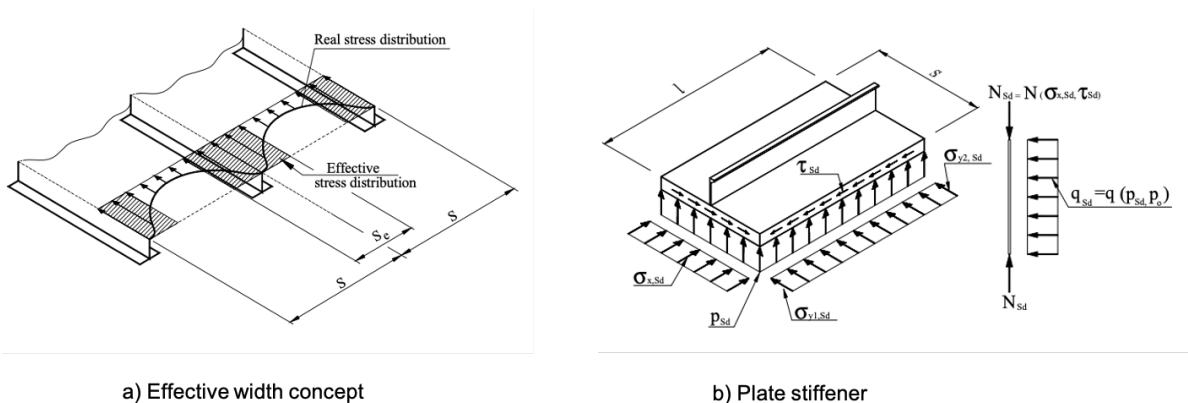


Figure 11.1: Schematic drawings of an effective width model (left) and a plate-stiffener (right)

Therefore, this research has studied whether buckling of the plate between the stiffeners causes an extensive degrading effect on the ultimate resistance of a plate-stiffener. Various non-linear plastic FEA experiments have been conducted on plate-stiffeners with various plate thicknesses to answer the following sub research question: 'Is the effective width method applicable in the case of extreme stress variations over plate-stiffeners?'

11.1. GENERAL OUTLINE OF EXPERIMENT

Several experiments by non-linear plastic FEA have been performed in order to determine the resistance of plate-stiffeners. Buckling of stiffened panels depend on many variables, as stated in Table 9.1. Due to the

lack of computing power and time, it will not be possible to investigate all possible geometries and loads. Therefore, the experiment will be performed on one plate-stiffener, shown in [Figure 11.4](#). The geometries of the plate-stiffener can be found in [Table 11.1](#).

Whether a degrading effect on the plate-stiffener will occur, in case of high local stress peaks, is believed to be dependent on the slenderness ($\bar{\lambda}_p = \frac{s}{t} \sqrt{\frac{f_y}{E}}$) of the plating. For this reason, the plate thickness in the experiment ranges from 8-30 mm. The lower limit of 8 mm has been chosen because thinner plates are likely to undergo unwanted extensive elastic deformations.

Buckling of unstiffened plates is induced by shear-, longitudinal- and transverse stresses. For slender stiffened panels, and therefore plate-stiffeners, the axial stress is averaged over the width of the plate-stiffener and a resultant force is constructed. The plate-stiffener is then checked for buckling as a beam, with the effective plate width acting as a second flange.

To avoid unnecessary complications, The experiment excludes shear- and transverse stresses, because it is assumed that the stiffener and its equivalent effective plate width are bearing the axial stresses of the plate between the stiffeners. For this reason, the plating between the stiffener is only checked to not exceed a threshold in shear- and transverse- stresses by DNV-RP-C201 [5] section 7.4 of which the formulas are presented by [Equation 11.1](#) to [Equation 11.3](#). To check whether the effective width method is applicable in case of high stress distributions over plate stiffeners, it is therefore sufficient to apply a uni-axial axial stress.

$$\tau_{Sd} \leq \tau_{Rd} = \frac{f_y}{\sqrt{3} \cdot \gamma_M} \quad (11.1)$$

$$\sigma_{y,Sd} \leq k_{sp} \cdot \sigma_{y,Rd} \quad (11.2)$$

$$k_{sp} = \sqrt{1.0 - 3 \cdot \left(\frac{\tau_{Sd}}{f_y} \right)^2} \quad (11.3)$$

11.2. STRESS DISTRIBUTIONS

It is desirable to perform experiments for situations found in the real world which may lead to failure of the plate-stiffener. The stress distribution obtained from the simulation presented in [section 7.3](#) is used to determine common stress distributions. [Figure 11.2](#) shows two panels drawn schematically on a stress distribution chart. Inside the panel, two plate-stiffeners have been drawn, with the plates indicated in shaded blue and the stiffeners denoted by a red line. From the figure it can be seen that panel 1 is subjected to a stress distribution in the form of a negative parabola, panel 2,3 and 4 are linear by approximation.

During the experiment, four types of functions will be considered:

1. Linear
2. sinusoidal
3. Positive parabola
4. Negative parabola

The portion of the total load that is variable will vary between 25% and 100%. The normalized functions that the plate-stiffeners will be subjected to is visualized in [Figure 11.3](#)

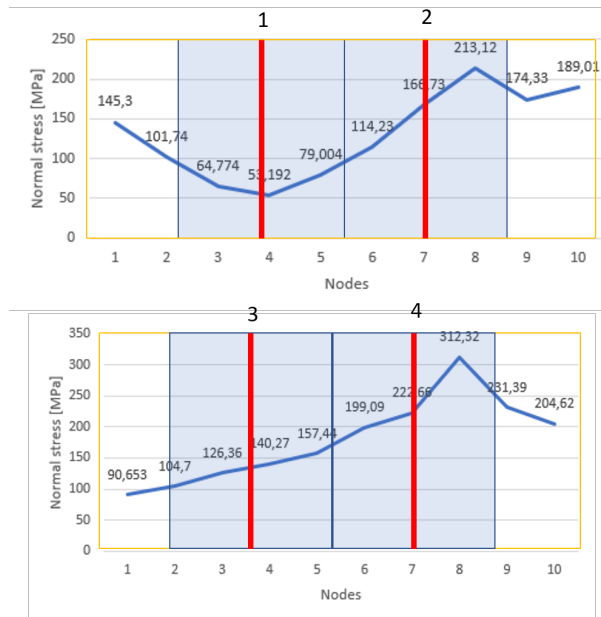


Figure 11.2: Schematic drawing of two plate stiffeners inside a panel with a stress distribution

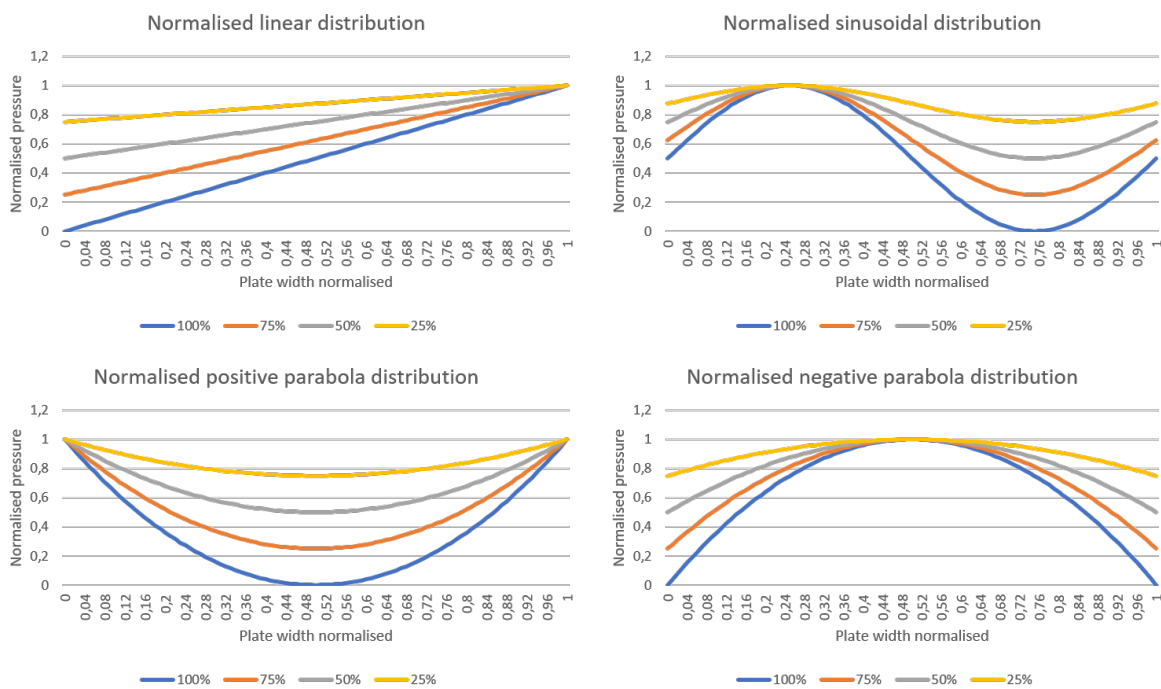


Figure 11.3: Normalized functions that the plate-stiffener will be subjected to

11.3. EXPERIMENTAL STEPS

Due to the varying plate thickness, a total of 14 analysis of the following plate thicknesses [mm] have been performed: 8,9,10,11,12,13,14,15,16,17,18,21,24,30.

Due to the large quantity of analysis, this process was automated with Ansys scripting. The relevant script can be found in [Appendix I](#). Each of the steps performed in the experiment are stated and briefly discussed:

1) GEOMETRY OF PLATE-STIFFENERS IS LOADED INTO THE FEA SOFTWARE

A 3D CAD-model of the plate-stiffener shown in [Figure 11.4](#) is loaded into Ansys finite element software. The exact geometries of the plate stiffener can be found in [Table 11.1](#).

Table 11.1: Plate-stiffener geometry used in experiment

Geometry	mm
Flange thickness	8
Flange width	30
Web height	145
Web thickness	8
Plate thickness	8-30
Plate width	833
Plate/stiffener length	3000



Figure 11.4: Plate-stiffener used in experiment

2) BOUNDARY CONDITIONS ARE APPLIED TO THE PLATE-STIFFENER

The plate stiffener is assumed to be simply supported, also known as sniped. Due to the little lateral pressure the plates endure, the reduced buckling length is limited, and simply supported can be assumed. More on this can be found in [section 4.8](#).

[Figure 11.5](#) shows the plate geometry loaded into Ansys with the boundary conditions applied. The position of the plate edge denoted by B is restricted in Z- and Y-direction, whereas plate face A is only restricted in Y-direction. The sides of the plate-stiffener denoted by C are positionally restricted in X-direction and rotationally restricted in Z-direction in order to simulate a plate stiffener as part of a larger panel.

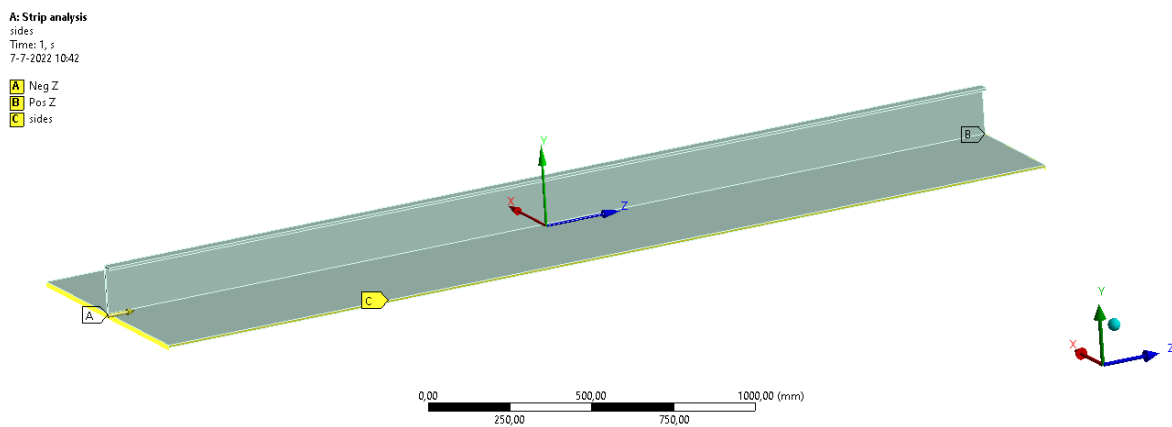


Figure 11.5: Plate-stiffener loaded into Ansys

3) EIGENVALUE ANALYSIS

In order to achieve a representative resistance of the plate stiffener, an initial deformation due to manufacturing imperfections must be applied. In order to do so, the buckling shape of the stiffener is found by an Eigenvalue analysis. [section 4.2](#) describes that, whenever the plate length is larger than its width ($a > b$), the plating tends to buckle in squares. Therefore, for this plate-stiffener, three half sinusoidal waves in the plating will lead to the minimum buckling resistance. The first 5 eigenvalues are retrieved and the one with three half sine waves is selected as initial deformation shape. The corresponding result of the eigenvalue analysis can be found by [Figure 11.6](#).

To account for residual stress in the plate-stiffener, additional structural imperfections may be added according to the commentary of EN1993-1-5 [15]. This is set to be the minimum of length/400 or width/200. On top of this, the geometrical imperfection should be added, which for the plate-stiffener used in this experiment accounts to length/300. For this plate-stiffener, this leads to a global imperfection of 17.5 mm, applied according to the shape obtained from the Eigenvalue buckling analysis.

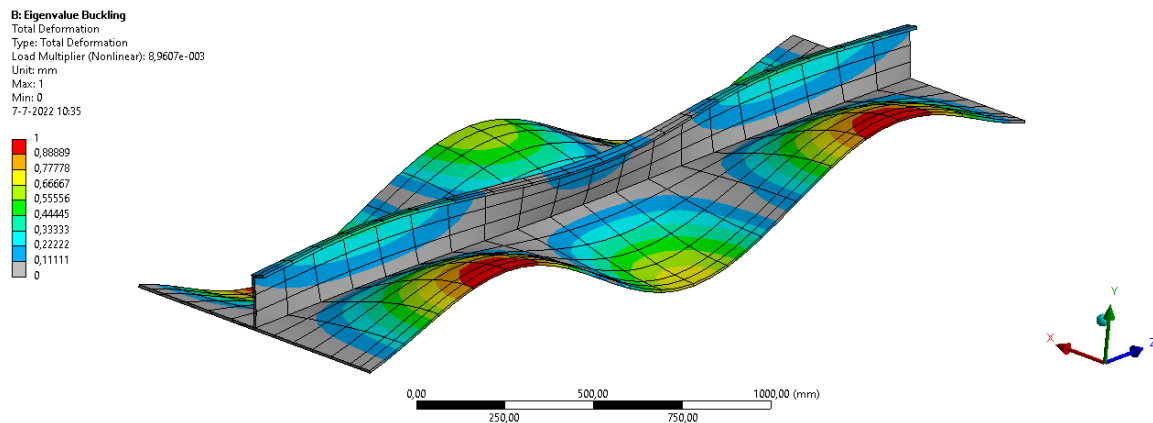


Figure 11.6: Eigenvalue buckling result

4) A LOAD DISTRIBUTION IS APPLIED IN THE FORM OF PRESSURE

Over the plate face indicated with 'A' in [Figure 11.5](#), a load is applied in the positive Z-direction. The load is applied in the form of varying pressure according to the functions shown in [Figure 11.3](#).

5) ULTIMATE RESISTANCE IS CALCULATED

The ultimate resistance of the plate-stiffener is calculated by non-linear plastic FEA. The load distribution is increased step by step until the plate-stiffener loses stability. Loss of stability is indicated by non-converging calculations. After loss of stability, the ultimate resistance, total deformation, equivalent stress, equivalent total strain and equivalent plastic strain is logged.

11.4. RESULTS OF PLATE-STIFFENER EXPERIMENT

[Figure 11.7](#) shows the result obtained by the non-linear plastic FEA. The legend indicates: 100%, 75%, 50%, 25% and a uniform distribution. On the vertical axis, the graph on the left side shows the obtained results normalized with respect to the yield stress, the graph on the right side shows the total force applied to the plate-stiffener, both at loss of stability. The horizontal axis denotes the plate slenderness ($\bar{\lambda}_p = \frac{s}{t} \sqrt{\frac{E_y}{E}}$), which changes because of varying plate thicknesses.

In case of a linear distribution, '100%' indicates a load distribution over the course of the plate-stiffener from 0 (at the negative X edge) to 1 (at the positive X edge). This means that the load applied at the positive X edge is twice the average resistance at which the plate-stiffener loses stability. [Figure 11.3](#) visualizes the pressure distributions the plate-stiffeners were subjected to in the experiment. [Figure 11.8](#) shows a graph of the peak stress on the outer edge of the plate-stiffener during the experiment with linear distributions. It can be seen from the graph that in almost all cases the peak stresses are: 1.25, 1.5, 1.75 and 2 times the uniform stress at

the stability limit.

The experiment has been conducted for all distributions shown in Figure 11.3. The sinusoidal-, positive parabola- and negative parabola- distribution results are shown in Figure 11.9, Figure 11.11 and Figure 11.12 respectively. The peak stresses encountered over the plate stiffener are represented in Figure 11.10, Figure 11.12 and Figure 11.14 respectively. From these graphs, it can be concluded that the peak stress over a plate stiffener at the stability limit may exceed the average resistance stress significantly.

It can be seen from the results that, independent of the slenderness, there is almost no deviation in resistance due to stress distributions, even in extreme cases with high stresses at the edge. This result is to be expected due to the effective width principle. Only in particular cases, high load distributions, lead to premature failure. More on that in section 11.5

LINEAR DISTRIBUTION

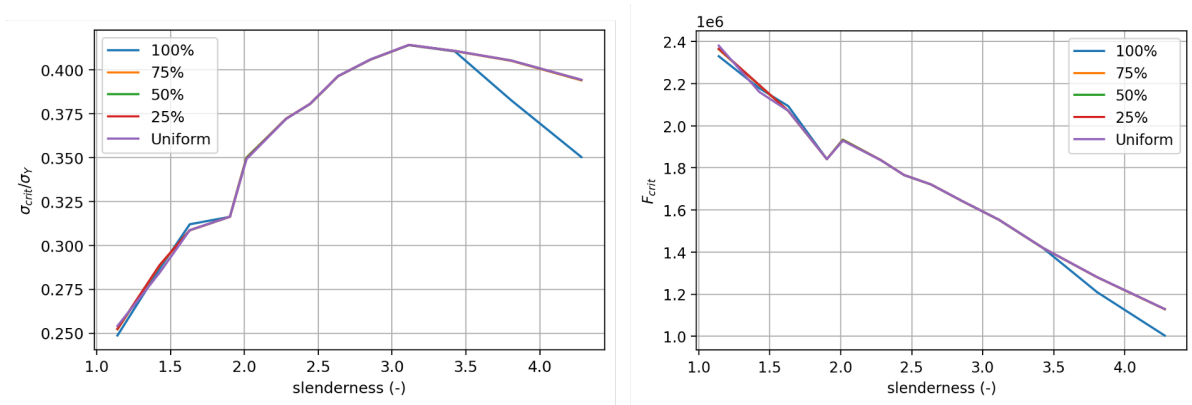


Figure 11.7: Resistance to linear load distribution in average stress (left) and total force (right).

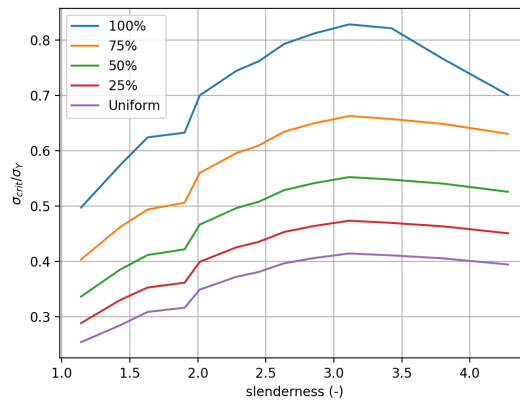


Figure 11.8: Peak stresses at positive edge for a linear distribution

SINUSOIDAL DISTRIBUTION

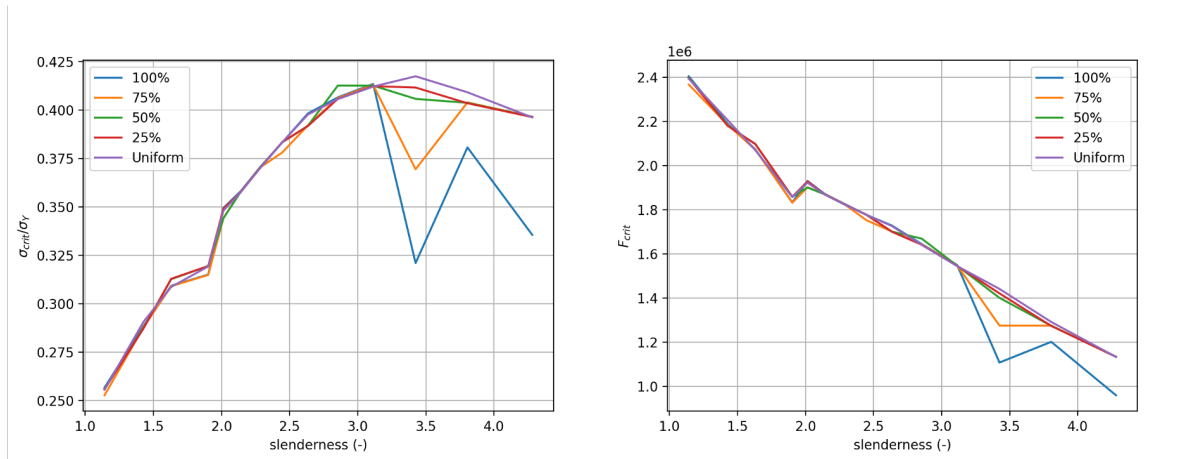


Figure 11.9: Resistance to Sinusoidal load distribution in average stress (left) and total force (right).

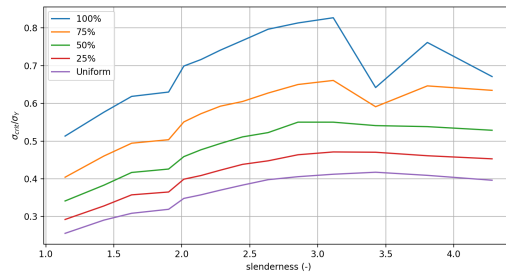


Figure 11.10: Peak stresses in sinusoidal distribution

POSITIVE PARABOLA DISTRIBUTION

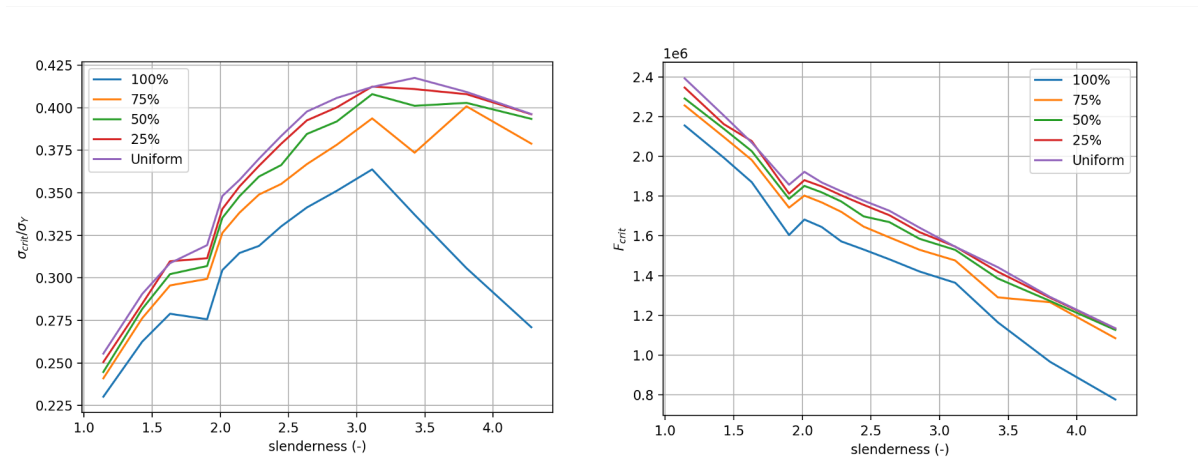


Figure 11.11: Resistance to Positive parabola load distribution in average stress (left) and total force (right).

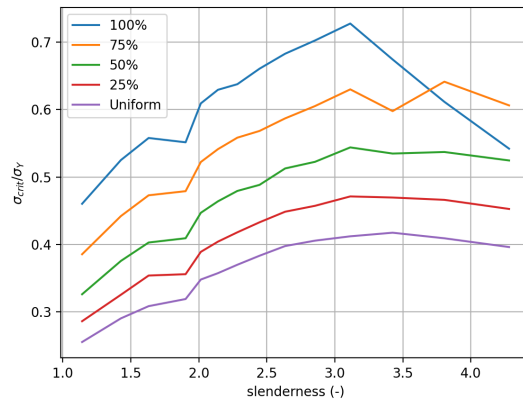


Figure 11.12: Peak stresses in positive parabolic load distribution

NEGATIVE PARABOLA DISTRIBUTION

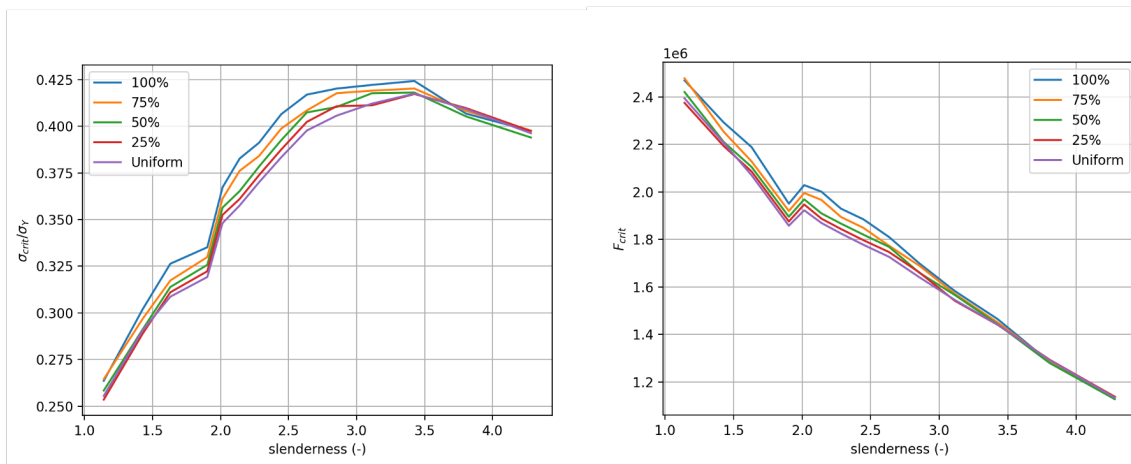


Figure 11.13: Resistance to negative parabolic load distribution in average stress (left) and total force (right).

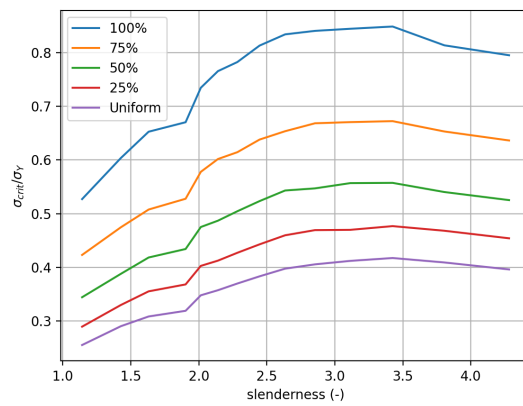


Figure 11.14: Peak stresses in positive parabolic load distribution

11.5. CONCLUSION

The experiment results show how stress distributions have a degrading effect on the resistance of plate-stiffeners when plate slenderness exceeds 3. In case of the negative parabola distribution over the plate-stiffener, no significant influence of the distribution can be determined. This supports the hypothesis that the effective width method, which averages stress over a plate stiffener, is applicable up to a certain limit. From the linear, sinusoidal and negative parabola analysis it can be seen from [Figure 11.7](#), [Figure 11.9](#) and [Figure 11.11](#) that the degrading effect disappears when 50% or more of the distribution is uniform (see [Figure 11.3](#)).

This analysis shows that for a plate slenderness between 3 and 4.28, the stress over the plate-stiffener should be averaged only when the peak of the distribution does not exceed twice the minimum.

12

LOAD REDISTRIBUTION IN CONTINUOUS PLATE STRUCTURE

Although SDC-Verifier is a powerful tool for post-processing FEA results, it allows the user to extract the average, minimum or maximum stress over a plate field only.

In order to safely apply the stiffener optimization algorithm, the effect of stress distributions on the ultimate resistance of a panel must be identified. The hypothesis question came up whether there is a redistributive effect among plate stiffeners. In order to study this, several non-linear plastic FEA experiments have been conducted to answer the question: 'Are stresses redistributed between plate-stiffeners inside a panel?'

For now, it has been assumed that slender stiffened panels can be cut up in so called plate-stiffeners. This simplification can be made because plate-stiffeners are checked based upon an equivalent force acting on them. This brings up the question whether there exists an interaction effect between the plate-stiffeners when one part of the plate stiffeners is loaded more than the rest, as in the case of a distributed load. For this reason, non-linear plastic FEA experiments have been conducted on a panel consisting of 5 plate stiffeners as described in the previous chapter. The geometry of the panel can be found in [Table 12.1](#).

Because the panel is simply supported on all sides, the redistributive effect, if present, will be the largest when the load peaks in the middle of the panel. The plate stiffener in the centre of the panel is after all the furthest away from a boundary condition. For this reason, a positive parabola has been chosen as load distribution shape. [Figure 12.1](#) shows a drawing of the panel used in the experiment, [Figure 12.2](#) shows that same panel in an upright view with the stress distribution it is subjected to drawn schematically.

In the experiments presented in [chapter 11](#), the resistance of a single plate stiffener has been studied. From these experiments, it can be concluded that it is correct to average stresses over the course of a stress distribution.

The non-linear analysis of this panel is far more computational expensive than a single plate stiffener. This is why the experiment is performed for the most extreme distribution only.

12.1. RESULT

For a plate thickness between 8-30 mm the resistance of the panel has been evaluated by non-linear plastic FEA. The results have been obtained by reading the force on the edge of the panel at the last converged solution obtained by Ansys, for a variety of plate thicknesses and therefore slenderness. [Figure 12.3](#) represents the average force reaction obtained from the non-linear plastic FEA analysis in blue, the resistance of a single plate-stiffener obtained in the previous experiment in green and the applied maximum stress to the middle plate-stiffener in orange.

Table 12.1: Panel geometry used in experiment

Geometry	[mm]
Flange thickness	8
Flange width	30
Web height	145
Web thickness	8
Plate thickness	8-30
panel width	5000
Plate/stiffener length	3000

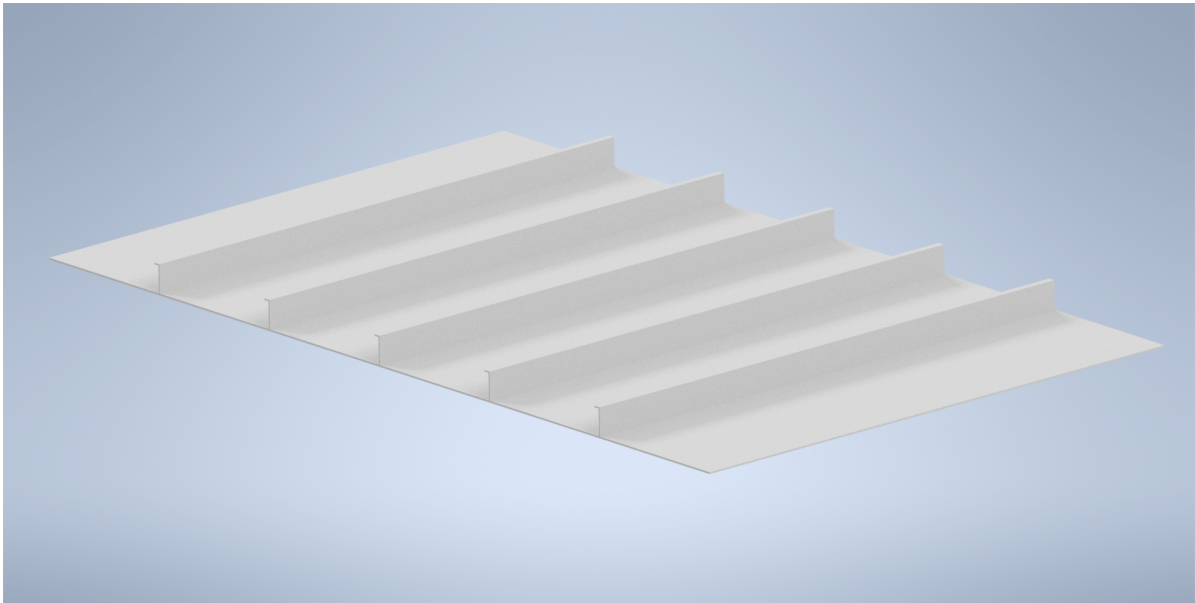


Figure 12.1: Drawing of panel used in experiment

The shape of the applied parabola, makes it possible to arrive at the maximum stress that the plate has encountered. The average lies at 0.66 which results in a maximum stress of ≈ 1.5 times the average. The results show that the pressure applied to the middle plate-stiffener is way higher than the resistance of a single plate-stiffener. Although the theoretical limit of the middle stiffener is reached however, the panel remained stable. The only explanation for this is that the middle plate-stiffener buckles elastically and that the surrounding plate stiffeners are able to take on the load partially.

12.2. CONCLUSION

From the experiment, it can be concluded that there is a redistributive effect between the plate-stiffeners inside a panel. Because only one geometry has been studied, it is not possible to say something generic about the interaction effect.

The redistribution effect enhances the ultimate resistance of the panel, so it can be concluded that the plate-stiffener approach is safe, even with large stress distributions over the panel. The result indicates that, in case of longitudinal stress distributions, it is conservative to select the design stress according to the largest stress average over a plate-stiffener. When taking the redistribution effect into account, less conservative configurations should be possible. More research is needed in order to investigate this interaction effect.

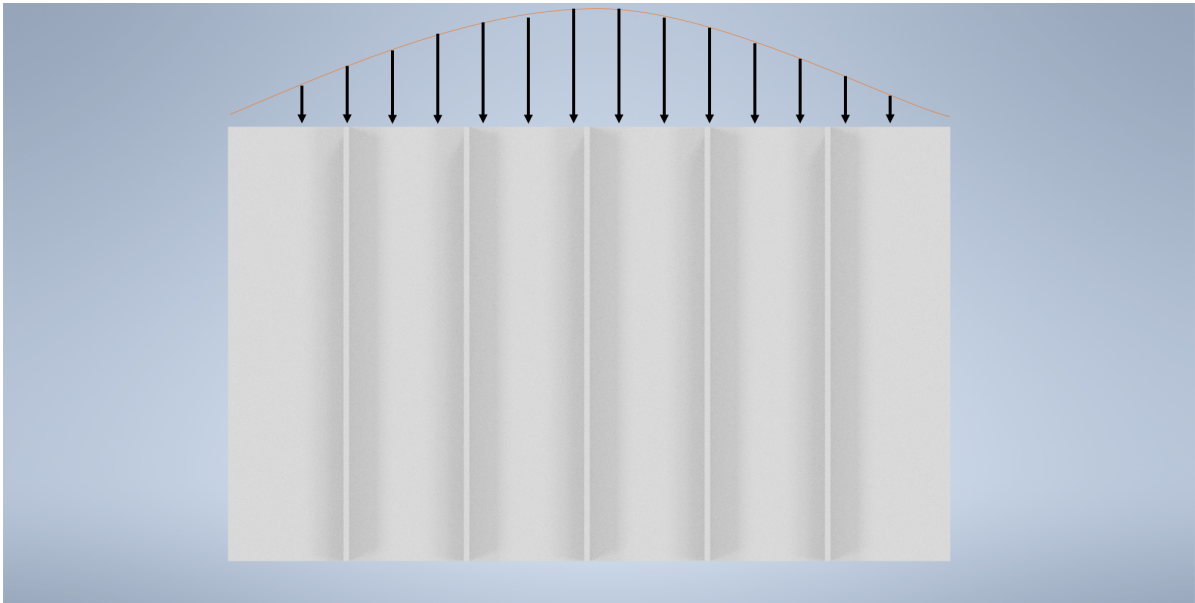


Figure 12.2: upright view of panel with stress distribution schematically drawn

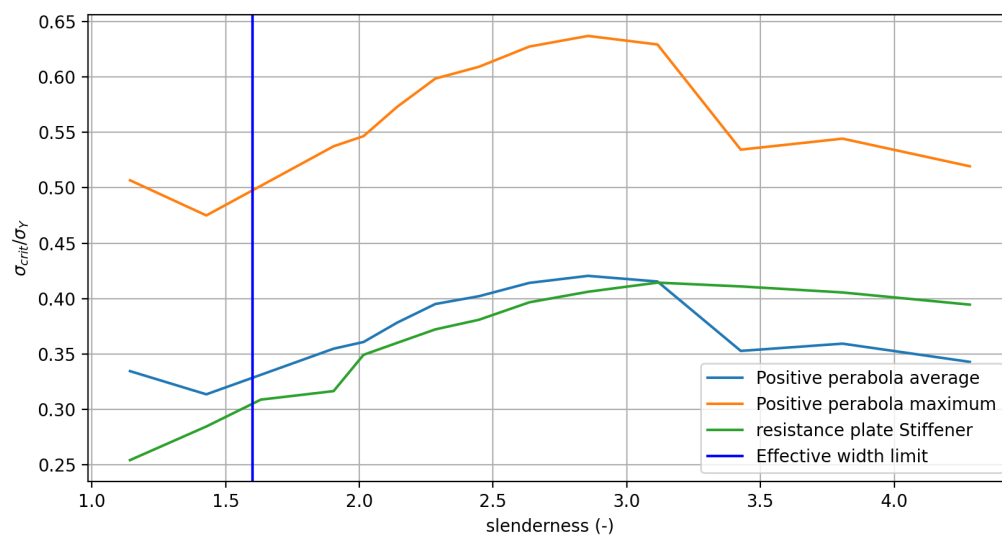


Figure 12.3: Maximum resistance of panel for the middle plate-stiffener, the panel on average and by DNV

13

VALIDATION AND VERIFICATION

13.1. CORRECT APPLICATION OF DNV-RP-C201

To validate the correct application of DNV-RP-C201 a variety of plates with load combinations has been checked against hand calculations done according to the design code. [Table 13.1](#) shows a list of the plate geometries and load cases that have been verified this way. The panels geometries are chosen so that the model is tested for a diverse selection of possibilities. A 6 x 5 meter panel was chosen for two different panel thicknesses and three different load cases, each with a different dominant direction. In case the model does not find sufficient stiffening with the provided stiffeners, it applies a stringer so that the panel length is cut in half and the process is repeated. Therefore, the last three geometries have been chosen as half the length of the panel.

The verification calculations of plate one and seven can be found in [Appendix G](#). Each interim calculation of the automated model has been compared with the hand calculation and did not differ more than 2%. The two percent difference is explained by rounding errors when calculating the distance from the neutral axis of the effective section to the working point of the axial force (z^*)[\[5\]](#).

The error is small enough to conclude that the design code was applied correctly.

Table 13.1: Verification plates

#Plate	Length [m]	Width [m]	Plate thickness [m]	Sx [MPa]	Sy [MPa]	Sxy [MPa]	Psd [MPa]
1	6	5	0.008	20	20	50	0.0021
2	6	5	0.008	20	50	20	0.0021
3	6	5	0.008	50	20	20	0.0021
4	6	5	0.016	20	20	20	0.0021
5	6	5	0.016	20	20	20	0.0021
6	6	5	0.016	20	20	20	0.0021
7	3	5	0.008	20	20	50	0.0021
8	3	5	0.008	20	50	20	0.0021
9	3	5	0.008	50	20	20	0.0021

13.2. VALIDATION OF STRESS CORRECTION

In [section 9.1](#) a simplification is justified for not implementing stiffeners in the optimization algorithm. Instead of modelling them, the plate stiffener stresses are artificially lowered according to the stiffener area applied to the plating.

In order to validate the applied stress correction, a linear elastic FEA experiment has been performed on panel one indicated by [Table 13.1](#). The experiment has been performed with and without stiffeners. [Figure 13.1](#) and [Figure 13.2](#) represent a panel with and without stiffeners, respectively. It is assumed that the panel is

uni-axially loaded in the direction of the stiffeners, with a distributed load of 12MN. It can be seen from the simulation that the stress without stiffeners under the same load is approximately 50% higher without stiffeners; just as predicted and validating the applied stress correction.

Table 13.2: Simulation data

F [MN]	$\sigma_{stiffeners}[MPa]$	$\sigma_{withoutStiffeners}[MPa]$	$A_{plate}[m^2]$	$A_{stiffeners}[m^2]$	$A_{stiffeners}/A_{plate}$
12	20	30	0.04	0.02112	0.528

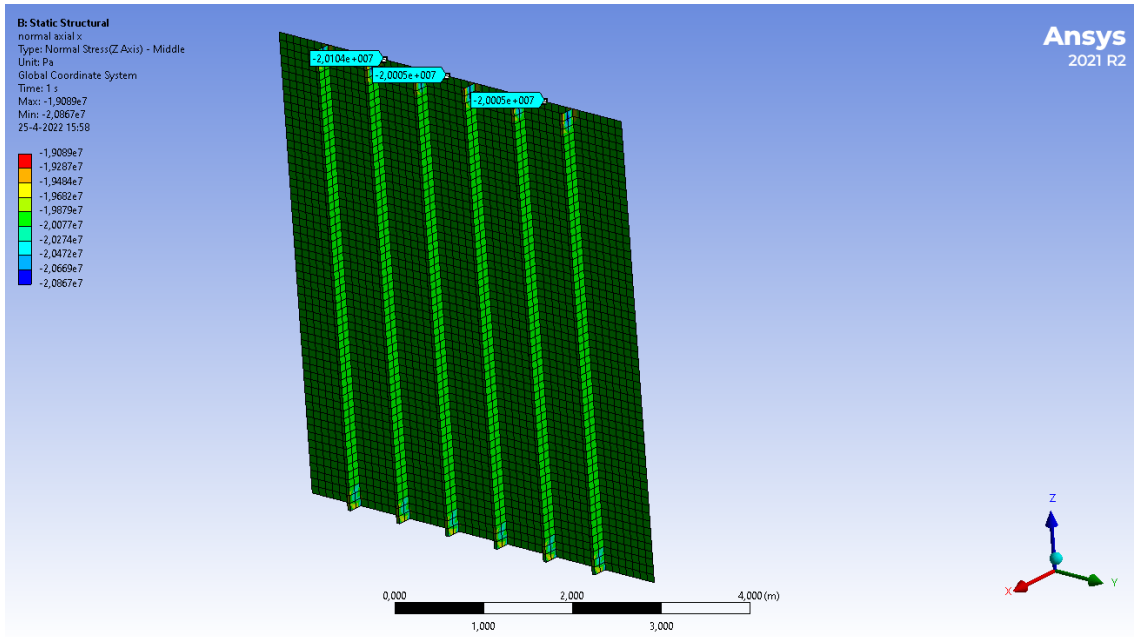


Figure 13.1: 20MPa stiffener direction axial stress simulation with ANSYS. Stiffeners modeled

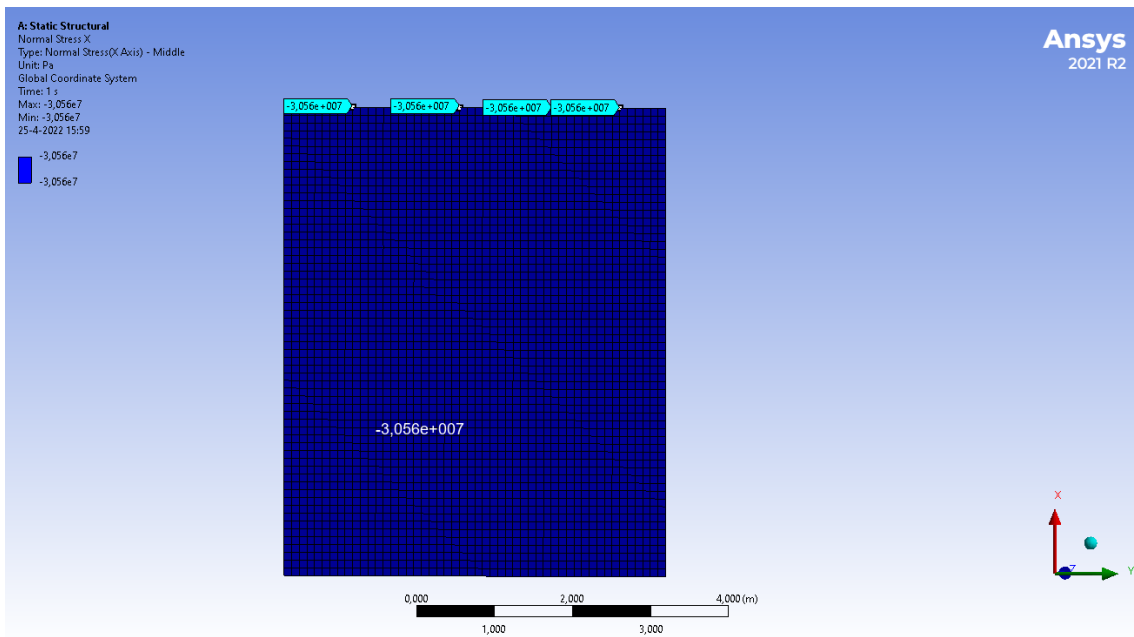


Figure 13.2: 20MPa stiffener direction axial stress simulation with ANSYS. Stiffeners not modeled

13.3. VALIDATION OF THE DEVELOPED MODEL ON A LARGE SET OF PANELS

In [section 13.1](#) the correct application of DNV-RP-C201 has been validated by hand calculations. After this validation, the method has been run on a large set of panels.

The validation of the method to a large scale structure is independent of the design stresses found in the linear elastic FEA analysis. In order to avoid the manual labour involved in selecting the reasonable maxima as described in [section 8.3](#), the average stresses over the panels have automatically been obtained with SDC-Verifier. It must therefore be noted that the results of this validation are not a representative stiffener configuration for the structure at hand. A full scale application of the model and the validation of its application can be found in [section 13.4](#)

For the validation of the method on a large scale structure, the side wall of the platform shown in [figure Figure 13.3](#) is used. The lower row of panels (lowest Z-coordinate) is excluded from the analysis, as stiffening is already applied in this area. This comes to a total of 60 panels. The input design stresses obtained by SDC-Verifier and the optimization method results are presented in [Appendix H](#).

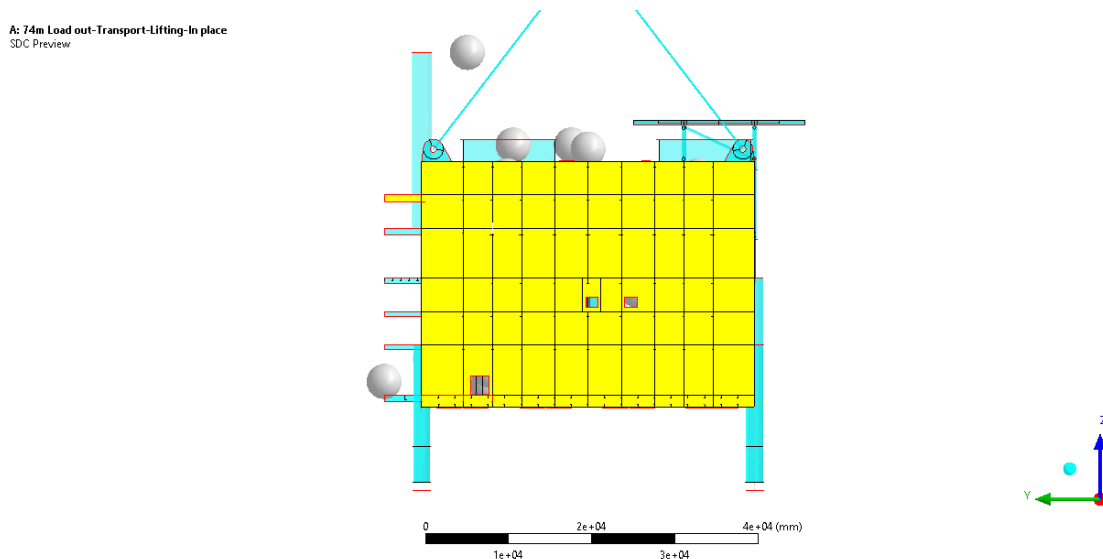


Figure 13.3: Wall on which the developed method is applied

13.4. FULL SCALE VALIDATION

In order to validate that the developed method stated in [chapter 9](#) is safe, a validation study was carried out. The study consists of three stages:

1. Linear elastic FEA of an unstiffened structure
2. Application of the stiffener placement method based on results obtained in stage one
3. Non-linear FEA analysis on stiffened structure to check for stability

The validation of the method requires drawing all suggested stiffeners back into a geometry. For a structure shown in [figure Figure 13.3](#), this is not feasible. Drawing all stiffeners back into the structure is simply too labour-intensive.

Therefore, a smaller stressed skin structure in the form of a stressed skin HV equipment module was chosen. A drawing of this structure is shown in [Figure E.1](#) found in [Appendix E](#). A considerable amount of effort has been spent on setting up a realistic FE model for the validation. Unfortunately, after completion of the FE model, a bug in SDC-Verifier did not allow the panel recognition tool to work properly. This was a surprise as the panel recognition tool worked fine previously, even when using larger models like shown in [Figure 13.3](#). After reviewing the model, the SDC-Verifier support service could also not resolve the issue, but noted that SDC-Verifier 2022 R1, which works with Ansys 2022 R1, presented no issues at all. Unfortunately, I did not

have this version of Ansys at my disposal so that I could not proceed with the validation of this model.

To still perform the necessary validation, another route was selected; to approximate a piece of the outer wall of a stressed skin platform.

GEOMETRY AND BOUNDARY CONDITIONS

A small scale validation of four panels has been performed, the geometry is shown in [Figure 13.4](#). In full scale stressed skin structures, panels around supports encounter the largest stresses and are subjected to distributed loads. For this reason, they are most likely to fail. Therefore, this situation is chosen for validation and these stress distributions are therefore approximated. The dimensions of the panel are stated in [Table 13.3](#).

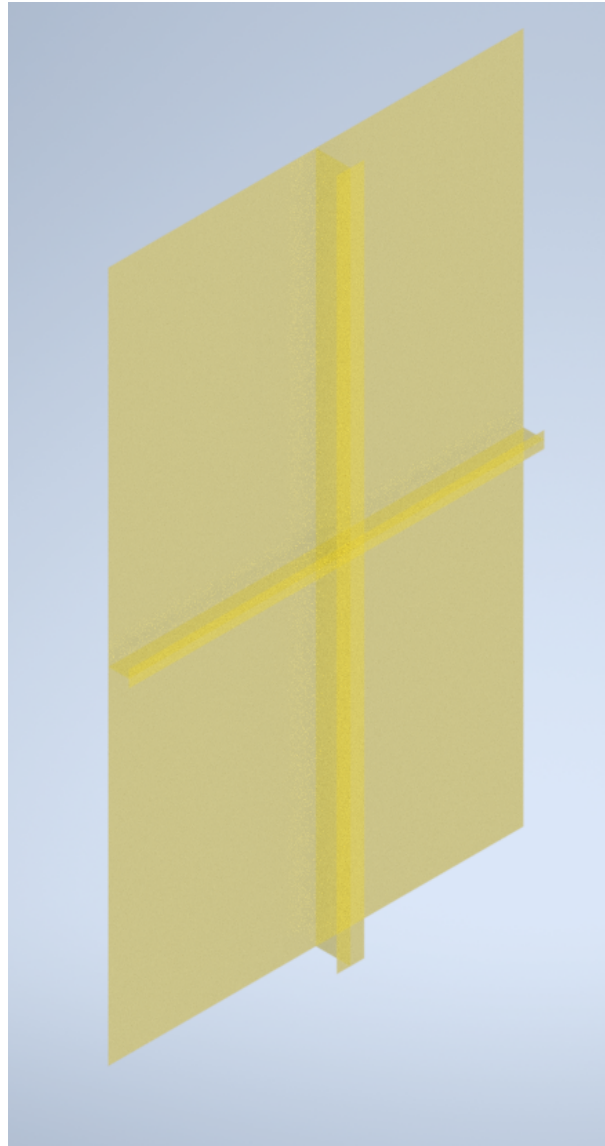


Figure 13.4: four-panel geometry used in validation

Table 13.3: Geometry of panel and stiffeners

Structural element	Length [m]	Width [m]	Flange width [m]	Flange thickness [m]	Web height [m]	Web thickness [m]	Plate Thickness [m]
Plating	10	6	-	-	-	-	0.008
Column	10	-	0.4	0.018	0.5	0.015	-
Stringer	6	-	0.24	0.011	0.3	9	-
Stiffener HP180x9	4.995	-	0.035	0.0176	0.162	9	-
Stiffener HP200x10	4.995	-	0.039	0.0197	0.18	10	-

In order to simulate stress developments near a support in a full scale analysis, the boundary conditions on the edges as shown in [Figure 13.5](#) have been applied to the linear elastic FEA model. All edges surrounding the panel are restricted in X-direction, as they are simply supported by the surrounding structural members. Only edge 'C' is restricted in all directions because it simulates a support pile of the structure. The boundary conditions are stated in [Table 13.4](#).

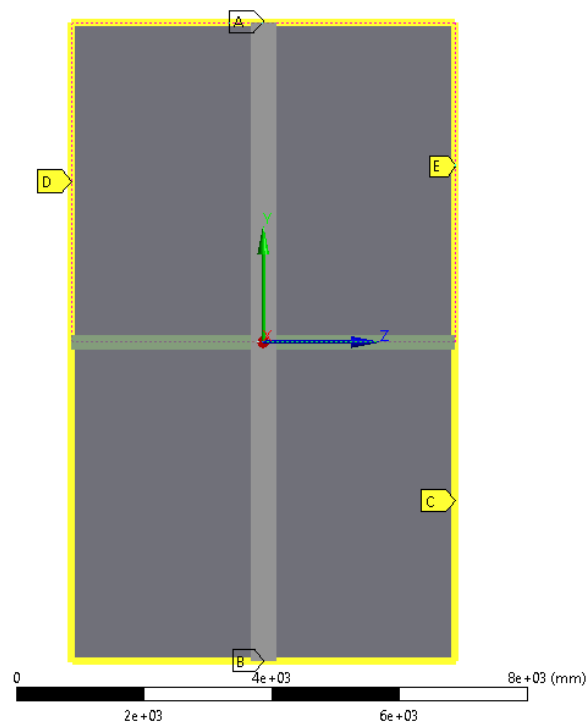


Figure 13.5: Boundary conditions applied to the validation geometry

Table 13.4: Boundary conditions

Label	Geometry	Displacement X	Displacement Y	Displacement Z
A	Edge	0	Free	Free
B	Edge	0	Free	Free
C	Edge	0	0	0
D	Edge	0	Free	Free
E	Edge	0	Free	Free

LOAD CASES

In order to simulate the stress developments found in a full scale topside, loads have been applied in the form of line pressures on edges A and B as shown in [Figure 13.6](#). Three different load cases have been studied. The load cases were simulated by altering the line pressures A and B. The values of these pressures for each load case can be found in [Table 13.5](#). For each of these load cases, a linear elastic FEA has been performed. The

gradient plots of these analyses can be found in appendix [Appendix F](#)

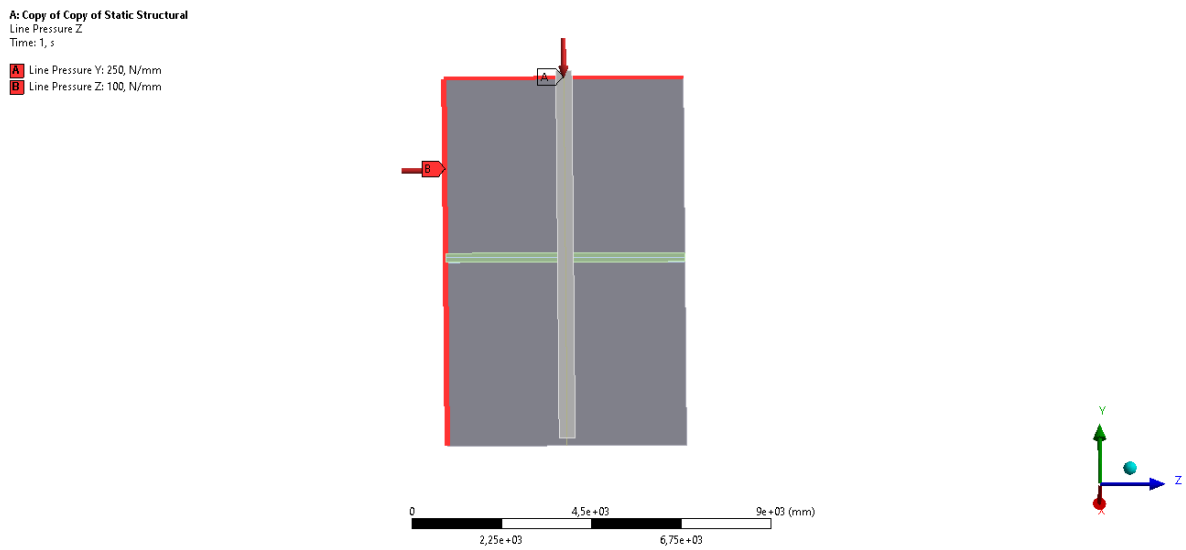


Figure 13.6: Line pressures applied to the geometry

Table 13.5: Line pressures per load case

Load case	Edge A [N/mm]	Edge B [N/mm]
1	250	100
2	250	50
3	300	50

EXTRACTION OF DESIGN STRESSES

With SDC-Verifiers panel recognition tool, the geometry of the panels is automatically identified and the average shear stress over the panels is extracted. Due to the stress distributions in the panels, reasonable maxima have been manually extracted from the FEA model. These results have been used as input for the automated stiffener placement method. The results of the stiffener placement method and its design stresses for load case 1,2 and 3 can be found in [Table 13.6](#), [Table 13.7](#), [Table 13.8](#), respectively. For each individual panel, the configuration with the most stiffeners, and the largest stiffener cross-section is selected as the stiffener proposal for that specific panel. [Table 13.9](#) represents the final result of the automated stiffener proposal method. [Figure 13.7](#) shows a drawing of the panel with the suggested stiffeners.

Table 13.6: Stiffener placement results load case 1

Plate	Sx (Mpa)	Sy (Mpa)	Sxy (Mpa)	L (m)	Lg (m)	Type	Number of stiffeners	Girders	UC	Weld Length	Plate thickness
1..Plate 3.2.1 (Y = -2500.05; Z = 1499.74)	14.89	22	20.8	5	3	HP200x10	5	0	0.94067	50	0.008
1..Plate 3.1.1 (Y = 2499.95; Z = 1499.74)	35.68	5.74	7.38	5	3	HP200x10	2	0	0.83708	20	0.008
1..Plate 3.3.1 (Y = 2499.95; Z = -1499.73)	27.55	12.34	3.12	5	3	HP180x09	3	0	0.95888	30	0.008
1..Plate 3.4.1 (Y = -2500.05; Z = -1499.73)	9.53	15.03	6.35	5	3	HP200x10	3	0	0.89301	30	0.008

Table 13.7: Stiffener placement results load case 2

Plate	Sx (Mpa)	Sy (Mpa)	Sxy (Mpa)	L (m)	Lg (m)	Type	Number of stiffeners	Girders	UC	Weld Length	Plate thickness
1..Plate 3.2.1 (Y = -2500.05; Z = 1499.74)	14.13	14.9	24.24	5	3	HP200x10	3	0	0.95732	30	0.008
1..Plate 3.1.1 (Y = 2499.95; Z = 1499.74)	33.1	1.31	3.92	5	3	HP200x10	1	0	0.96030	10	0.008
1..Plate 3.3.1 (Y = 2499.95; Z = -1499.73)	11.8	8.99	8.06	5	3	HP180x9	2	0	0.92763	20	0.008
1..Plate 3.4.1 (Y = -2500.05; Z = -1499.73)	29.21	6.53	1.54	5	3	HP180x9	2	0	0.94816	20	0.008

Table 13.8: Stiffener placement results load case 3

Plate	Sx (Mpa)	Sy (Mpa)	Sxy (Mpa)	L (m)	Lg (m)	Type	Number of stiffeners	Girders	UC	Weld Length	Plate thickness
1..Plate 3.2.1 (Y = -2500.05; Z = 1499.74)	16.53	16.25	29.96	5	3	HP200x10	4	0	0.85128	40	0.008
1..Plate 3.1.1 (Y = 2499.95; Z = 1499.74)	14.31	9.4	9.84	5	3	HP200x10	2	0	0.78832	20	0.008
1..Plate 3.3.1 (Y = 2499.95; Z = -1499.73)	38.89	0.52	3.97	5	3	HP180x9	2	0	0.78839	20	0.008
1..Plate 3.4.1 (Y = -2500.05; Z = -1499.73)	35.07	6.5	1.66	5	3	HP200x10	2	0	0.87462	20	0.008

Table 13.9: Maximum number of stiffeners out of every load case

Plate	Sx (Mpa)	Sy (Mpa)	Sxy (Mpa)	L (m)	Lg (m)	Type	Number of stiffeners	Girders	UC	Weld Length	Plate thickness
1..Plate 3.2.1 (Y = -2500.05; Z = 1499.74)	14.89	22	20.75	5	3	HP200x10	5	0	0.94067	50	0.008
1..Plate 3.1.1 (Y = 2499.95; Z = 1499.74)	35.68	5.74	7.38	5	3	HP200x10	2	0	0.83708	20	0.008
1..Plate 3.3.1 (Y = 2499.95; Z = -1499.73)	27.55	12.34	3.12	5	3	HP180x09	3	0	0.95888	30	0.008
1..Plate 3.4.1 (Y = -2500.05; Z = -1499.73)	9.53	15.03	6.35	5	3	HP200x10	3	0	0.89301	30	0.008

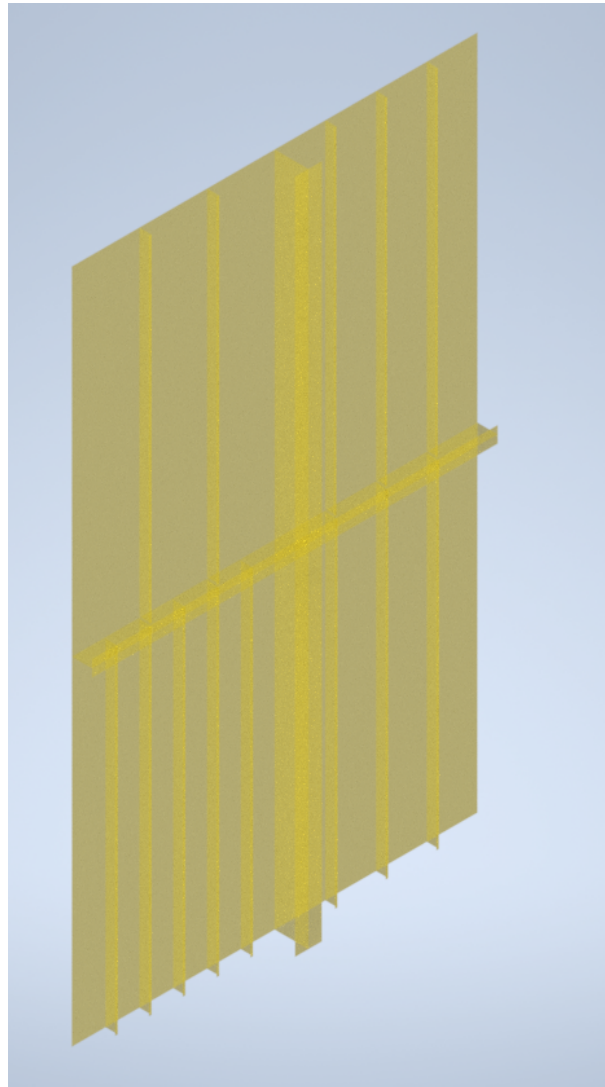


Figure 13.7: Validation geometry with proposed stiffeners

VALIDATION BY MEANS OF NON-LINEAR PLASTIC FEA ANALYSIS

In order to validate the stiffener proposal of the method, a non-linear FEA analysis has been performed. Therefore, the stiffener proposal found in [Table 13.9](#) is drawn into the initial geometry. This, now stiffened panel, is shown in [Figure 13.7](#). The same boundary conditions and loads are applied to this new geometry as in the linear elastic FEA. Only now, plastic material properties and deflections will be accounted for during the FEA analysis.

Prior to the Non-linear plastic FEA analysis, an eigenvalue analysis has been performed to retrieve the buckling shape of the panel, this is shown in [Figure 13.8](#). This shape is used in the analysis to account for initial deformations.

It can be seen from the buckling shape that the outer right plate in the upper right panel tends to buckle first. Therefore, based on the dimensions of this plating bounded by larger compression members, initial deformations are set at this location based on the commentary of EN1993-1-5 [15]. The commentary prescribes an initial deformation of length/400 or width/200, whichever is the largest. On top of that, an additional deformation is added of length/300 for residual welding stresses. This results in a total initial deformation of 29.1 mm.

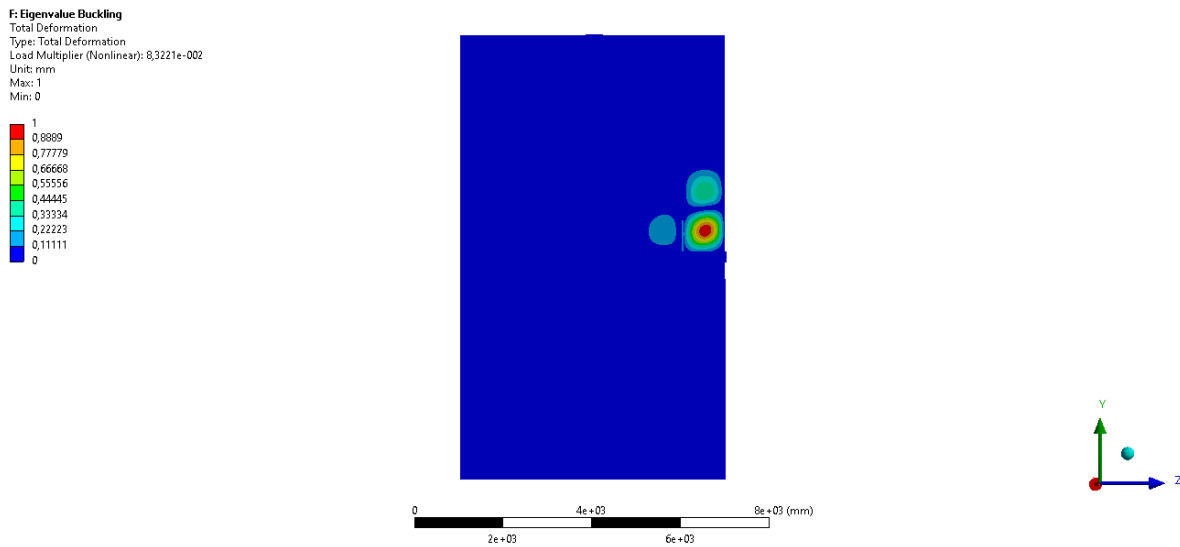


Figure 13.8: First buckling mode of panels

The non-linear FEA analysis results in a stable structure with deformations not larger than 9 mm. Therefore, it can be concluded that the stiffener proposal method is valid and safe. Contour plots of the non-linear FEA solution for each load-case are shown in [Figure 13.9](#), [Figure 13.10](#) and [Figure 13.11](#).

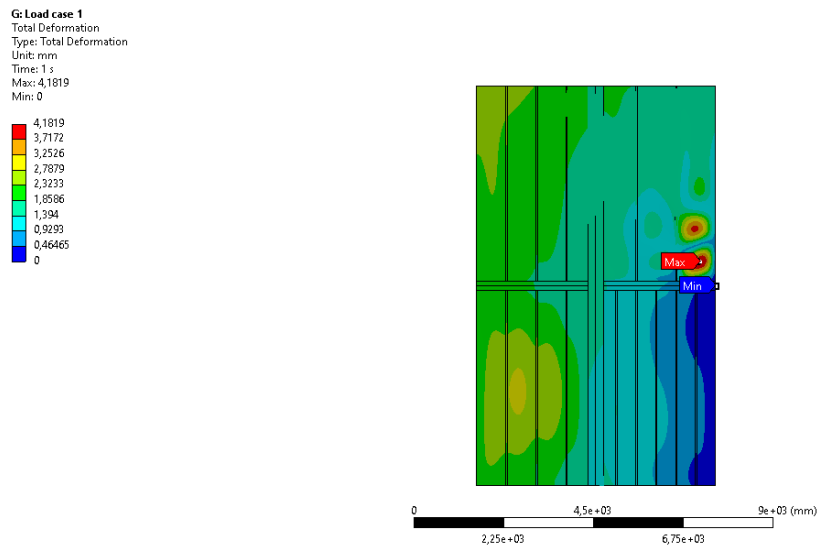


Figure 13.9: Total deformation due to load case 1

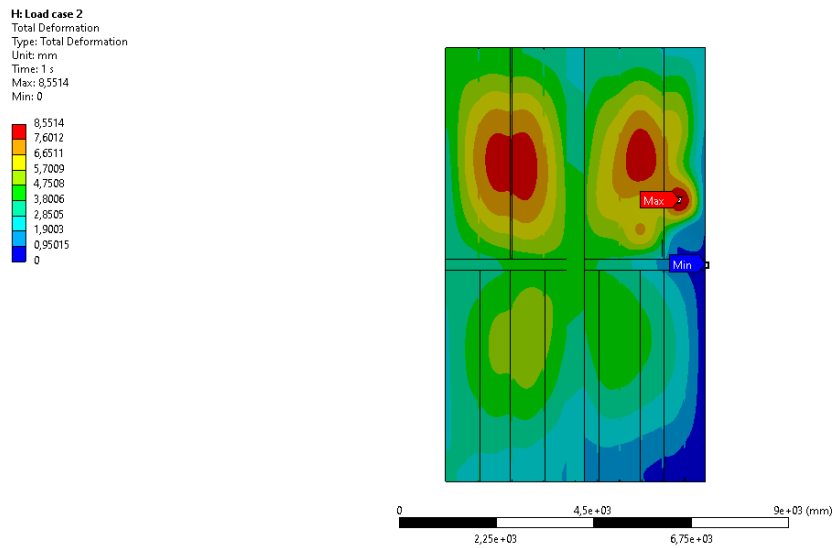


Figure 13.10: Total deformation due to load case 2

! Load case 3
Total Deformation
Type: Total Deformation
Unit: mm
Time: 1 s
Max: 9,4904
Min: 0

9,4904
8,4359
7,3814
6,3269
5,2725
4,218
3,1635
2,109
1,0545
0

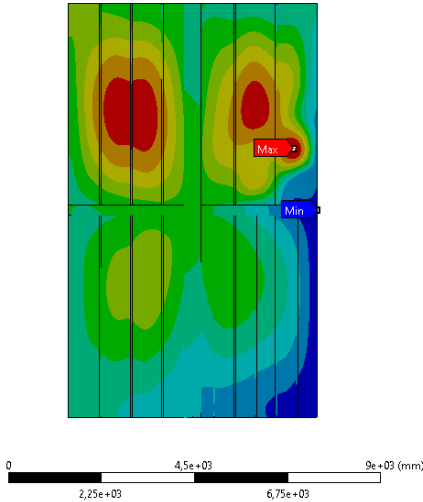


Figure 13.11: Total deformation due to load case 3

14

CONCLUSION

This thesis answers the research question: "How to develop a method with which stiffener placement in stability governed thin walled structures can be automated and optimized for cost of execution?"

Stressed skin offshore platforms are stability governed structures due to their slender nature and the relatively small amount of lateral pressure they are subjected to. Because stiffeners and stringers encounter little out-of-plane loads, it is possible to leave them out of the linear elastic FEA. This leads to a major simplification of the FEA model and opens up the possibility for automation and optimization.

By means of linear elastic FEA the stresses throughout the platform are obtained. With the help of SDC-Verifiers panel recognition tool, the geometry and stresses over each panel can be automatically extracted from the model. For panels subjected to distributed loads however, design stresses can only be manually extracted from the linear elastic FEA solution.

With these input stresses, an optimization method has been developed as described in [chapter 9](#). Taking into account the boundaries stated in [chapter 8](#), this method has been automated using the programming language Python. The method yields an optimal stiffener configuration with respect to weld volume, that ensures stability for a specific load case based on DNV-RP-C201. However, this model assumes uniform stresses, equivalent to the reasonable maximum stress found over a panel's edge; in case of a distributed stress distribution this is a conservative overestimation. Once software is available that allows for stress distribution extraction over panels, a refinement method is proposed in [chapter 10](#).

The application of the effective width method in case of extreme stress distributions has been validated by non-linear plastic FEA in [chapter 11](#). These experiments show that for plates with a slenderness range from 3 to 4.28, the peak of a distribution should not exceed twice the minimum when the effective width method is applied. An additional experiment has been conducted on a stiffened panel as a whole. From this experiment, it can be concluded that there exists a redistribution effect between plate-stiffeners in a panel.

The stiffener optimization tool developed in this thesis allows engineers to design stability governed structures without modelling each individual stiffener. This enhances design flexibility and majorly simplifies the FE model. Later on in the design process, the stiffener optimization tool will quickly generate the optimal stiffener and stringer configuration. It has been identified that cost of execution is mainly dependent on weld volume, which in this particular case study is solely dependent on weld length. Therefore, an efficiency optimum is realized by applying a minimum number of stiffeners. Due to the many calculations involved in finding such an optimum, the method has been automated.

In very heavily loaded panels, it may happen that the method cannot provide a realistic solution because the combination of design stresses is too high. In these cases, the plate thickness will have to be increased and the panel will have to be re-evaluated (manually). However, this only occurs in a small percentage of panels.

It is therefore safe to conclude that the application of the method developed in this thesis will drastically lower the manual labour in the design- and execution process of topsides.

15

RECOMMENDATIONS AND FURTHER RESEARCH

Manual selection of design stresses, described in [section 8.3](#), requires a substantial amount of man-hours, increasing not only project costs but also the risk of human error.

Therefore, software to extract stress distributions from a linear elastic FEA solution should be developed. Once this software is available, the method as described in [chapter 10](#), allows for a more accurate way of determining the design stress, which leads to less conservative results, therefore saving costs.

[chapter 12](#) identifies a redistribution effect between plate-stiffeners within a stiffened panel. This redistribution effect is currently not covered by DNV-RP-C201, which means that stiffened panels are conservatively designed when subjected to load distributions. Further research on this effect is needed so that less conservative designs may be achieved.

BIBLIOGRAPHY

- [1] American Bureau of Shipping (ABS). *Buckling and ultimate strength assessment for offshore structures*. 2004.
- [2] Y. Bai and W.-L. Jin. *Chapter 17 - Ultimate Strength of Plates and Stiffened Plates*. Butterworth-Heinemann, second edition edition, 2016. ISBN 978-0-08-099997-5. URL <https://www.sciencedirect.com/science/book/pii/B9780080999975000174>.
- [3] K.-J. Bathe. *Finite element procedures in engineering analysis*. 1982.
- [4] D. Beg, U. Kuhlmann, L. Davaine, B. Braun, and U. Kuhlmann. *Design of Plated Structures : Eurocode 3: Design of Steel Structures, Part 1-5: Design of Plated Structures*. 2011. ISBN 9783433601174. URL <http://ebookcentral.proquest.com/lib/delft/detail.action?docID=838192>.
- [5] Det Norske Veritas (DNV). *Design of offshore steel structures, general - LRFD method*. 2015.
- [6] Det Norske Veritas (DNV). *DNVGL-OS-C101: Design of offshore steel structures, general - LRFD method*. 2019.
- [7] ECCS - European Convention for Constructional Steelwork and Associação Portuguesa de Construção. *Design of Steel Structures : Eurocode 3: Design of Steel Structures, Part 1-1: General Rules and Rules for Buildings*. 2016. ISBN 9783433031650. URL <http://ebookcentral.proquest.com/lib/delft/detail.action?docID=4711450>.
- [8] European Committee for Standardization. *Design of steel structures. Part 1.1 General rules and rules for buildings. ENV 1993-1-1*. 1997.
- [9] European Committee for Standardization. *EN 1993-1-5:2006 - Eurocode 3: Design of steel structures – Part 1-5: Plated structural elements*. 2006.
- [10] O. Hillers. *Automatic buckling checks on stiffened panels based on finite element results*. 2011.
- [11] O. F. Hughes and J. K. Paik. *12. Elastic Buckling of Plates*. Society of Naval Architects and Marine Engineers (SNAME), 2010. ISBN 978-0-939773-78-3. URL <https://app.knovel.com/hotlink/khtml/id:kt008RRIS3/ship-structural-analysis/elastic-buckling-plates>.
- [12] Institute of steel development and growth. *Teaching material - chapter 6*. . URL <http://www.steel-insdag.org/TeachingMaterial/Chapter6.pdf>.
- [13] Institute of steel development and growth. *Teaching material - chapter 7*. . URL <http://www.steel-insdag.org/TeachingMaterial/Chapter7.pdf>.
- [14] Institute of steel development and growth. *Teaching material - chapter 8*. . URL <http://www.steel-insdag.org/TeachingMaterial/Chapter8.pdf>.
- [15] B. Johansson, R. Maquoi, G. Sedlacek, C. Muller, and D. Beg. *Commentary and worked examples to en 1993-1-5 'Plated structural elements'*. 2007.
- [16] Kalmar Industries BV. *Lastechnisch Construeren*, volume 1.
- [17] R. E. Melchers. *The effect of corrosion on the structural reliability of steel offshore structures*, volume 47. 2005. URL <https://www.sciencedirect.com/science/book/pii/S0010938X05001034>.
- [18] Može and Primož. Lecture 7.2: Cross-section classification. URL <http://fgg-web.fgg.uni-lj.si/~/pmoze/esdep/master/wg07/10200.htm>.

- [19] D. Nethercot and L. Gardner. *Designers' Guide to Eurocode 3*. ICE Publishing, 2011. ISBN 978-0-7277-4172-1. URL <https://app.knovel.com/hotlink/khtml/id:kt00C60NVE/designers-guide-eurocode/structural-analysis>.
- [20] M. Okereke and S. Keates. *Finite Element Applications*. Springer International Publishing, 2018. ISBN 978-3-319-67124-6. doi: 10.1007/978-3-319-67125-3.
- [21] J. K. Paik and A. K. Thayamballi. *Ultimate Limit State Analysis and Design of Plated Structures*. John Wiley Sons, Incorporated, 2018. ISBN 9781119367789. URL <http://ebookcentral.proquest.com/lib/delft/detail.action?docID=5317467>.
- [22] J. M. Pons-Poblet. *The vierendeel truss: past and present of an innovative typology*. 2019.
- [23] L. Ramsden. *Talisman energy : AUK platform*. URL <https://leeramsden.com/blog/talisman-40-year-old-north-sea-oil-rig-auk>.
- [24] Steelconstruction. *Continuous and discontinuous stiffeners*. URL <https://www.steelconstruction.info/Stiffeners>.
- [25] T.-L. Teng, P.-H. Chang, and W.-C. Tseng. *Effect of welding sequences on residual stresses*, volume 81. 2003. URL <https://www.sciencedirect.com/science/book/pii/S0045794902004479>.
- [26] J. R. Thomas and O. Hughes. *Finite Element Method - Linear Static and Dynamic Finite Element Analysis*. Dover Publications. ISBN 978-0-486-41181-1. URL <https://app.knovel.com/hotlink/toc/id:kpFEMLSDF1/finite-element-method/finite-element-method>.
- [27] S. Timoshenko and S. Woinowsky-Krieger. *Theory of plates and shells*. McGraw-Hil, 2nd edition, 1970.
- [28] K. Weynand and J.-P. Jaspart. *4. Welded Connections*. John Wiley Sons, 2017. ISBN 978-3-433-03216-9. URL <https://app.knovel.com/hotlink/khtml/id:kt011R4C02/design-joints-in-steel/welded-connections>.
- [29] C. Yu and B. Schafer. *Effect of Longitudinal Stress Gradients on Elastic Buckling of Thin Plates*, volume 133. 04 2007.

A

DERIVATION OF EULER BUCKLING CRITERION

In this appendix, the derivation of Euler's beam buckling stress is given. [Figure A.1](#) denotes the idealized, pin-ended uniform beam for which the theory can be applied. It makes use of the following assumptions:

- The beam material is homogeneous and elastic.
- The beam is perfectly straight and has no imperfections.
- The applied load is at the centroid of both ends/

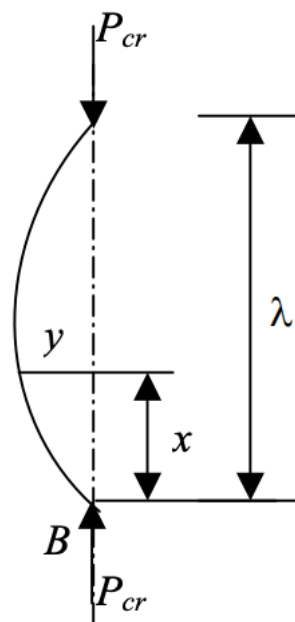


Figure A.1: Pin ended beam [12]

Initially the column will remain straight under load P except for a certain value $P = P_{cr}$ where it starts to buckle. The buckling deformation at a distance x from B is called y , so that the bending moment in the beam is $P_{cr} \cdot y$. The differential equation for a small buckling deformation is therefore given by [Equation A.1](#).

$$-EI \frac{d^2 y}{dx^2} = P_{cr} \cdot y \quad (\text{A.1})$$

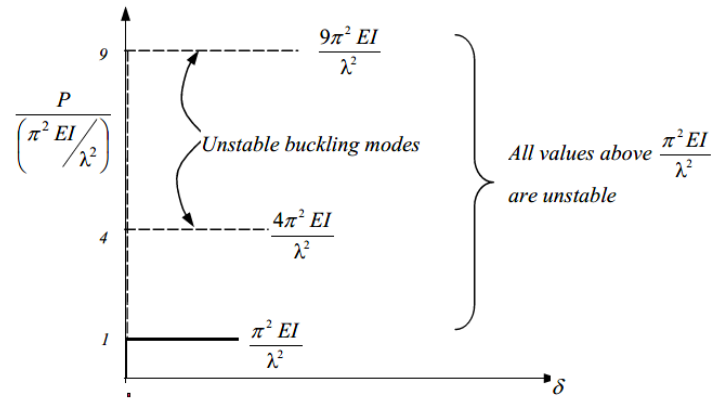


Figure A.2: Graph of buckling load solutions [12]

The solution for this equation is given by Equation A.2, with A_1 and B_1 constants.

$$y = A_1 \cos x \sqrt{\frac{P_{cr}}{EI}} + B_1 \sin x \sqrt{\frac{P_{cr}}{EI}} \quad (\text{A.2})$$

Taking into account the boundary condition for $y = 0$ at $x = 0$ and $y = 0$ at $x = \lambda$ yields $A_1 = 0$ and $\sin \lambda \sqrt{\frac{P_{cr}}{EI}} = 0$ as $B_1 = 0$ would yield the trivial solution were $y = 0$ for all values of x . This can only be satisfied when $\lambda \sqrt{\frac{P_{cr}}{EI}} = 0, \pi, 2\pi, \text{etc.}$ This leads to a solution for P_{cr} equal to Equation A.3, with n an integer.

$$P_{cr} = \frac{\pi^2 EI}{\lambda^2}, \frac{4\pi^2 EI}{\lambda^2}, \dots, \frac{n^2 \pi^2 EI}{\lambda^2} \quad (\text{A.3})$$

Figure A.2 shows the various for P_{cr} . However, all solutions above the first buckling mode are unstable. This means that they are possible but tend to return to the first mode in case of a small disturbance. Therefore, the first buckling mode is governing.

B

PLATE BUCKLING

This appendix will give the critical buckling strength derivation of a simply supported uniaxially loaded plate under compression. The derivation is presented as described by Hughes and Paik [11]. Consider the uniform, simply supported plate denoted in [Figure B.1](#) under a uni-axial compressive load N_x . The equilibrium equation for such a plate is given by [Equation B.1](#).

$$\frac{\partial^4 w}{\partial x^4} + \frac{2\partial^4 w}{\partial x^2 \partial y^2} + \frac{\partial^4 w}{\partial y^4} = \frac{12(1-\nu^2)}{Et^3} \left(-N_x \frac{\partial^2 w}{\partial x^2} \right) \quad (\text{B.1})$$

The simply supported boundary condition gives the following boundary condition: $w = 0$ at $x = 0, x = a, y = 0$ and $y = b$. Substitution of these boundary conditions into [Equation B.1](#) gives [Equation B.3](#) after some simplification. Just as in the column buckling derivation of [Appendix A](#), the lowest buckling stress is the only stable mode and therefore $n = 1$ for all practical applications.

$$\left(\frac{m^4 \pi^4}{a^4} + 2 \frac{m^2 n^2 \pi^4}{a^2 b^2} + \frac{n^4 \pi^4}{b^4} \right) = \frac{12(1-\nu^2)}{Et^3} (N_x)_{cr} \frac{m^2 \pi^2}{a^2} \quad (\text{B.2})$$

$$(N_x)_{cr} = \frac{\pi^2 Et^3}{12(1-\nu^2)} \frac{(m^2/a^2 + n^2/b^2)^2}{m^2/a^2} = \frac{\pi^2 Et^3}{12(1-\nu^2)} \left(\frac{m}{a} + \frac{n^2 a}{mb^2} \right)^2 \quad (\text{B.3})$$

Substitution of $n = 1$ and $k = \left(\frac{m}{a} + \frac{n^2 a}{mb^2} \right)^2$ gives the critical buckling stress σ_{cr} in [Equation B.5](#). k can be determined analytically or extracted from [Figure 4.2](#). This is the case for simply supported edges, for other conditions like fixed or free the value of k can vary from 0.5 to 7 as can be seen in [Figure B.2](#)

$$(N_x)_{cr} = \frac{\pi^2 Et^3}{12(1-\nu^2) b^2} \left(m \frac{b}{a} + \frac{1}{m} \frac{a}{b} \right)^2 \quad (\text{B.4})$$

$$\sigma_{cr} = \frac{k \pi^2 E}{12(1-\nu^2) (b/t)^2} \quad (\text{B.5})$$

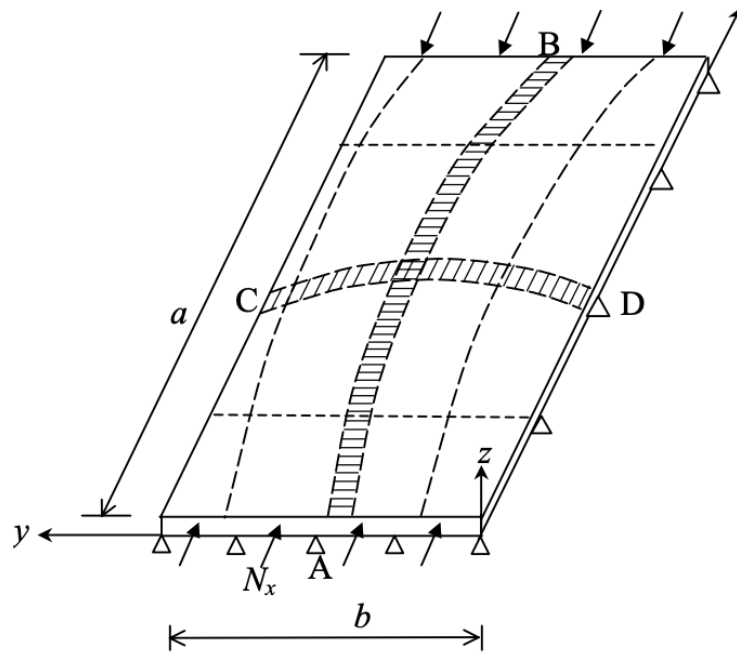


Figure B.1: Buckling of Plate under Uni-axial Compression [13]

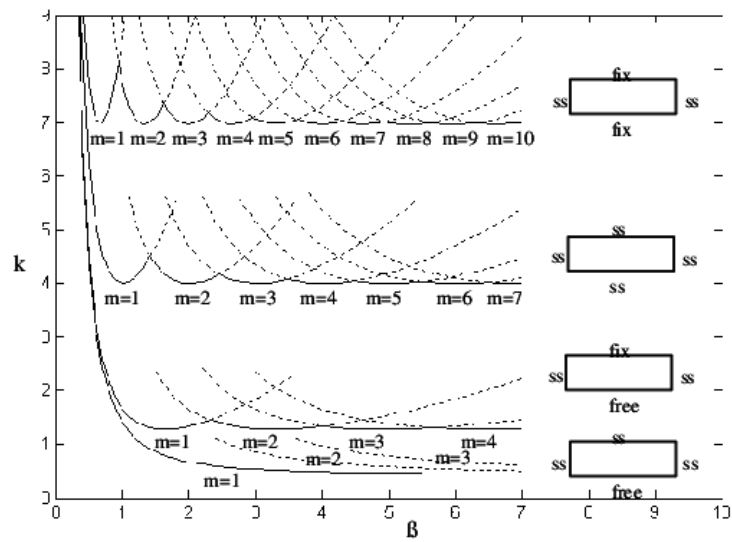


Figure B.2: Coefficient k for uniformly compressed rectangular plates under different boundary conditions [29]

C

EFFECTIVE WIDTHS FOR STRESS DISTRIBUTIONS

Figure C.1: Effective widths for stress distributions [4]

Stress distribution (compression positive)				Effective ^p width b_{eff}		
				$\psi = 1$ $b_{eff} = \rho b$ $b_{e1} = 0.5b_{eff}$ $b_{e2} = 0.5b_{eff}$		
				$1 > \psi \geq 0$ $b_{eff} = \rho b$ $b_{e1} = \frac{2}{5-\psi}b_{eff}$ $b_{e2} = b_{eff} - b_{e1}$		
				$\psi < 0$ $b_{eff} = \rho b_c = \rho b / (1 - \psi)$ $b_{e1} = 0.4b_{eff}$ $b_{e2} = 0.6b_{eff}$		
$\psi = \sigma_2 / \sigma_1$	1	$1 > \psi > 0$	0	$0 > \psi > -1$	-1	$-1 > \psi > -3$
Buckling coefficient k_σ	4.0	$8.2 / (1.05 + \psi)$	7.8	$7.81 - 6.29\psi + 9.78\psi^2$	23.9	$5.98(1 - \psi)^2$

D

LOAD DISTRIBUTION PLOTS

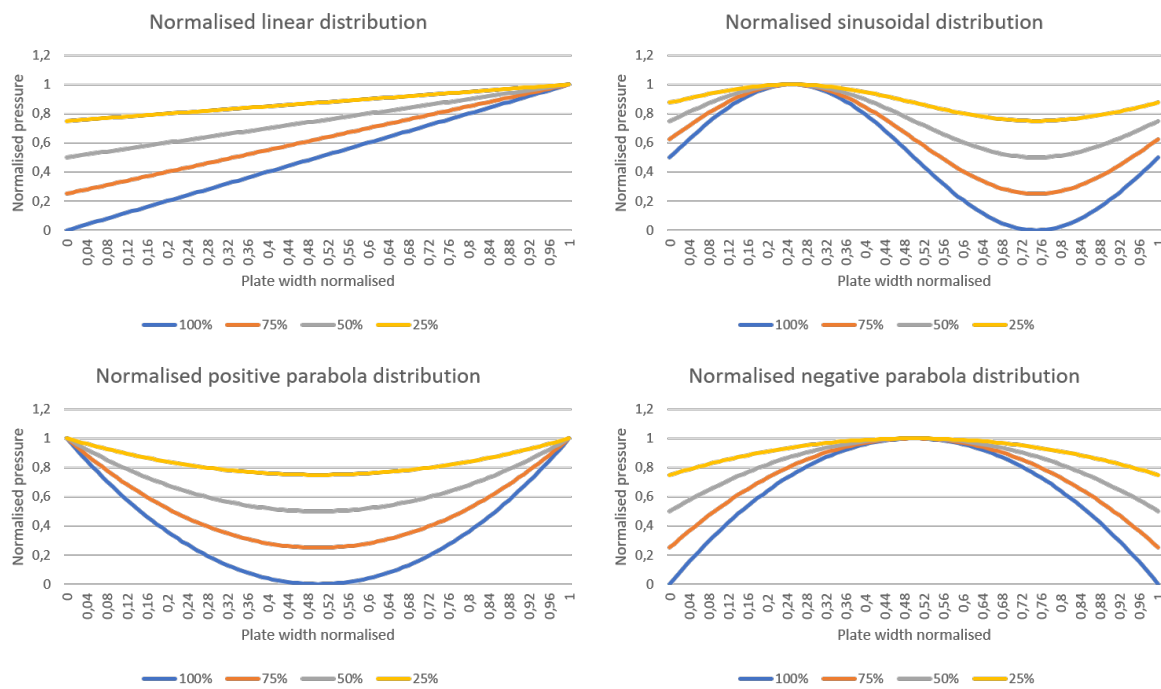


Figure D.1: Function 1, negative parabola

E

STRESSED SKIN MODULE

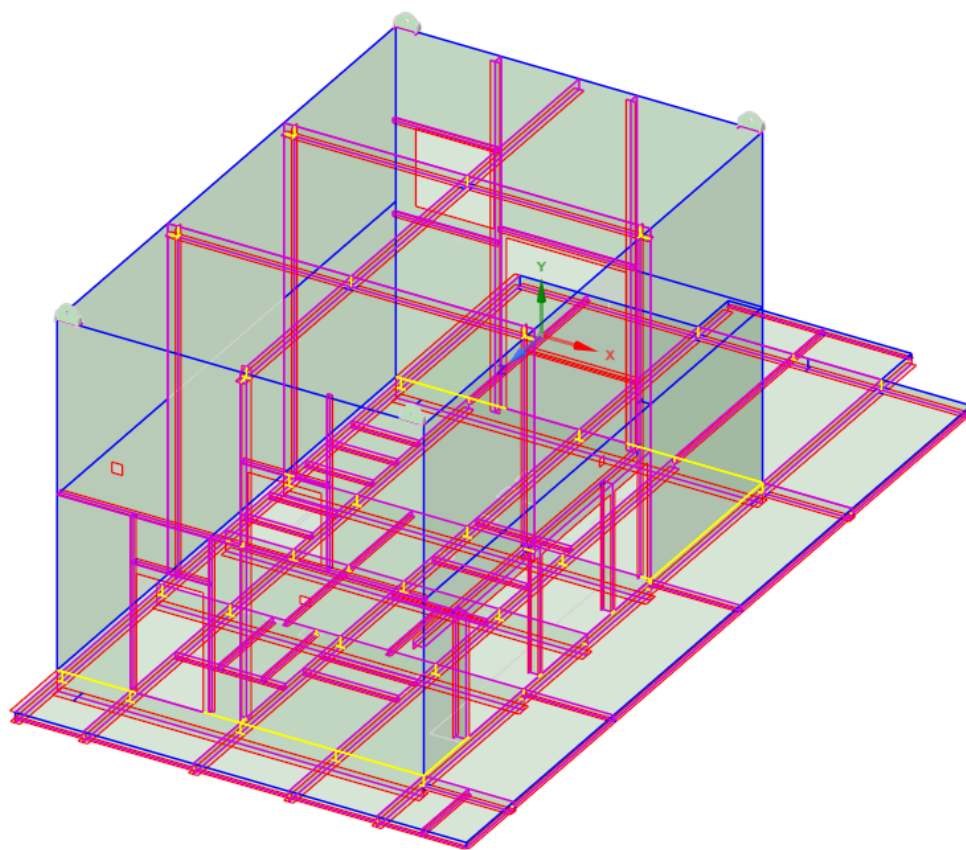


Figure E.1: HV equipment module

F

CONTOUR PLOTS FULL SCALE VALIDATION

LOAD CASE 1

A: Copy of Copy of Static Structural
Y Axis - Normal Stress - End Time 2
Type: Normal Stress(Y Axis) - Middle
Unit: MPa
Global Coordinate System
Time: 1 s
Max: 37,068
Min: -367,02

37,068
0
-21,429
-42,857
-64,286
-85,714
-107,14
-128,57
-150
-367,02

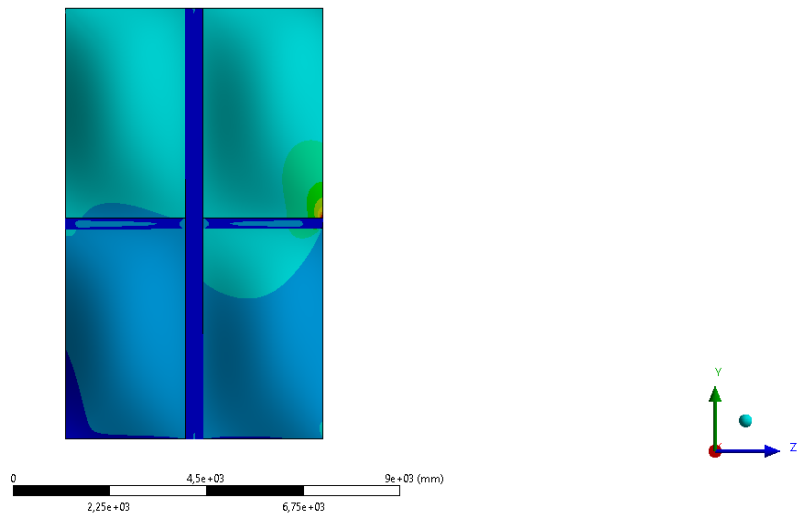


Figure F.1: Contour plot of normal stress in longitudinal direction

A: Copy of Copy of Static Structural
 Z Axis - Normal Stress - End Time
 Type: Normal Stress(Z Axis) - Middle
 Unit: MPa
 Global Coordinate System
 Time: 1 s
 Max: 299,91
 Min: -222,3

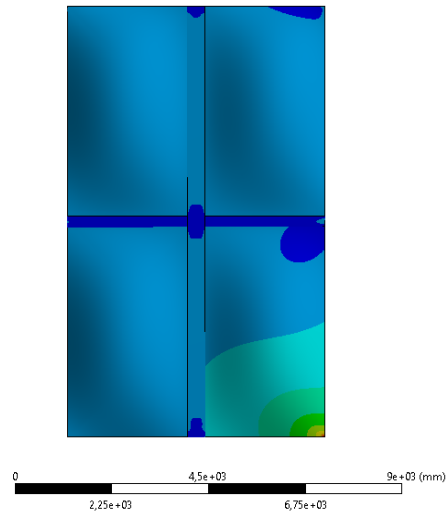
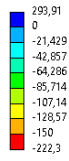


Figure E2: Contour plot of normal stress in transverse direction

A: Copy of Copy of Static Structural
 YZ Component - Shear Stress - End Time
 Type: Shear Stress(YZ Component) - Middle
 Unit: MPa
 Global Coordinate System
 Time: 1 s
 Max: 142,72
 Min: -4,651

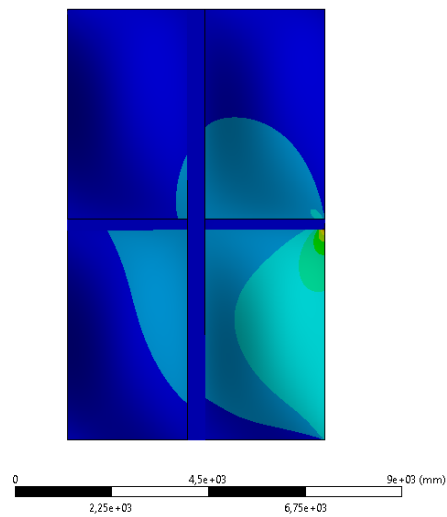
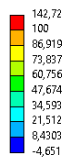


Figure E3: Contour plot shear stress

LOAD CASE 2

B: Copy of Copy of Copy of Static Structural

Y Axis - Normal Stress - End Time
 Type: Normal Stress(Y Axis) - Middle
 Unit: MPa
 Global Coordinate System
 Time: 1 s
 Max: 74,043
 Min: -195,59

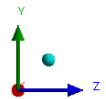
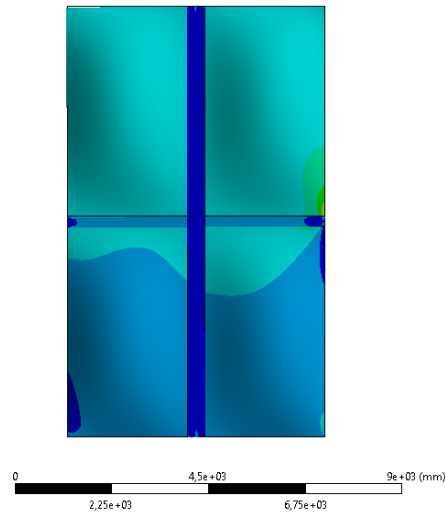
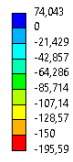


Figure F4: Contour plot of normal stress in longitudinal direction

B: Copy of Copy of Copy of Static Structural

Z Axis - Normal Stress - End Time
 Type: Normal Stress(Z Axis) - Middle
 Unit: MPa
 Global Coordinate System
 Time: 1 s
 Max: 466,29
 Min: -258,64

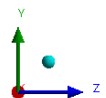
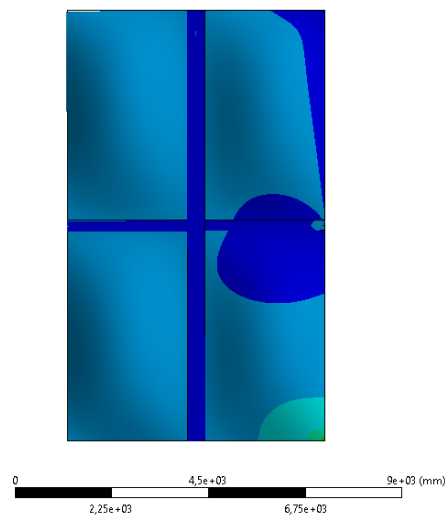
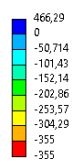


Figure F5: Contour plot of normal stress in transverse direction

B: Copy of Copy of Copy of Static Structural
 YZ Component - Shear Stress - End Time
 Type: Shear Stress(YZ Component) - Middle
 Unit: MPa
 Global Coordinate System
 Time: 1 s
 Max: 107,45
 Min: -27,335

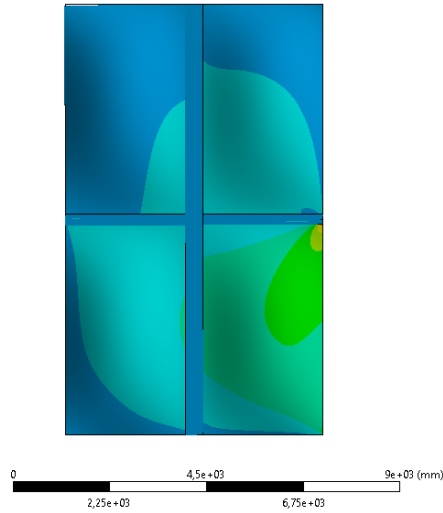


Figure E6: Contour plot shear stress

LOAD CASE 3

C: Copy of Copy of Copy of Static Structural
 Y Axis - Normal Stress - End Time
 Type: Normal Stress(Y Axis) - Middle
 Unit: MPa
 Global Coordinate System
 Time: 1 s
 Max: 95,654
 Min: -217,13

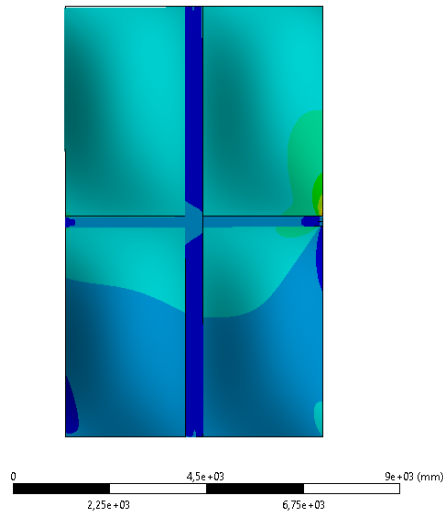


Figure E7: Contour plot of normal stress in longitudinal direction

C: Copy of Copy of Copy of Copy of Static Structural
 Z Axis - Normal Stress - End Time
 Type: Normal Stress(Z Axis) - Middle
 Unit: MPa
 Global Coordinate System
 Time: 1 s
 Max: 585,96
 Min: -318,72

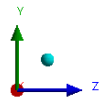
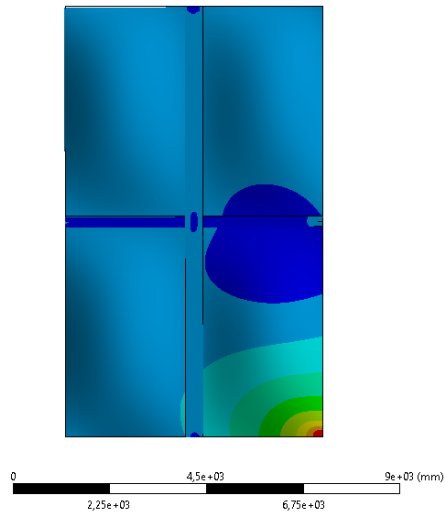


Figure E8: Contour plot of normal stress in transverse direction

C: Copy of Copy of Copy of Copy of Static Structural
 YZ Component - Shear Stress - End Time
 Type: Shear Stress(YZ Component) - Middle
 Unit: MPa
 Global Coordinate System
 Time: 1 s
 Max: 120,94
 Min: -44,457

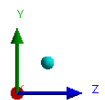
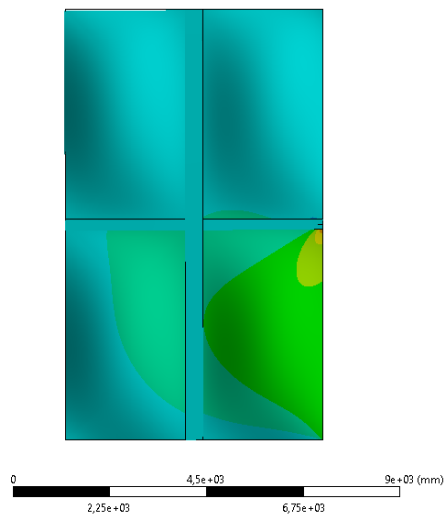


Figure E9: Contour plot shear stress

G

VERIFICATION OF DESIGN CODE APPLICATION

#stiffeners = 6
Stiffeners Type = HP200x10

pSd	=	design lateral pressure	=	0.0021 [MPa]
σx1,Sd	=	largest occurring longitudinal stress	=	20 [MPa]
σx2,Sd	=	smallest occurring longitudinal stress	=	20 [MPa]
σy1,Sd	=	largest occurring transverse stress	=	20 [MPa]
σy2,Sd	=	smallest occurring transverse stress	=	20 [MPa]
τSd	=	occurring shear stress	=	50 [MPa]

Pannel data				
l	=	plate length	=	6000 [mm]
L _G	=	plate width / girder length	=	5000 [mm]
t	=	plate thickness	=	8 [mm]
L _p	=	length of pannel	=	18000 [mm]

		Hand calculation	Automated result	Difference %	
Stiffeners / Girders					
hw	=	height of web	180 [mm]	180.26 [mm]	0.00
b	=	width of flange	39 [mm]	38.90 [mm]	0.00
ef	=	eccentricity of flange	14 [mm]	14.45 [mm]	0.00
tw	=	thickness of web	10 [mm]	10.00 [mm]	-
tf	=	thickness of flange	19.7 [mm]	19.74 [mm]	0.00
Aw	=	hw tw	1803 [mm ²]	1,802.61 [mm ²]	0.00
Af	=	b tf	768 [mm ²]	767.94 [mm ²]	-
n	=	number of stiffeners	6 [-]	6 [-]	-
s	=	Width between stiffeners	714 [mm]	714.2857143 [mm]	0.00

		Hand calculation	Automated result	Difference %	
7.3 Effective plate width					
se	=	s Cxs Cys	302.24 mm	302.24 mm	0.00
Ae	=	Aw + Af + (se(n)/2 + se(n+1)/2) t	4,988.46 mm ²	4,988.46 mm ²	-
zpe	=	((t/2 + hw/2) Aw + (t/2 + hw + tf/2) Af) / Ae	63.90 mm	63.90 mm	0.00
zte	=	t/2 + hw + tf - zpe	140.10 mm	140.10 mm	0.00
le	=	1/12 se t ³ + zpe ² se t + 1/12 tw hw ³ + (t/2 + hw/2 - zpe) ² Aw + 1/12 b tf ³ + (t/2 + hw + tf/2 - zpe) ² Af	29,463.46 mm ⁴	29,463.46 mm ⁴	0.00
ie	=	√(le / Ae)	76.85 mm	76.85 mm	0.00
Wep	=	le / (zpe + t/2)	433,925.56 mm ³	433,925.56 mm ³	0.00
Wes	=	le / zte	210,302.80 mm ³	210,302.80 mm ³	0.00
A	=	Aw + Af + s t	8,284.84 mm ²	8,284.84 mm ²	0.00
zp	=	((t/2 + hw/2) Aw + (t/2 + hw + tf/2) Af) / A	38.48 mm	38.48 mm	0.00
zt	=	t/2 + hw + tf - zp	165.52 mm	165.52 mm	0.00
ls	=	1/12 s t ³ + zp ² s t + 1/12 tw hw ³ + (t/2 + hw/2 - zp) ² Aw + 1/12 b tf ³ + (t/2 + hw + tf/2 - zp) ² Af	37,585.40 mm ⁴	37,585.40 mm ⁴	0.00
lp	=	t ³ s / 10.9	33,551.77 mm ⁴	33,551.77 mm ⁴	0.00

		Hand calculation	Automated result	Difference %	
7.2 Forces in the idealised stiffened plate					
τcrl	=	k l 0.904 E (t/s) ²	128.51 MPa	128.51 MPa	0.00
NSd	=	σx,Sd (Aw + Af + s t) + τtf s t	165,696.75 N/mm	165,696.75 N/mm	0.00
ψ	=	σy2,Sd / σy1,Sd	1.00	1.00	-
kc	=	2 (1 + √(1 + (10.9 ls) / (t ³ s)))	68.97	68.97	0.00
C0	=	(Wes fy mc) / (kc E t ² s)	0.00	0.00	0.00
p0	=	(0.6 + 0.4 ψ) C0 σy1,Sd if ψ > -1,5; 0 if ψ ≤ -1,5	0.03 N/mm	0.03 N/mm	0.00
qSd	=	(pSd + p0) s	22.92 MPa	22.92 MPa	0.00

		Hand calculation	Automated result	Difference %	
7.4 Resistance of plate between stiffeners					
ksp	=	√(1.0 - 3 (τSd/fy) ²)	0.97	0.97	-
τRd	=	fy / (√3 γM)	178.23	178.23	-
UCr	=	τSd / τRd	0.28	0.28	-
UCσ	=	σy,Sd / ksp σy,Rd	0.48	0.48	-

7.5 Characteristic buckling strength of stiffeners

		Hand calculation	Automated result	Difference %	
7.5.2 Torsional buckling of stiffeners					
IT	=	l	2,350.00 mm	2,350.00 mm	-
Iz	=	(1/12) Af b ² + ef ² Af / (1+ Af/Aw)	209,341.99 mm ⁴	209,341.99 mm ⁴	-
c	=	2 - s/l	1.88	1.88	0.00
fEpx	=	3.62 E (t/s) ²	95.36 MPa	95.36 MPa	-
fEpy	=	0.9 E (t/s) ²	23.71 MPa	23.71 MPa	-
fEpt	=	5.0 E (t/s) ²	131.71 MPa	131.71 MPa	-
σj,Sd	=	√(σx2,Sd + σy2,Sd - σx,Sd σy,Sd + 3τ2Sd)	88.88 MPa	88.88 MPa	0.00
λe	=	√((fy / σj,Sd) ((σx,Sd/fEpx)c + (σy,Sd/fEpy)c + (τSd/fEpt)c) 1/c)	1.97	1.97	0.00
fep	=	fy / √(1 + λ4e)	88.88 MPa	88.88 MPa	-
η	=	σj,Sd / fep; η ≤ 1.0	1.00	1.00	-
C	=	hw/s (t/tw) ³ √(1-h)	0.00	0.00	0.00
β	=	if s > l; 1.0	1.01	1.01	0.00
		if s ≤ l; (3C+0.2) / (C+0.2)			
fET	=	l; (b + 2(hw/IT) ²) G (tw/hw) ²	236.38 MPa	236.38 MPa	0.00
		L,T; b Aw+(tf/tw)2Af/(Aw+3Af)G(tw/hw)2+p2Elz/(Aw/3+Af)IT2			
λT	=	√(fy/fET)	1.23	1.23	-
μ	=	0.35(λT - 0.6)	0.22	0.22	0.00
fT / fy	=	if λT ≤ 0.6; 1.0	0.51	0.51	-
		if λT > 0.6; (1+μ+λT ² - √((1+μ+λT ²) ² - 4λT ²)) / (2 λT ²)			
fT	=	(fT / fy) fy	181.96 MPa	181.96 MPa	0.00
UCT	=	σx,Sd / fT	0.11	0.11	0.00

		Hand calculation	Automated result	Difference %	
7.5.1 General					
pf	=	(12 W) / (l2 s) (fy / γM); W is MIN(Wep and Wes)	0.03 MPa	0.03 MPa	0.00
lk	=	l (1 - 0.5 pSd/pf)	5,792.05 mm	5,792.05 mm	0.00
fE	=	π ² E (ie/lk) ²	364.90 MPa	364.90 MPa	0.00
frp	=	fy	355.00 MPa	355.00 MPa	-
frs	=	fy if λIT ≤ 0.6; fT (see eq. 7.28) if λIT > 0.6	181.96 MPa	181.96 MPa	0.00
λp	=	√(frp/fE)	0.99	0.99	0.00
λs	=	√(frs/fE)	0.71	0.71	0.00
μp	=	(0.34 + 0.08 (zpe/ie)) (- 0.2)	0.32	0.32	0.00
μs	=	(0.34 + 0.08 (zte/ie)) (- 0.2)	0.25	0.25	0.00
fkp/frp	=	if λ ≤ 0.2; 1.0	0.58	0.58	0.00
		if λ > 0.2; (1+μp+λ ² -√((1+μp+λ ²) ² -4λ ²)) / (2λ ²)			

fks/frs	=	if $\lambda \leq 0.2$; 1.0	=	0.72	0.72	-	0.00
		if $\lambda > 0.2$; $(1+\mu s+\lambda^2-v((1+\mu s+\lambda^2)^2-4\lambda^2)/(2\lambda^2))$					
fkp	=	(fkp / frp) frp	=	205.17	205.17	MPa	0.00
fks	=	(fks / frs) frs	=	131.44	131.44	MPa	0.00

7.6 Resistance of stiffened panels to shear stresses			Hand calculation	Automated result	Difference %	
τ_{crs}	=	$((36 E) / (s t l^2)) (l p l s^3)^{1/4}$	238.75	238.75	Mpa	-
τ_{Rdy}	=	$f_y / (\sqrt{3} yM)$	178.23	178.23	Mpa	-
τ_{Rdl}	=	τ_{crl} / yM	111.75	111.75	Mpa	-
τ_{Rds}	=	τ_{crs} / yM	207.61	207.61	Mpa	-
τ_{Rd}	=	minimum of τ_{Rdy} , τ_{Rdl} and τ_{Rds}	111.75	111.75	Mpa	-
UCt	=	τ_{Sd} / τ_{Rd}	0.45	0.45	-	-

7.7 Interaction formulas for axial compression and lateral pressure			Hand calculation	Automated result	Difference %	
7.7.3 Resistance parameters for stiffeners						
NRd	=	$A_e (f_y / yM)$	1,539,915.07	1,539,915.07	N	0.00
Nks,Rd	=	$A_e (f_{ks} / yM)$	570,161.19	570,161.19	N	0.00
Nkp,Rd	=	$A_e (f_{kp} / yM)$	889,986.57	889,986.57	N	0.00
Ms1,Rd	=	$W_{es} (f_r / yM)$	38,206,925.35	38,206,925.35	Nmm	0.00
Ms2,Rd	=	$W_{es} (f_r / yM)$	33,831,198.14	33,831,198.14	Nmm	0.00
Mst,Rd	=	$W_{es} (f_y / yM)$	64,919,561.42	64,919,561.42	Nmm	0.00
Mp,Rd	=	$W_{ep} (f_y / yM)$	133,950,932.74	133,950,932.74	Nmm	0.00
u	=	$(\tau_{Sd} / \tau_{Rd})^2$	0.20	0.20	-	0.00
NE	=	$(\pi^2 E A_e) / (l_k / i_e)^2$	1,820,279.89	1,820,279.89	N	0.00

7.7.1 Continuous stiffeners			Hand calculation	Automated result	Difference %	
M1,Sd	=	$Abs(q_{Sd} l_2 / 12)$	68,771,928.80	68,771,928.80	Nmm	0.00
M2,Sd	=	$Abs(q_{Sd} l_2 / 24)$	34,385,964.40	34,385,964.40	Nmm	0.00

Lateral pressure on plate side:						
	=	$(NSd/NksRd) + ((M1Sd-NSd z^*) / (Ms1Rd (1-(NSd/NE)))) + u$	2.17	2.17	-	0.20
	=	$(NSd/NkpRd) - 2 (NSd/NRd) + ((M1Sd-NSd z^*) / (MpRd (1-(NSd/NE)))) + u$	0.65	0.65	-	0.19
	=	$(NSd/NksRd) - 2 (NSd/NRd) + ((M2Sd+NSd z^*) / (MstRd (1-(NSd/NE)))) + u$	1.04	1.04	-	0.24
	=	$(NSd/NkpRd) + ((M2Sd+NSd z^*) / (MpRd (1-(NSd/NE)))) + u$	0.76	0.75	-	0.16
UCmax	=		2.17	2.17	-	0.20
Lateral pressure on stiffener side:						
	=	$(NSd/NksRd) - 2 (NSd/NRd) + ((M1Sd+NSd z^*) / (MstRd (1-(NSd/NE)))) + u$	1.48	1.50	-	1.13
	=	$(NSd/NkpRd) + ((M1Sd+NSd z^*) / (MpRd (1-(NSd/NE)))) + u$	0.97	0.98	-	0.83
	=	$(NSd/NksRd) + ((M2Sd-NSd z^*) / (Ms2Rd (1-(NSd/NE)))) + u$	1.53	1.50	-	2.09
	=	$(NSd/NkpRd) - 2 (NSd/NRd) + ((M2Sd-NSd z^*) / (MpRd (1-(NSd/NE)))) + u$	0.43	0.43	-	1.86
UCmax	=		1.53	1.50	-	2.09

VERIFICATION PANEL 7

#stiffeners = 5.00
 Stiffeners Type = HP160x8

pSd	=	design lateral pressure	=	0.0021 [MPa]
$\sigma_{1,Sd}$	=	largest occurring longitudinal stress	=	20 [MPa]
$\sigma_{2,Sd}$	=	smallest occurring longitudinal stress	=	20 [MPa]
$\sigma_{y1,Sd}$	=	largest occurring transverse stress	=	20 [MPa]
$\sigma_{y2,Sd}$	=	smallest occurring transverse stress	=	20 [MPa]
τ_{Sd}	=	occurring shear stress	=	50 [MPa]

Pannel data				
l	=	plate length	=	3000 [mm]
L_G	=	plate width / girder length	=	5000 [mm]
t	=	plate thickness	=	8 [mm]
L_p	=	length of pannel	=	18000 [mm]

Stiffeners / Girders		Hand calculation	Automated result	Difference %	
hw	=	height of web	= 145	144.61 [mm]	0.00
b	=	width of flange	= 32	31.58 [mm]	0.00
ef	=	eccentricity of flange	= 12	11.79 [mm]	0.00
tw	=	thickness of web	= 8	8.00 [mm]	-
tf	=	thickness of flange	= 15.4	15.39 [mm]	0.00
Aw	=	hw tw	= 1157	1,156.87 [mm ²]	0.00
Af	=	b tf	= 486	486.11 [mm ²]	0.00
n	=	number of stiffeners	= 5	5.00 [-]	0.00
s	=	Width between stiffeners	= 833	833.33	0.00

7.3 Effective plate width		Hand calculation	Automated result	Difference %	
se	=	s Cxs Cys	= 316.33	316.33 mm	0.00
Ae	=	Aw + Af + (se(n)/2 + se(n+1)/2) t ((t/2 + hw/2) Aw + (t/2 + hw + tf/2) Af)	= 4,173.64	4,173.64 mm ²	0.00
zpe	=	/ Ae	= 39.36	39.36 mm	0.00
zte	=	t/2 + hw + tf - zpe	= 124.64	124.64 mm	0.00
le	=	1/12 se t ³ + zpe ² se t + 1/12 tw hw ³ + (t/2 + hw/2 - zpe) ² Aw + 1/12 b tf ³ + (t/2 + hw + tf/2 - zpe) ² Af	= 14,186.64	14,186.64 ·10 ³ mm ⁴	0.00
ie	=	√(le / Ae)	= 58.30	58.30 mm	0.00
Wep	=	le / (zpe + t/2)	= 327,217.55	327,217.55 mm ³	0.00
Wes	=	le / zte	= 113,816.73	113,816.73 mm ³	0.00
A	=	Aw + Af + s t ((t/2 + hw/2) Aw + (t/2 + hw + tf/2) Af)	= 8,309.65	8,309.65 mm ²	0.00
zp	=	/ A	= 19.77	19.77 mm	0.00
zt	=	t/2 + hw + tf - zp	= 144.23	144.23 mm	0.00
ls	=	1/12 s t ³ + zp ² s t + 1/12 tw hw ³ + (t/2 + hw/2 - zp) ² Aw + 1/12 b tf ³ + (t/2 + hw + tf/2 - zp) ² Af	= 17,426.23	17,426.23 ·10 ³ mm ⁴	0.00
lp	=	t ³ s / 10.9	= 39,143.73	39,143.73 mm ⁴	0.00

7.2 Forces in the idealised stiffened plate		Hand calculation	Automated result	Difference %	
τ_{cr}	=	kl 0.904 E (t/s) ²	= 98.83	98.83 MPa	0.00
NSd	=	$\sigma_{x,Sd}$ (Aw + Af + s t) + τ_{tf} s t	= 166,192.92	166,192.92 N/mm	0.00
Ψ	=	$\sigma_{y2,Sd} / \sigma_{y1,Sd}$	= 1.00	1.00 -	-
kc	=	2 (1 + √(1 + (10.9 ls) / (t ³ s)))	= 44.25	44.25 -	0.00
C0	=	(Wes fy mc) / (kc E t ² s)	= 0.00	0.00 MPa	0.00
p0	=	(0.6 + 0.4 Ψ) C0 $\sigma_{y1,Sd}$ if $\Psi > -1,5$; 0	= 0.02	0.02 N/mm	0.00
qSd	=	(pSd + p0) s	= 19.82	19.82 MPa	0.00

7.4 Resistance of plate between stiffeners		Hand calculation	Automated result	Difference %	
ksp	=	√(1.0 - 3 (tSd/fy) ²)	= 0.97	0.97	0.00
τ_{Rd}	=	fy / (√3 γ_M)	= 178.23	178.23	0.00
UC τ	=	τ_{Sd} / τ_{Rd}	= 0.28	0.28	0.00
UC σ	=	$\sigma_{y,Sd} / ksp \sigma_{y,Rd}$	= 0.40	0.40	0.00

7.5 Characteristic buckling strength of stiffeners

7.5.2 Torsional buckling of stiffeners		Hand calculation	Automated result	Difference %	
IT	=	l	= 3,000.00	mm	0.00
Iz	=	(1/12) Af b ² + ef ² Af / (1+ Af/Aw)	= 88,000.81	88,000.81 mm ⁴	0.00

VERIFICATION PANEL 7

c	=	2- s/l	=	1.72	1.72	-	0.00
fEpx	=	3.62 E (t/s)2	=	70.06	70.06	MPa	0.00
fEpy	=	0.9 E (t/s)2	=	17.42	17.42	MPa	0.00
fEpt	=	5.0 E (t/s)2	=	96.77	96.77	MPa	0.00
σj,Sd	=	$\sqrt{(\sigma_{x,Sd} + \sigma_{y,Sd} - \sigma_{x,Sd} \sigma_{y,Sd} + 3\tau_{Sd})}$	=	88.88	88.88	Mpa	0.00
λe	=	$\sqrt{((f_y / \sigma_{j,Sd}) ((\sigma_{x,Sd}/f_{Epx})c + (\sigma_{y,Sd}/f_{Epy})c + (\tau_{Sd}/f_{Ept})c) / c)}$	=	2.33	2.33	-	0.00
fep	=	$f_y / \sqrt{1 + \lambda 4e}$	=	64.13	64.13	MPa	0.00
η	=	σj,Sd / fep; h ≤ 1.0	=	1.00	1.00	-	-
C	=	hw/s (t/tw)3 √(1-h)	=	-	-	-	-
β	=	if s > l; 1.0	=	1.00	1.00	-	-
fET	=	if s ≤ l; (3C+0.2) / (C+0.2) l; (b + 2(hw/IT)2) G (tw/hw)2	=	241.20	241.20	MPa	0.00
		L,T; b Aw+(tf/tw)2Af / (Aw+3Af)G(tw/hw)2 + p2Eiz/(Aw/3+Af)IT2					
λT	=	√(fy/fET)	=	1.21	1.21	-	0.00
μ	=	0.35(λT - 0.6)	=	0.21	0.21	-	0.00
fT / fy	=	if λT ≤ 0.6; 1.0	=	0.52	-	-	-
		if λT > 0.6; (1+μ+λT2 - √((1+μ+λT2)2 - 4λT2)) / (2 λT2)					
fT	=	(fT / fy) fy	=	184.92	184.92	MPa	0.00
UCT	=	σx,Sd / fT	=	0.11	0.11	-	0.00

7.5.1 General			Hand calculation	Automated result	Difference %	
pf	=	(12 W) / (l2 s) (fy / γM); W is MIN(WeI =	0.06	0.06	MPa	0.00
lk	=	l (1 - 0.5 pSd/pf)	2,943.97	2,943.97	mm	0.00
fE	=	π2 E (ie/lk)2	812.86	812.86	MPa	0.00
frp	=	fy	355.00	355.00	MPa	-
frs	=	fy if λIT ≤ 0.6; fT (see eq. 7.28) if λT > =	184.92	184.92	MPa	0.00
λp	=	√(frp/fE)	0.66	0.66	-	0.00
λs	=	√(frs/fE)	0.48	0.48	-	0.00
μp	=	(0.34 + 0.08 (zpe/ie)) (1 - 0.2)	0.18	0.18	-	0.00
μs	=	(0.34 + 0.08 (zte/ie)) (1 - 0.2)	0.14	0.14	-	0.00
fkp/frp	=	if λ ≤ 0.2; 1.0	0.78	0.78	-	0.00
		if λ > 0.2; (1+μp+λ2-√((1+μp+λ2)2)-4λ2) / (2λ2)				
fks/frs	=	if λ ≤ 0.2; 1.0	0.85	0.85	-	0.00
		if λ > 0.2; (1+μs+λ2-√((1+μs+λ2)2)-4λ2) / (2λ2)				
fkp	=	(fkp / frp) frp	278.20	278.20	MPa	0.00
fks	=	(fks / frs) frs	157.31	157.31	MPa	0.00

7.6 Resistance of stiffened panels to shear stresses			Hand calculation	Automated result	Difference %	
τcrs	=	((36 E) / (s t l2)) (lp ls3)1/4	478.01	478.01	Mpa	0.00
τRdy	=	fy / (√3 γM)	178.23	178.23	Mpa	0.00
τRdl	=	τcrl/γM	85.94	85.94	Mpa	-
τRds	=	τcrs/γM	415.66	415.66	Mpa	0.00
τRd	=	minimum of τRdy, τRdl and τRds	85.94	85.94	Mpa	-
UCt	=	τSd / τRd	0.58	0.58	-	-

7.7 Interaction formulas for axial compression and lateral pressure

7.7.3 Resistance parameters for stiffeners			Hand calculation	Automated result	Difference %	
NRd	=	Ae (fy / γM)	1,288,384.57	1,288,384.57	N	0.00
Nks,Rd	=	Ae (fks / γM)	570,918.44	570,918.44	N	0.00
Nkp,Rd	=	Ae (fkp / γM)	1,009,660.64	1,009,660.64	N	0.00
Ms1,Rd	=	Wes (fr / γM)	24,573,864.03	24,573,864.03	Nmm	0.00
Ms2,Rd	=	Wes (fr / γM)	19,078,823.99	19,078,823.99	Nmm	0.00
Mst,Rd	=	Wes (fy / γM)	35,134,728.94	35,134,728.94	Nmm	0.00
Mp,Rd	=	Wep (fy / γM)	101,010,633.92	101,010,633.92	Nmm	0.00
u	=	(τSd / τRd)2	0.34	0.34	-	0.00
NE	=	(π2 E Ae) / (lk/ie)2	3,392,603.99	3,392,603.99	N	0.00

VERIFICATION PANEL 7

7.7.1 Continuous stiffeners							
M1,Sd	=	Abs(qSd I2 / 12)	=	14,867,576.70	14,867,576.70	Nmm	0.00
M2,Sd	=	Abs(qSd I2 / 24)	=	7,433,788.35	7,433,788.35	Nmm	0.00

Lateral pressure on plate side:							
	=	$(NSd/NksRd) + ((M1Sd-NSd z^*) / (Ms1Rd (1-(NSd/NE)))) + u$	=	0.985929789	0.988457051	-	0.26
	=	$(NSd/NkpRd) - 2 (NSd/NRd) + (M1Sd-NSd z^*) / (MpRd (1-(NSd/NE))) + u$	=	0.331821591	0.332436423	-	0.19
	=	$(NSd/NksRd) - 2 (NSd/NRd) + (M2Sd+NSd z^*) / (MstRd (1-(NSd/NE))) + u$	=	0.789857485	0.788089873	-	0.22
	=	$(NSd/NkpRd) + (M2Sd+NSd z^*) / (MpRd (1-(NSd/NE))) + u$	=	0.648596767	0.647981935	-	0.09
UCmax	=		=	0.985929789	0.988457051	-	0.26
Lateral pressure on stiffener side:							
	=	$(NSd/NksRd) - 2 (NSd/NRd) + (M1Sd+NSd z^*) / (MstRd (1-(NSd/NE)))) + u$	=	0.894887708	0.896170187	-	0.14
	=	$(NSd/NkpRd) + (M1Sd+NSd z) / (MpRd (1-(NSd/NE))) + u$	=	0.685129637	0.685575725	-	0.07
	=	$(NSd/NksRd) + (M2Sd-NSd z) / (Ms2Rd (1-(NSd/NE))) + u$	=	0.895134347	0.892772588	-	0.26
	=	$(NSd/NkpRd) - 2 (NSd/NRd) + (M2Sd-NSd z) / (MpRd (1-(NSd/NE))) + u$	=	0.295288721	0.294842633	-	0.15
UCmax	=		=	0.895134347	0.896170187	-	0.12

H

OPTIMIZER RESULTS

OUTPUT SDC VERIFIER

Plate	Length	Width	Plate thi Sx	Sy	Sxy	
1..Section X 1 (X = 99.5)	6,000	5,000	0.008	-26399836.00	-9839720.00	79554872.00
1..Plate 1.11.1 (Y = 203.53; Z = 27.54)	6,000	5,000	0.008	-26399836.00	-9839720.00	79554872.00
1..Plate 1.22.1 (Y = 238.48; Z = 27.46)	6,000	5,000	0.008	-29540166.00	-8802524.00	74646712.00
1..Plate 1.40.1 (Y = 238.47; Z = 41.52)	6,000	5,000	0.008	-20893986.00	-4370551.00	48090424.00
1..Plate 1.75.1 (Y = 203.58; Z = 41.54)	6,000	5,000	0.008	-17513928.00	-4499604.50	41751136.00
1..Plate 1.23.1 (Y = 238.43; Z = 32.54)	5,000	4,000	0.008	-6131736.50	-43642440.00	66334048.00
1..Plate 1.12.1 (Y = 203.57; Z = 32.54)	5,000	4,000	0.008	-9435537.00	-40771136.00	62571500.00
1..Plate 1.72.1 (Y = 238.5; Z = 36.5)	5,000	4,000	0.008	-5236715.00	-34955268.00	59291180.00
1..Plate 1.76.1 (Y = 203.57; Z = 36.54)	5,000	4,000	0.008	-6020830.00	-30780778.00	51855160.00
1..Plate 1.4.1 (Y = 215.01; Z = 27.54)	6,000	4,000	0.008	0.00	-9207215.00	40168744.00
1..Plate 1.25.1 (Y = 227.01; Z = 41.55)	6,000	4,000	0.008	-5462136.50	-13968919.00	35307324.00
1..Plate 1.77.1 (Y = 238.5; Z = 46.53)	5,000	4,000	0.008	-2722987.00	-10692586.00	39141864.00
1..Plate 1.64.1 (Y = 215.01; Z = 41.55)	6,000	4,000	0.008	-9402414.00	-10687616.00	32605648.00
1..Plate 1.17.1 (Y = 227; Z = 32.6)	4,000	4,000	0.008	-12169524.00	-7827793.00	40138508.00
1..Plate 1.7.1 (Y = 215; Z = 32.6)	4,000	4,000	0.008	-9392923.00	-4782604.00	39239892.00
1..Plate 1.8.1 (Y = 219.01; Z = 27.54)	6,000	4,000	0.008	0.00	-6077623.00	29379866.00
1..Plate 1.61.1 (Y = 215.04; Z = 36.57)	4,000	4,000	0.008	-7407215.00	-10270659.00	35276624.00
1..Plate 1.79.1 (Y = 203.54; Z = 46.52)	5,000	4,000	0.008	-5236250.50	-6141173.00	28943610.00
1..Plate 1.29.1 (Y = 226.98; Z = 46.56)	4,000	4,000	0.008	-9074569.00	-19978230.00	31493280.00
1..Plate 1.49.1 (Y = 222.99; Z = 41.48)	6,000	4,000	0.008	-6029504.00	-11139336.00	22896008.00
1..Plate 1.50.1 (Y = 219.01; Z = 41.55)	6,000	4,000	0.008	-7315335.50	-10934181.00	22884848.00
1..Plate 1.9.1 (Y = 219.01; Z = 32.6)	4,000	4,000	0.008	-10589694.00	-3303855.00	27911330.00
1..Plate 1.14.1 (Y = 223.01; Z = 27.54)	6,000	4,000	0.008	0.00	-4339016.00	33401574.00
1..Plate 1.33.1 (Y = 227.04; Z = 50.56)	4,000	4,000	0.008	-147261.69	-31327252.00	22137560.00
1..Plate 1.70.1 (Y = 222.97; Z = 46.61)	4,000	4,000	0.008	-8160674.50	-17498624.00	22203802.00
1..Plate 1.67.1 (Y = 215; Z = 46.6)	4,000	4,000	0.008	-14085619.00	-9256890.00	20434914.00
1..Plate 1.16.1 (Y = 227.01; Z = 27.54)	6,000	4,000	0.008	0.00	-4100438.00	38654104.00

1..Plate 1.36.1 (Y = 238.45; Z = 50.53)	5,000	4,000	0.008	-3087215.50	-3278166.25	15576588.00
1..Plate 1.55.1 (Y = 203.55; Z = 50.53)	5,000	4,000	0.008	-7415888.50	-2570144.00	14998853.00
1..Plate 1.15.1 (Y = 222.96; Z = 32.67)	4,000	4,000	0.008	-10329553.00	-6486261.50	30605786.00
1..Plate 1.68.1 (Y = 219.01; Z = 46.58)	4,000	4,000	0.008	-16118991.00	-8682129.00	12395273.00
1..Plate 1.27.1 (Y = 227.01; Z = 36.54)	4,000	4,000	0.008	-11151584.00	-332512.06	42029924.00
1..Plate 1.41.1 (Y = 223; Z = 50.55)	4,000	4,000	0.008	-27880776.00	0.00	17211812.00
1..Plate 1.52.1 (Y = 219.01; Z = 50.54)	4,000	4,000	0.008	-25930316.00	0.00	10230353.00
1..Plate 1.56.1 (Y = 215; Z = 50.56)	4,000	4,000	0.008	-22424420.00	0.00	9684314.00
1..Plate 1.10.1 (Y = 207.73; Z = 27.56)	6,000	3,500	0.008	-12190649.00	-14666018.00	61203988.00
1..Plate 1.21.1 (Y = 234.25; Z = 32.61)	4,000	3,500	0.008	-13907179.00	-11274843.00	68313296.00
1..Plate 1.39.1 (Y = 234.21; Z = 41.56)	6,000	3,500	0.008	-9994427.00	-11434294.00	52971572.00
1..Plate 1.5.1 (Y = 211.23; Z = 27.56)	6,000	3,500	0.008	-5035807.00	-12418841.00	50340044.00
1..Plate 1.57.1 (Y = 234.22; Z = 36.53)	4,000	3,500	0.008	-11948322.00	-11492116.00	62920068.00
1..Plate 1.24.1 (Y = 230.75; Z = 41.56)	6,000	3,500	0.008	-5922845.00	-13857062.00	46103332.00
1..Plate 1.13.1 (Y = 207.75; Z = 32.61)	4,000	3,500	0.008	-18458972.00	-13894804.00	57531980.00
1..Plate 1.73.1 (Y = 207.75; Z = 41.57)	6,000	3,500	0.008	-14543143.00	-10186173.00	44867272.00
1..Plate 1.18.1 (Y = 234.27; Z = 27.79)	6,000	3,500	0.008	-2756687.00	-9346697.00	53887176.00
1..Plate 1.74.1 (Y = 207.75; Z = 36.61)	4,000	3,500	0.008	-15678899.00	-11953117.00	54476112.00
1..Plate 1.26.1 (Y = 230.75; Z = 36.57)	4,000	3,500	0.008	-1145758.50	-11332574.00	53337564.00
1..Plate 1.20.1 (Y = 230.73; Z = 32.62)	4,000	3,500	0.008	-7195259.00	-11862909.00	52975676.00
1..Plate 1.65.1 (Y = 211.25; Z = 41.56)	6,000	3,500	0.008	-11415466.00	-10458456.00	38917932.00
1..Plate 1.6.1 (Y = 211.25; Z = 32.61)	4,000	3,500	0.008	-11820678.00	-9941207.00	47960696.00
1..Plate 1.62.1 (Y = 211.23; Z = 36.57)	4,000	3,500	0.008	-10098492.00	-11845936.00	47938524.00
1..Plate 1.71.1 (Y = 234.28; Z = 46.59)	4,000	3,500	0.008	-9970944.00	-12719573.00	42543252.00
1..Plate 1.28.1 (Y = 230.76; Z = 46.57)	4,000	3,500	0.008	-9478555.00	-17761218.00	39996072.00
1..Plate 1.78.1 (Y = 207.78; Z = 46.58)	4,000	3,500	0.008	-8205061.00	-11729452.00	29877626.00

1..Plate 1.19.1 (Y = 230.78; Z = 27.52)	6,000	3,500	0.008	0.00	-1988736.25	44049300.00
1..Plate 1.66.1 (Y = 211.23; Z = 46.62)	4,000	3,500	0.008	-9096751.00	-12147768.00	26273778.00
1..Plate 1.32.1 (Y = 230.76; Z = 50.61)	4,000	3,500	0.008	-171852.19	-26320800.00	25208358.00
1..Plate 1.34.1 (Y = 234.24; Z = 50.61)	4,000	3,500	0.008	-1339460.50	-16167078.00	23114538.00
1..Plate 1.54.1 (Y = 207.73; Z = 50.56)	4,000	3,500	0.008	-2328931.25	-15047404.00	15968358.00
1..Plate 1.53.1 (Y = 211.25; Z = 50.57)	4,000	3,500	0.008	-697474.50	-18220022.00	13656769.00
1..Plate 1.45.1 (Y = 223.38; Z = 36.53)	4,000	3,300	0.008	-767763.56	-8186313.50	27398708.00
1..Plate 1.60.1 (Y = 218.22; Z = 36.54)	4,000	2,500	0.008	-4343770.00	-6120954.00	24645436.00

OPTIMIZATION RESULTS

	Plate	SigmaxSd	SigmaySd	TauSd	I	Lg	Type	#stiffeners	girders	UCMaxPSzStar	WeldLength	plateThickness
0	1..Section X 1 (X = 99.5)	26.399836	9.83972	79.554872	3	5	HP120x7	6	1	0.988795318	36	0.008
1	1..Plate 1.11.1 (Y = 203.53; Z = 27.54)	26.399836	9.83972	79.554872	3	5	HP120x7	6	1	0.988795318	36	0.008
2	1..Plate 1.22.1 (Y = 238.48; Z = 27.46)	29.540166	8.802524	74.646712	3	5	HP120x7	6	1	0.901752593	36	0.008
3	1..Plate 1.40.1 (Y = 238.47; Z = 41.52)	20.893986	4.370551	48.090424	6	5	HP180x9	5	0	0.966019075	60	0.008
4	1..Plate 1.75.1 (Y = 203.58; Z = 41.54)	17.513928	4.4996045	41.751136	6	5	HP180x9	5	0	0.874413444	60	0.008
5	1..Plate 1.23.1 (Y = 238.43; Z = 32.54)	6.1317365	43.64244	66.334048	2.5	4	HP200x10	4	1	0.964994273	20	0.008
6	1..Plate 1.12.1 (Y = 203.57; Z = 32.54)	9.435537	40.771136	62.5715	2.5	4	HP200x10	4	1	0.882479521	20	0.008
7	1..Plate 1.72.1 (Y = 238.5; Z = 36.5)	5.236715	34.955268	59.29118	2.5	4	HP180x9	4	1	0.880113431	20	0.008
8	1..Plate 1.76.1 (Y = 203.57; Z = 36.54)	6.02083	30.780778	51.85516	2.5	4	HP160x8	4	1	0.871596496	20	0.008
9	1..Plate 1.4.1 (Y = 215.01; Z = 27.54)	0	9.207215	40.168744	6	4	HP200x10	4	0	0.953830854	48	0.008
10	1..Plate 1.25.1 (Y = 227.01; Z = 41.55)	5.4621365	13.968919	35.307324	3	4	HP140x8	3	1	0.96273342	18	0.008
11	1..Plate 1.77.1 (Y = 238.5; Z = 46.53)	2.722987	10.692586	39.141864	5	4	HP180x9	4	0	0.910001293	40	0.008
12	1..Plate 1.64.1 (Y = 215.01; Z = 41.55)	9.402414	10.687616	32.605648	6	4	HP200x10	5	0	0.854789672	60	0.008
13	1..Plate 1.17.1 (Y = 227; Z = 32.6)	12.169524	7.827793	40.138508	4	4	HP180x9	3	0	0.923961913	24	0.008
14	1..Plate 1.7.1 (Y = 215; Z = 32.6)	9.392923	4.782604	39.239892	4	4	HP140x8	3	0	0.925811963	24	0.008
15	1..Plate 1.8.1 (Y = 219.01; Z = 27.54)	0	6.077623	29.379866	6	4	HP200x10	3	0	0.877356044	36	0.008
16	1..Plate 1.61.1 (Y = 215.04; Z = 36.57)	7.407215	10.270659	35.276624	4	4	HP180x9	3	0	0.938298643	24	0.008
17	1..Plate 1.79.1 (Y = 203.54; Z = 46.52)	5.2362505	6.141173	28.94361	5	4	HP160x8	3	0	0.943941923	30	0.008
18	1..Plate 1.29.1 (Y = 226.98; Z = 46.56)	9.074569	19.97823	31.49328	4	4	HP200x10	4	0	0.855472863	32	0.008
19	1..Plate 1.49.1 (Y = 222.99; Z = 41.48)	6.029504	11.139336	22.896008	6	4	HP200x10	4	0	0.983538439	48	0.008
20	1..Plate 1.50.1 (Y = 219.01; Z = 41.55)	7.3153355	10.934181	22.884848	6	4	HP200x10	4	0	0.97389296	48	0.008
21	1..Plate 1.9.1 (Y = 219.01; Z = 32.6)	10.589694	3.303855	27.91133	4	4	HP180x9	2	0	0.967535477	16	0.008
22	1..Plate 1.14.1 (Y = 223.01; Z = 27.54)	0	4.339016	33.401574	6	4	HP180x9	3	0	0.923396222	36	0.008
23	1..Plate 1.33.1 (Y = 227.04; Z = 50.56)	0.14726169	31.327252	22.13756	2	4	HP100x8	2	1	0.999869834	8	0.008
24	1..Plate 1.70.1 (Y = 222.97; Z = 46.61)	8.1606745	17.498624	22.203802	4	4	HP200x10	3	0	0.859363251	24	0.008
25	1..Plate 1.67.1 (Y = 215; Z = 46.6)	14.085619	9.25689	20.434914	4	4	HP180x9	2	0	0.990022286	16	0.008
26	1..Plate 1.16.1 (Y = 227.01; Z = 27.54)	0	4.100438	38.654104	6	4	HP200x10	3	0	0.911502609	36	0.008
27	1..Plate 1.36.1 (Y = 238.45; Z = 50.53)	3.0872155	3.27816625	15.576588	5	4	HP140x8	2	0	0.939827598	20	0.008
28	1..Plate 1.55.1 (Y = 203.55; Z = 50.53)	7.4158885	2.570144	14.998853	5	4	HP140x8	2	0	0.898285432	20	0.008
29	1..Plate 1.15.1 (Y = 222.96; Z = 32.67)	10.329553	6.4862615	30.605786	4	4	HP140x8	3	0	0.867784819	24	0.008
30	1..Plate 1.68.1 (Y = 219.01; Z = 46.58)	16.118991	8.682129	12.395273	4	4	HP160x8	2	0	0.975252156	16	0.008

31	1..Plate 1.27.1 (Y = 227.01; Z = 36.54)	11.151584	0.33251206	42.029924	4	4	HP100x7	3	0	0.967435248	24	0.008
32	1..Plate 1.41.1 (Y = 223; Z = 50.55)	27.880776	0	17.211812	4	4	HP120x8	2	0	0.971844429	16	0.008
33	1..Plate 1.52.1 (Y = 219.01; Z = 50.54)	25.930316	0	10.230353	4	4	HP180x9	1	0	0.914105528	8	0.008
34	1..Plate 1.56.1 (Y = 215; Z = 50.56)	22.42442	0	9.684314	4	4	HP160x8	1	0	0.891711987	8	0.008
35	1..Plate 1.10.1 (Y = 207.73; Z = 27.56)	12.190649	14.666018	61.203988	3	3.5	HP180x9	3	1	0.979870265	18	0.008
36	1..Plate 1.21.1 (Y = 234.25; Z = 32.61)	13.907179	11.274843	68.313296	4	3.5	HP160x8	4	0	0.909979724	32	0.008
37	1..Plate 1.39.1 (Y = 234.21; Z = 41.56)	9.994427	11.434294	52.971572	6	3.5	HP200x10	5	0	0.882258922	60	0.008
38	1..Plate 1.5.1 (Y = 211.23; Z = 27.56)	5.035807	12.418841	50.340044	6	3.5	HP200x10	5	0	0.912230025	60	0.008
39	1..Plate 1.57.1 (Y = 234.22; Z = 36.53)	11.948322	11.492116	62.920068	4	3.5	HP160x8	4	0	0.858580475	32	0.008
40	1..Plate 1.24.1 (Y = 230.75; Z = 41.56)	5.922845	13.857062	46.103332	6	3.5	HP200x10	5	0	0.988846763	60	0.008
41	1..Plate 1.13.1 (Y = 207.75; Z = 32.61)	18.458972	13.894804	57.53198	4	3.5	HP160x8	4	0	0.936305474	32	0.008
42	1..Plate 1.73.1 (Y = 207.75; Z = 41.57)	14.543143	10.186173	44.867272	6	3.5	HP200x10	4	0	0.957979626	48	0.008
43	1..Plate 1.18.1 (Y = 234.27; Z = 27.79)	2.756687	9.346697	53.887176	6	3.5	HP200x10	4	0	0.924998751	48	0.008
44	1..Plate 1.74.1 (Y = 207.75; Z = 36.61)	15.678899	11.953117	54.476112	4	3.5	HP200x10	3	0	0.993943471	24	0.008
45	1..Plate 1.26.1 (Y = 230.75; Z = 36.57)	1.1457585	11.332574	53.337564	4	3.5	HP200x10	3	0	0.938697141	24	0.008
46	1..Plate 1.20.1 (Y = 230.73; Z = 32.62)	7.195259	11.862909	52.975676	4	3.5	HP200x10	3	0	0.957310013	24	0.008
47	1..Plate 1.65.1 (Y = 211.25; Z = 41.56)	11.415466	10.458456	38.917932	6	3.5	HP200x10	4	0	0.924640257	48	0.008
48	1..Plate 1.6.1 (Y = 211.25; Z = 32.61)	11.820678	9.941207	47.960696	4	3.5	HP180x9	3	0	0.867892682	24	0.008
49	1..Plate 1.62.1 (Y = 211.23; Z = 36.57)	10.098492	11.845936	47.938524	4	3.5	HP200x10	3	0	0.871890541	24	0.008
50	1..Plate 1.71.1 (Y = 234.28; Z = 46.59)	9.970944	12.719573	42.543252	4	3.5	HP180x9	3	0	0.971112518	24	0.008
51	1..Plate 1.28.1 (Y = 230.76; Z = 46.57)	9.478555	17.761218	39.996072	4	3.5	HP200x10	3	0	0.961791704	24	0.008
52	1..Plate 1.78.1 (Y = 207.78; Z = 46.58)	8.205061	11.729452	29.877626	4	3.5	HP160x8	3	0	0.832960809	24	0.008
53	1..Plate 1.19.1 (Y = 230.78; Z = 27.52)	0	1.98873625	44.0493	6	3.5	HP140x8	3	0	0.890306926	36	0.008
54	1..Plate 1.66.1 (Y = 211.23; Z = 46.62)	9.096751	12.147768	26.273778	4	3.5	HP200x10	2	0	0.916035566	16	0.008
55	1..Plate 1.32.1 (Y = 230.76; Z = 50.61)	0.17185219	26.3208	25.208358	4	3.5	HP200x10	4	0	0.931534271	32	0.008
56	1..Plate 1.34.1 (Y = 234.24; Z = 50.61)	1.3394605	16.167078	23.114538	4	3.5	HP200x10	2	0	0.98111771	16	0.008
57	1..Plate 1.54.1 (Y = 207.73; Z = 50.56)	2.32893125	15.047404	15.968358	4	3.5	HP180x9	2	0	0.985911454	16	0.008
58	1..Plate 1.53.1 (Y = 211.25; Z = 50.57)	0.6974745	18.220022	13.656769	4	3.5	HP200x10	2	0	0.880980675	16	0.008
59	1..Plate 1.45.1 (Y = 223.38; Z = 36.53)	0.76776356	8.1863135	27.398708	4	3.3	HP160x8	2	0	0.967538472	16	0.008
60	1..Plate 1.60.1 (Y = 218.22; Z = 36.54)	4.34377	6.120954	24.645436	4	2.5	HP160x8	1	0	0.991700253	8	0.008



**CODE FOR SECOND ORDER
PLATE-STIFFENER ANALYSIS**

```

1 #workbench script for distributed load analysis
2
3 #%% data pre processing
4 execfile('C:\Strip experiment with finer mesh\Scripting files\Strip\second
step\Workbench second step pre processing.py')
5
6 #%% End data pre processing
7
8
9 #set scripting version
10 SetScriptVersion(Version="21.2.209")
11 system1 = GetSystem(Name="SYS")
12 InventorfilePath = 'C:\Strip experiment with finer mesh\inventor files refined mesh'
13 resultsPath = 'C:\Strip experiment with finer mesh\Results'
14 scriptPath = 'C:\Strip experiment with finer mesh\Scripting files\Strip\second step'
15
16 for subdir, dirs, files in os.walk(InventorfilePath):
17     for file in files:
18         #Import new geometry and update the model
19         geometry1 = system1.GetContainer(ComponentName="Geometry")
20         geometry1.SetFile(FilePath=InventorfilePath+file)
21         modelComponent1 = system1.GetComponent(Name="Model")
22         modelComponent1.Update(AllDependencies=True)
23         model1 = system1.GetContainer(ComponentName="Model")
24         model1.Edit()
25
26         #load mechanical stript for eigenvalue analysis
27         DSscript = open(scriptPath+"\Eigenvalue strip second step.py", "r")
28         DSscriptcommand=DSscript.read()
29         DSscript.close()
30
31         # Send the command
32         model1.SendCommand(Language='Python', Command = DSscriptcommand)
33
34         #geometry is now fully loaded
35         #get plate thickness from file name
36
37         plateThickness = ''
38         for num in file[7:]: #extracts number from path # becaurefull!!! brackets
ignore characters was only necessary for certain name
39             if num.isdigit() or num == '.':
40                 plateThickness += num
41         plateThickness = int(float(plateThickness))
42
43         #Define scale factor according to slenderness ratio
44         with open(scriptPath + '/Variables.txt') as csv_file:
45             csv_reader = csv.reader(csv_file)
46             header = next(csv_reader)
47             variables = next(csv_reader)
48             w0 =float(variables[0])
49             Thickness = int(float(variables[1]))
50
51         if Thickness != plateThickness:
52             raise ValueError('plate thickness form file name does not mach the plate
chicknes from the first mechanical execution')
53
54         #get the mode at which the maximum force is present
55         with open(resultsPath + '/maxforces.txt') as file:
56             csv_reader = csv.reader(file)

```

```
57     for row in csv_reader:
58         if row[3] == str(Thickness):
59             mode1 = row[1]
60
61
62
63     system2 = GetSystem(Name="SYS 1")
64     solution2 = system2.GetContainer(ComponentName="Solution")
65     modalUpdateOptionsForCdbTransfer1 =
solution2.GetModalUpdateOptionsForCdbTransfer(Name="ModalUpdateOptionsForCdbTransfer"
)
66     modalUpdateOptionsForCdbTransfer1.ScaleFactor = w0
67     modalUpdateOptionsForCdbTransfer1.Mode = mode1
68
69     system3 = GetSystem(Name="SYS 2")
70     modelComponent2 = system3.GetComponent(Name="Model")
71     modelComponent2.Update(AllDependencies=True)
72     model2 = system3.GetContainer(ComponentName="Model")
73     model2.Edit()
74
75
76     #load mechanical script for eigenvalue analysis
77     DSscript = open(scriptPath+ "/Non-linear second step.py", "r")
78     DSscriptcommand1=DSscript.read()
79     DSscript.close()
80
81     # Send the command
82     model2.SendCommand(Language='Python', Command = DSscriptcommand1)
83
84
```

```

1 # Non-linear analysis of distributed loads
2
3 import os
4 import csv
5 import math
6
7 #variables
8 plateWidth = 833
9 webHeight = 145
10 flangeWidth = 30
11 flangeWebThickness = 8
12
13 Model.Analyses[0].Children[4].Suppressed = True #supresses displacement
14 Model.Analyses[0].Children[3].Suppressed = False #unsupresses the pressure
15
16 InventorfilePath = 'C:\Strip experiment with finer mesh\inventor files refined mesh'
17 resultsPath = 'C:\Strip experiment with finer mesh\Results'
18 scriptPath = 'C:\Strip experiment with finer mesh\Scripting files\Strip\second step'
19
20
21 #check if plate thickness is same as elsewhere in the script
22 with open(scriptPath + '/Variables.txt') as csv_file:
23     csv_reader = csv.reader(csv_file)
24     header = next(csv_reader)
25     variables = next(csv_reader)
26     w0 = float(variables[0])
27     Thickness = int(float(variables[1]))
28
29 plateThickness = Thickness
30 A = plateWidth*plateThickness+(flangeWidth+webHeight)*flangeWebThickness
31
32 PressurePath = resultsPath + '/Analysis {} mm/pressureVectors {}
mm.txt'.format(plateThickness,plateThickness)
33 path = resultsPath + '/Analysis {} mm'.format(plateThickness)
34
35 #open the csv file with pressure vectorswith open(resultsPath+'Analysis {}
mm\pressureVectors {} mm.txt'.format(plateThickness,plateThickness), 'r') as file:
36 with open(PressurePath, 'r') as csvFile:
37
38     csv_reader = csv.reader(csvFile)
39     rowCount = 0
40     for row in csv_reader:
41         if rowCount == 0:
42             header = row
43             rowCount += 1
44         elif row == []:
45             continue
46         elif rowCount == 1:
47             xvector = row
48             xvectorQuantity = ''
49             for index,value in enumerate(xvector):
50                 xvectorQuantity = xvectorQuantity + 'Quantity("{} [mm]"),
'.format(round(float(xvector[index]),2))
51                 xvectorQuantity = xvectorQuantity[:-2]
52                 xvectorQuantity = '['+xvectorQuantity+']'
53                 #load values into ansys
54                 Model.Analyses[0].Children[3].Magnitude.Inputs[0].DiscreteValues =
eval(xvectorQuantity)
55

```

```

56         rowCount += 1
57     else:
58         globals()['function%s' % str(rowCount-1)] = row
59         #convert the forces into pressures
60         globals()['function%s Quantity' % str(rowCount-1)] = ''
61         for index,value in enumerate(globals()['function%s' % str(rowCount-1)]):
62             globals()['function%s' % str(rowCount-1)][index] = float(value)/A
63             globals()['function%s Quantity' % str(rowCount-1)] = globals()
['function%s Quantity' % str(rowCount-1)] + 'Quantity("{} [MPa]"),
'.format(round(globals()['function%s' % str(rowCount-1)][index],3))
64             globals()['function%s Quantity' % str(rowCount-1)] = globals()
['function%s Quantity' % str(rowCount-1)][:-2]
65             globals()['function%s Quantity' % str(rowCount-1)] = '['+globals()
['function%s Quantity' % str(rowCount-1)]+']'
66             #load values into ansys
67             Model.Analyses[0].Children[3].Magnitude.Output.DiscreteValues =
eval(globals()['function%s Quantity' % str(rowCount-1)])
68
69             #solve
70             Model.Solve(True)
71             #save results
72             newpath = path + '/function%s' % str(rowCount-1)
73             if not os.path.exists(newpath):
74                 os.makedirs(newpath)
75             # script to export all results in the tree to AVZ (3D image) files.
76             # get a list of all the results in the project
77             results
=ExtAPI.DataModel.GetObjectsByType(DataModelObjectCategory.Result)
78             #loop over the results
79             for n in range(0,results.Count):
80                 # select and activate the result
81                 result = results[n]
82                 result.Activate()
83
84                 # export the result to avz file using the result name for the filename
85                 mvm = ExtAPI.Graphics.ModelViewManager
86                 avzFilename = newpath + '/' + result.Name + '.avz'
87                 ExtAPI.Graphics.Export3D(avzFilename)
88                 #export as textFile
89                 result.ExportToTextFile(newpath + '\ '+result.Name+'.txt')
90
91             forces = []
92             for i in range(100):
93
94                 forces.append(abs(Model.Analyses[0].Solution.Children[5].InternalObject.SequenceZVec
tor(i)))
95                 forces.append(max(forces))
96
97                 #write force probe values to file
98                 with open(newpath+'\Force Reaction.txt', 'a') as f:
99
100                     fwriter = csv.writer(f, delimiter=',')
101                     fwriter.writerow(forces)
102
103                 forces = []
104                 for i in range(100):
105
106                     forces.append(abs(Model.Analyses[0].Solution.Children[6].InternalObject.SequenceZVec
tor(i)))
107                     forces.append(max(forces))

```

```
106
107     #write displacement probe values to file
108     with open(newpath+'\Displacement Reaction.txt', 'a') as f:
109
110         fwriter = csv.writer(f, delimiter=',')
111         fwriter.writerow(forces)
112
113     rowCount += 1
114
115
116     #get the values as pressures and loaded into ansys
117     # code for updating tabular data in gui
118     # pressure_36.Magnitude.Output.DiscreteValues = [Quantity("10 [MPa]"),
Quantity("20 [MPa]")]
119     # pressure_36.Magnitude.Inputs[0].DiscreteValues = [Quantity("0 [mm]"),
Quantity("10 [mm]")]
120
121
122
123
```

```
1 #Eigenvalue anlyais of distributed loads
2
3 import os
4 import csv
5
6 InventorfilePath = 'C:\Strip experiment with finer mesh\inventor files refined mesh'
7 resultsPath = 'C:\Strip experiment with finer mesh\Results'
8 scriptPath = 'C:\Strip experiment with finer mesh\Scripting files\Strip\second step'
9
10
11 def NumFromString(string):
12     stringNumbers = ''
13     for num in string:
14         if num.isdigit():
15             stringNumbers += num
16         if num == '.':
17             stringNumbers += num
18     return float(stringNumbers)
19
20
21
22 #get the body
23 Model = ExtAPI.DataModel.Project.Model
24 #set its material to structural steel NL
25 Model.Children[0].Children[0].Material = "4720b8bb-0d5c-4e4c-96cf-1810ac75e2e7"
26
27 Model.Children[4].ElementSize = Quantity(30, "mm")
28
29 #length in x
30 PlateWidth = str(Model.Children[0].Children[0].LengthX)
31 PlateWidth = NumFromString(PlateWidth)
32
33 #height of body
34 Height = str(Model.Children[0].Children[0].LengthY)
35 Height = NumFromString(Height)
36 #height of body
37 Length = str(Model.Children[0].Children[0].LengthZ)
38 Length = NumFromString(Length)
39
40 #variables
41 flangeThickness = 8
42 WebHeight = 145
43 yieldStrength = 355e6
44 E = 210e9
45
46 B = PlateWidth
47 t = Height - flangeThickness - WebHeight
48 slendernessRatio = B/t*(yieldStrength/E)**0.5
49 w0 = 0.1*slendernessRatio**2*t
50
51 with open(scriptPath+'/Variables.txt', 'w') as f:
52     fwriter = csv.writer(f, delimiter=',')
53     header = ['Initial imperfection', 't', 'slendernessRatio']
54     fwriter.writerow(header)
55     fwriter.writerow([w0, round(t, 3), slendernessRatio])
56
57
58
```

```
1 #Pre processing of uniformly loaded ultimate resistances
2 #
3 import os
4 import csv
5 import math
6
7 plateWidth = 833
8
9 InventorfilePath = 'C:\higher resistance thinner plate test\inventor files refined
mesh'
10 resultsPath = 'C:\higher resistance thinner plate test\Results'
11 scriptPath = 'C:\higher resistance thinner plate test\Scripting files\Strip\First
step'
12
13
14 header = ['Directory','mode','maxForce','plateThickness']
15 with open(resultsPath+'/maxforces.txt', 'w') as file:
16
17     writer = csv.writer(file)
18     writer.writerow(header)
19     file.close()
20
21 #%%
22
23 for subdir, dirs, files in os.walk(resultsPath):
24     for file in files:
25         if file == 'Force Reaction.txt':
26             with open(subdir+'/Force Reaction.txt') as csvFile: #iterate through
results and construct a file with the ultimate resistance at a certain mode
27                 csv_reader = csv.reader(csvFile, delimiter=',')
28                 lineCount = 0
29                 maxForceMode = []
30                 mode = 0
31                 for row in csv_reader:
32                     if lineCount == 0:
33                         lineCount += 1
34                         continue
35                     elif row == []:
36                         lineCount += 1
37                         continue
38                     else:
39                         mode += 1
40                         maxForceMode.append([mode,row[-1]])
41                         lineCount += 1
42                 csvFile.close()
43
44                 minMaxForcePerMode = [0,1e10]
45                 for mode in maxForceMode:
46                     if float(mode[1]) < float(minMaxForcePerMode[1]):
47                         minMaxForcePerMode = mode
48
49                 plateThickness = ''
50                 for num in subdir: #extracts number from path
51
52                     if num.isdigit() or num == '.':
53                         plateThickness += num
54                 #write result to file
55                 data = [subdir, minMaxForcePerMode[0],
minMaxForcePerMode[1],plateThickness]
```

```

56         with open(resultsPath+'/maxforces.txt', 'a') as file:
57
58             writer = csv.writer(file)
59             writer.writerow(data)
60             file.close()
61
62
63
64
65
66
67
68
69
70
71
72
73
74
75
76
77
78
79
80
81
82
83
84
85
86
87
88
89
90
91
92
93
94
95
96
97
98
99
100
101
102
103
104
105
106
107
108
109

```

```

110 #%%
111
112
113 for subdir, dirs, files in os.walk(resultsPath):
114     for index01, dirss in enumerate(dirs):
115         print(dirss)
116         resistance = listOfMaxForces[index01] #gets the resistance. Must me in right
order ofcourse
117
118
119         #create file for pressure vectors
120         header = ['xvector, first is spacial the latter are functions:'+
str(functions)]
121         with open(resultsPath+'/'+dirss+'/pressureVectors {}
mm.txt'.format(listOfPlateThicknesses[index01]), 'w') as file:
122
123             writer = csv.writer(file)
124             writer.writerow(header)
125             writer.writerow(xvector)
126             file.close()
127             for index02, func in enumerate(functions):
128                 #turns the force over the plate into pressure over the plate
129                 #A = (plateWidth*plateThickness)+(145+30)*8
130
131
132                 #create variables to store functions
133                 globals()['function%s' % functions[index02]] = []
134                 for index, element in enumerate(xvector):
135                     x = element
136                     x = eval(functions[index02])#/A
137                     globals()['function%s' % functions[index02]].append(x)
138
139                 # #plot a graph
140                 # plt.figure(dpi = 200)
141                 # plt.plot(xvector, globals()['function%s' % functions[index02]])
142                 # # plt.plot(time, X2)
143
144                 # # plt.ylim(ymax=2.5, ymin=-2.5)
145                 # # plt.legend(["X", "Y", "Z"], loc = "best")
146                 # plt.title('Function: '+functions[index02])
147                 # #plt.ylim([-ampl_acc_plot, ampl_acc_plot])
148                 # plt.xlabel('x-location [mm]')
149                 # #plt.ylabel('Rot. [$deg/s$]')
150                 # plt.ylabel('Pressure [MPa]')
151                 # #plt.legend()
152                 # plt.tight_layout()
153                 # plt.show()
154
155                 #store the vectors in a CSV file
156
157                 with open(resultsPath+'/'+dirss+'/pressureVectors {}
mm.txt'.format(listOfPlateThicknesses[index01]), 'a') as file:
158
159                     writer = csv.writer(file)
160                     writer.writerow(globals()['function%s' % functions[index02]])
161                     file.close()
162
163
164

```

```
1 #Ultimate resistance for each mode, uniformly loaded
2
3 import os
4 import csv
5 import math
6
7 #set scripting version
8 SetScriptVersion(Version="21.2.209")
9 system1 = GetSystem(Name="SYS")
10
11
12 InventorfilePath = 'C:\higher resistance thinner plate test\inventor files refined
mesh'
13 resultsPath = 'C:\higher resistance thinner plate test\Results'
14 scriptPath = 'C:\higher resistance thinner plate test\Scripting files\Strip\First
step'
15
16
17 for subdir, dirs, files in os.walk(InventorfilePath):
18     for file in files:
19         print(file)
20
21         #Import new geometry and update the model
22         geometry1 = system1.GetContainer(ComponentName="Geometry")
23         geometry1.SetFile(FilePath=InventorfilePath+'/'+file)
24         modelComponent1 = system1.GetComponent(Name="Model")
25         modelComponent1.Update(AllDependencies=True)
26         model1 = system1.GetContainer(ComponentName="Model")
27         model1.Edit()
28
29         #load mechanical stript for eigenvalue analysis
30         DSscript = open(scriptPath+"\Eigenvalue strip.py", "r")
31         DSscriptcommand=DSscript.read()
32         DSscript.close()
33
34         # Send the command
35         model1.SendCommand(Language='Python', Command = DSscriptcommand)
36
37         #geometry is now fully loaded
38         #Define scale factor according to slenderness ratio
39
40         with open(scriptPath+'\Variables.txt') as csv_file:
41             csv_reader = csv.reader(csv_file)
42             header = next(csv_reader)
43             variables = next(csv_reader)
44             w0 =float(variables[0])
45             Thickness = int(float(variables[1]))
46
47         print(Thickness)
48
49
50         system2 = GetSystem(Name="SYS 1")
51         solution2 = system2.GetContainer(ComponentName="Solution")
52         modalUpdateOptionsForCdbTransfer1 =
solution2.GetModalUpdateOptionsForCdbTransfer(Name="ModalUpdateOptionsForCdbTransfer"
)
53         modalUpdateOptionsForCdbTransfer1.ScaleFactor = w0
54
55
```

```
56
57     #loop through all nodal solutions
58     modesToCheck = 50
59
60     if os.path.isfile(resultsPath+'\\Analysis %s mm\\Force Reaction.txt' %
Thickness):
61         os.remove(resultsPath+'\\Analysis %s mm\\Force Reaction.txt' % Thickness)
62
63     newpath = resultsPath+'\\Analysis %s mm' % Thickness
64     if not os.path.exists(newpath):
65         os.mkdir(newpath)
66
67     with open(newpath+'\\Force Reaction.txt', 'a+') as f:
68         fwriter = csv.writer(f, delimiter=',')
69         header = ['ForceZ', 'MaxForce']
70         fwriter.writerow(header)
71
72
73     for mode in range(1,modesToCheck+1):
74         modalUpdateOptionsForCdbTransfer1.Mode = mode
75         system3 = GetSystem(Name="SYS 2")
76         modelComponent2 = system3.GetComponent(Name="Model")
77         modelComponent2.Update(AllDependencies=True)
78         model2 = system3.GetContainer(ComponentName="Model")
79         model2.Edit()
80
81
82     #load mechanical script for eigenvalue analysis
83     DSscript = open(scriptPath+"/Non-linear mechanical strip.py", "r")
84     DSscriptcommand1=DSscript.read()
85     DSscript.close()
86
87     # Send the command
88     model2.SendCommand(Language='Python', Command = DSscriptcommand1)
89
90
91
92
93
94
```

```
1 #Non-linear mechanical solver
2
3 import os
4 import csv
5 Model.Solve(True)
6 #reads the variables file
7
8 resultsPath = 'C:\higher resistance thinner plate test\Results'
9 scriptPath = 'C:\higher resistance thinner plate test\Scripting files\Strip\First
step'
10
11 Model.Analyses[0].Children[4].Suppressed = False #supresses displacement
12 Model.Analyses[0].Children[3].Suppressed = True #unsupresses the pressure
13
14 with open(scriptPath+'/Variables.txt') as csv_file:
15     csv_reader = csv.reader(csv_file)
16     header = next(csv_reader)
17     variables = next(csv_reader)
18     w0 =float(variables[0])
19     Thickness = int(float(variables[1]))
20
21
22 #create new folder
23 newpath = resultsPath+'\Analysis %s mm' % Thickness
24
25 if not os.path.exists(newpath):
26     os.mkdir(newpath)
27
28
29 forces = []
30 for i in range(99):
31
32     forces.append(abs(Model.Analyses[0].Solution.Children[5].InternalObject.SequenceZVec
tor(i)))
33     forces.append(max(forces))
34
35 #write force probe values to file
36 with open(newpath+'\Force Reaction.txt', 'a') as f:
37
38     fwriter = csv.writer(f, delimiter=',')
39     fwriter.writerow(forces)
40
```

```
1 #Non-linear eigenvalue analysis
2
3 import os
4 import csv
5 scriptPath = 'C:\higher resistance thinner plate test\Scripting files\Strip\First
step'
6
7
8 def NumFromString(string):
9     stringNumbers = ''
10    for num in string:
11        if num.isdigit():
12            stringNumbers += num
13        if num == '.':
14            stringNumbers += num
15    return float(stringNumbers)
16
17
18
19 #get the body
20 Model = ExtAPI.DataModel.Project.Model
21 #set its material to structural steel NL
22 Model.Children[0].Children[0].Material = "4720b8bb-0d5c-4e4c-96cf-1810ac75e2e7"
23
24 Model.Children[4].ElementSize = Quantity(50, "mm")
25
26
27
28 #length in x
29 PlateWidth = str(Model.Children[0].Children[0].LengthX)
30 PlateWidth = NumFromString(PlateWidth)
31
32 #height of body
33 Height = str(Model.Children[0].Children[0].LengthY)
34 Height = NumFromString(Height)
35 #height of body
36 Length = str(Model.Children[0].Children[0].LengthZ)
37 Length = NumFromString(Length)
38
39 #variables
40 flangeThickness = 8
41 WebHeight = 145
42 yieldStrength = 355e6
43 E = 210e9
44
45 B = PlateWidth
46 t = Height - flangeThickness - WebHeight
47 slendernessRatio = B/t*(yieldStrength/E)**0.5
48 w0 = 10
49
50 with open(scriptPath+'\Variables.txt', 'w') as f:
51     fwriter = csv.writer(f, delimiter=',')
52     header = ['Initial imperfection', 't']
53     fwriter.writerow(header)
54     fwriter.writerow([w0, round(t, 3)])
55
56
57
```